THE HONG KONG
POLYTECHNIC UNIVERSITY
香港理工大學
Pao Yue-kong Library
包玉剛圖書館

Copyright Undertaking

This thesis is protected by copyright, with all rights reserved.

By reading and using the thesis, the reader understands and agrees to the following terms:

1. The reader will abide by the rules and legal ordinances governing copyright regarding the use of the thesis.
2. The reader will use the thesis for the purpose of research or private study only and not for distribution or further reproduction or any other purpose.
3. The reader agrees to indemnify and hold the University harmless from and against any loss, damage, cost, liability or expenses arising from copyright infringement or unauthorized usage.

If you have reasons to believe that any materials in this thesis are deemed not suitable to be distributed in this form, or a copyright owner having difficulty with the material being included in our database, please contact lbsys@polyu.edu.hk providing details. The Library will look into your claim and consider taking remedial action upon receipt of the written requests.

Pao Yue-kong Library, The Hong Kong Polytechnic University, Hung Hom, Kowloon, Hong Kong

http://www.lib.polyu.edu.hk

ADVANCED CHEMICAL OXIDATION TREATMENT OF DYE WASTEWATER AND REMEDIATION OF CHLORINATED AROMATIC DYES (CADs) POLLUTED SOIL BY SURFACTANT MICELLAR/UV SYSTEM

by

Chi Wai Ma

A Thesis for the Degree of Doctor of Philosophy

Department of Civil and Structural Engineering

THE HONG KONG POLYTECHNIC UNIVERSITY

JANUARY 2001

Pao Yue-Kong Library
PolyU • Hong Kong

DECLARATION

I hereby declare that this thesis entitled "Advanced Chemical Oxidation Treatment of Dye Wastewater and Remediation of Chlorinated Aromatic Dyes (CADs) Polluted Soil by Surfactant Micellar/UV System" has not been, either in whole or in part, previously submitted to any other institution for a degree or other qualification, and contains no material previously published or written by another person. except where due reference is made in the text.

Chi Wai Ma

ACKNOWLEDGEMENTS

First of all, I would like to express my sincere gratitude to my chief supervisor, Dr. WEI CHU for his invaluable advice, continued guidance and personal encouragement throughout my study. I also thank for his patience and efforts on reviewing all my papers and thesis, thus making the research possible.

I wish to extend my gratitude to Mr. W.S.LAM of Waste & Wastewater Laboratory and Mr. W.K.HO of Dyeing & Finishing Laboratory for their helping me to solve instrumental, and technical problems during the research period.

I would like to thank Mr. C.W.LAU and K.H.NG of Waste & Wastewater Laboratory, for their kindness and technical support during the research period.

Finally, I am very grateful to the University Research Fund from the Hong Kong Polytechnic University for financial support.

RESEARCH PLAN

Part I
Advanced Chemical Oxidation (ACO)

(ACO I)
Ozonation of 6 purified aromatic dyes

(ACO II)
Photodegradation of aromatic dyes

Preliminary test of 16 commercial dyes

Further test of 6 purified aromatic dyes

Part II
Remediation of Chlorinated Aromatic Dyes (CADs) polluted soil

Photodegradation of CADs in surfactant micellar/UV system

Effect of humics

This research consisted of two parts: The first part was the "Advanced Chemical Oxidation (ACO) Treatment of dye wastewater" which including the ozonation of 6 purified aromatic dyes and photodegradation of 16 commercial aromatic dyes & 6 purified aromatic dyes. The second part was the "remediation of Chlorinated Aromatic Dyes (CADs) polluted soil by surfactant micellar/UV system" which including the photodegradation of Disperse Red 13 and the effect of humics on this system.

Abstract of thesis entitled

"Advanced Chemical Oxidation Treatment of Dye Wastewater

And

Remediation of Chlorinated Aromatic Dyes (CADs) Polluted Soil by

Surfactant Micellar/UV System"

Submitted by Chi Wai Ma

for the degree of Doctor of Philosophy

at Hong Kong Polytechnic University in January, 2001

ABSTRACT

A quantitative estimation of direct ozonation and indirect free radical oxidation of dyes with assorted chromophores was studied through the examination of reaction kinetics in the ozonation process. The reaction kinetics of dye ozonation under different conditions was determined by adjusting the ozone doses, dye concentration, and reaction pH. The ozonation of dyes was found dominant by pseudo first-order reaction, and the rate constants decreased as the dye/ozone ratio increased. For all selected azo dyes, the dye decay rates increased as the initial pH of the solution increased, yet the decay rates of anthraquinone dyes would decrease in the same situation. The ozonation of dyes at a high pH contributed by hydroxyl free radicals was qualitatively verified by the use of a free radical scavenger. A proposed model, in another way, quantitatively determines the fraction of contribution for dye decomposition between free radical oxidation and direct ozonation.

Besides the ozonation reaction, the six selected dyes were UV-irradiated under 253.7 nm of UV light. Experimental results indicated that photo-degradation of all selected dyes following pseudo first order decay and the reaction mechanism was dominated by free radical reactions where acidic photo-products were formed. Moreover, the solubility of the dye molecules was found very important to determine the efficiency of photo-degradation. Dyes with higher water solubility were much easier to be decayed than that with lower water solubility. However, photo-sensitizer such as acetone could greatly enhance the photo-degradation rates for all dyes even for the ones with lower water solubility. In general, the higher the initial pH, the higher the reaction rates constants.

Surfactant soil washing of hydrophobic dye contaminated soil was believed to be a useful technique to extract the contaminants to the aqueous solution in order to facilitate the wastewater treatment. Therefore, a typical soil contaminant, insoluble Chlorinated Aromatic Dye (CAD) - Disperse Red 13 (DR), was used to explore the reaction mechanism and kinetics of photodegradation in non-ionic surfactant solutions. Additional hydrogen source and photosensitizer could improve the decay rates. The decay rate of dye in surfactants depended on its micelle-water partition coefficient (K_m) within surfactants. Basically, the photodegradation of CAD could be divided into three stages: initial lag stage, fast degradation stage and final retardation stage. However, no lag stage and higher degradation rate were observed after adding hydrogen source ($NaBH_4$) or photosensitizer (acetone) to the surfactant micellar solution. Additional hydrogen source or photosensitizer had dosage limitations in such applications. The photoreduction of DR was the main reaction mechanism, in which photodechlorination was observed first with the generation of HCl as the final product, then followed by photodecolourization via the breaking of the azo bond of the chromophore.

After surfactant soil washing, the humic materials will be extracted and present within micelle solution. Experimental results indicated that low dose of humics mainly acted as an additional hydrogen source to improve the photodegradation rate. However, high dose of humics would embed the characteristics of being a hydrogen source, but acted more like a quencher. A mathematical model (Stern-Volmer plot) based on possible reaction mechanisms in this system was proposed and successfully described the quantum yield's improving and quenching processes.

TABLE OF CONTENTS

	Page
DECLARATION	i
ACKNOWLEDGEMENTS	ii
RESEARCH PLAN	iii
ABSTRACT	iv
TABLE OF CONTENT	vii
LIST OF TABLE	xi
LIST OF FIGURE	xii
CHAPTER 1: INTRODUCTION	1
1.1. Advanced Chemical Oxidation (ACO) Treatment of Dye Wastewater	1
1.2. Remediation of Chlorinated Aromatic Dyes (CADs) Polluted Soil by Surfactant Micellar/UV System	3
CHAPTER 2: THEORY AND LITERATURE REVIEW	5
2.1. Dyes and wastewater treatment system	5
2.1.1. Dyes	5
2.1.2. Review of the treatment for dye removal from wastewater	6
2.2. Ozonation	8
2.2.1. Ozone and its decomposed free-radicals	8
2.2.2. Stability of ozone in aqueous solution	10
2.2.3. Ozonation of Aromatic Dyes	11
2.2.4. Ozonation system	13
2.3. Photochemical Reaction of Aromatic Azo Dyes	15
2.3.1. Photooxidation	16
2.3.2. Photoreduction	18
2.3.3. Photochemical reaction of chlorinated aromatic halides	20
2.3.4. Quenching mechanism: Stern-Volmer Plots	22
2.3.5. Hydrogen source/electron source	25
2.3.6. Photosensitization	26
2.4. Photochemical Reaction within Surfactant Micelles	27
2.4.1. Surfactant micelles	27
2.4.2. Enhanced solubility	30

2.4.3. Catalytic effect of micelles 32
2.4.4. Photochemical reaction mechanism within micelles 35

2.5. Soil Washing with Surfactant Micelle 38
2.5.1. Soil washing 38
2.5.2. Extraction of naturally occurring humic materials 42
2.5.3. The humics/fulvic acids ratio 45
2.5.4. Effect of humic materials in photodegradation 46

CHAPTER 3: MATERIAL AND METHODS 47
3.1. Experimental Approach 47
3.1.1. Advanced Chemical Oxidation (ACO) treatment of dye wastewater 47
3.1.2. Remediation of Chlorinated Aromatic Dyes (CADs) polluted soil by surfactant micellar/UV system 48

3.2. Chemical and Reagents 49
3.2.1. Selection of dyes 49
3.2.2. pH & pH buffer 55
3.2.3. Surfactants 56
3.2.4. Soil & humic materials 56
3.2.5. Other chemical 57

3.3. Experiments and Dye's Quantitative Analysis 58
3.3.1. Ozonation of Aromatic Dyes 58
3.3.2. Photodegradation of Aromatic Dyes 60
3.3.3. Photodegradation of Chlorinated Aromatic Dyes (CADs) in micelle 61

3.4. Data Analysis 62
3.4.1. Quantum yield determination 62

3.5. Summary of Experiments 63
3.5.1. Ozonation of Aromatic Dyes 64
3.5.2. Photodegradation of Aromatic Dyes: Preliminary Test 65
3.5.3. Photodegradation of Aromatic Dyes: Further Test 66
3.5.4. Photodegradation of Chlorinated Aromatic Dyes (CADs) in micelle 67
3.5.5. Photodegradation of Chlorinated Aromatic Dyes (CADs) in micelle with the presence of humic materials 68

CHAPTER 4: RESULTS AND DISCUSSION: ADVANCED CHEMICAL OXIDATION (ACO) TREATMENT OF DYE WASTEWATER – OZONATION OF AROMATIC DYES 72

4.1. Ozonation of Aromatic Dyes 72
4.1.1. The mass transfer of ozone 72
4.1.2. Reaction kinetics of ozonation 73
4.1.3. Effect of initial pH 74
4.1.4. Quantitative prediction 76

CHAPTER 5: RESULTS AND DISCUSSION: ADVANCED CHEMICAL OXIDATION (ACO) TREATMENT OF DYE WASTEWATER – PHOTODEGRADATION OF AROMATIC DYES 86

5.1. Preliminary Test 86
5.2. Further Test 91
5.2.1. Effect of initial pH 91
5.2.2. Buffer test 92
5.2.3. Reaction kinetics of photodegradation 92
5.2.4. Free radical 93
5.2.5. Chromophore 94
5.2.6. Solubility 95
5.2.7. Photo-sensitization 95

CHAPTER 6: RESULTS AND DISCUSSION: REMEDIATION OF CHLORINATED AROMATIC DYES (CADs) POLLUTED SOIL BY SURFACTANT MICELLAR/UV SYSTEM 105

6.1. Photodegradation of Chlorinated Aromatic Dyes (CADs) in Micelle 105
6.1.1. The role of surfactants in the photodegradation of DR 105
6.1.2. Three-Stage kinetics 107
6.1.3. Reaction mechanism of photodecay of dye 108
6.1.4. Improvement and inhibition of the reaction 110

6.2. Photodegradation of Chlorinated Aromatic Dyes (CADs) in Micelle with the Presence of Humic Materials 120

6.2.1. Effect of humic materials 120

6.2.2. Stern Volmer Plot 121

CHAPTER 7: CONCLUSION AND RECOMMENDATION 134

7.1. Conclusion 134
7.2. Recommendation 137

APPENDIX A 138
APPENDIX B 147
APPENDIX C 157
APPENDIX D 165

REFERENCE 170

LIST OF TABLE

Table 1: Physical properties of ozone 8

Table 2: Oxidation potential of various oxidation agents 9

Table 3: Bond dissociation Energies for Carbon-Halides 22

Table 4: Enhanced solubility of DR at different non-ionic surfactants 32

Table 5: Physical and/or chemical properties of sixteen commercial dyes 52

Table 6: The physical and/or chemical properties of six purified dyes 53

Table 7: The characteristic of the non-ionic surfactants 56

Table 8: Ozonation of Aromatic Dyes 64

Table 9: Photodegradation of Aromatic Dyes (Preliminary test) 65

Table 10: Photodegradation of Aromatic Dyes (Further test) 66

Table 11: Photodegradation of Chlorinated Aromatic Dyes (CADs) in micelle 67

Table 12: Photodegradation of Chlorinated Aromatic Dyes (CADs) in micelle with the presence of humic materials 68

Table 13: The analysis of constants k_o, k_{OOH} and k 78

Table 14: The results of colour removal of sixteen commercial dyes by UV-irradiation 88

Table 15: Summary of the reaction rate and deactivation rate of DR photodegradation in the presence of different humic substances 127

Table 16: The values of ozone calibration curve 139

LIST OF FIGURE

Figure 1: Basic Structure of an Anionic Surfactant Micelle 29

Figure 2: Reactions in Micelles 37

Figure 3a: A two-phase soil/aqueous system in the absence of surfactant 39

Figure 3b: A system after nonionic surfactant added to the aqueous phase 40

Figure 3c: A system consists of soil, CAD and nonionic surfactant micellar solution 41

Figure 4: Chemical properties of humic substances 43

Figure 5: Model structure of humic acids 44

Figure 6: Model structure of fulvic acids 45

Figure 7: Distribution of humus forms in grassland and forest soil 45

Figure 8: Chemical structures of sixteen commercial dyes in preliminary test 50

Figure 9: Chemical structure of the six selected dyes used in photodegradation and ozonation 54

Figure 10: Chemical structures of the Chlorinated Aromatic Dye (CAD) - DR 2-chloro-4-nitroaniline →2-(N-ethylanilino) ethanol 55

Figure 11: Diagram of ozonation system 70

Figure 12: The Rayonet photochemical reactor 71

Figure 13: Ozone concentration at different pH 4, pH 7 and pH 10 under different air input flowrates 79

Figure 14: The rate of ozone transfer from the gaseous phase to the aqueous phase; and the amount of the saturated ozone at different pHs and flowrates 80

Figure 15: The pseudo first-order decay rate constants of dye ozonation at different initial pH 4, pH 7 and pH 10 81

Figure 16: Quenching of free radical reaction in ozonation of Polyazo dye AZ5 82

Figure 17: Pseudo first-order decay of A1 at different initial dye concentrations & Ozonation of three different dyes at various dye/ozone ratios 83

Figure 18: Variation of pseudo first-order rate constants at different pH 84

Figure 19: The correlation between $\Delta k/\Delta pH$ vs. $3k_{OOH}/k_o$ 85

Figure 20: The change of the dye (C/C_0) during photodegradation at different initial pH with and without photosensitizer 97

Figure 21: The change of pH during photodegradation at different initial pH with or without photosensitizer 98

Figure 22: The change of the dye (C/C_0) during UV irradiation at initial pH 7 & 10 and pH buffer 7 & 10 99

Figure 23: The pseudo first-order photodecay of dyes at initial pH 4, pH 7 & pH 10 100

Figure 24: The pseudo first-order constants at different initial pH 101

Figure 25: Photodegradation of Polyazo dye (AZ5) with and without quencher (0.1 M carbonate) 102

Figure 26: Photosensitization reaction of six purified aromatic dyes 103

Figure 27: The change of the UV/VIS spectra during the photodegradation reaction of dye AZ5 with & without acetone (sensitizer) 104

Figure 28: Photodegradation of DR in various non-ionic surfactant solutions. Lag phases were observed for all samples 113

Figure 29: The solubility enhancement of DR at different non-ionic surfactants 114

Figure 30: The effect of K_m to the reaction rates of DR: i) DR in different Brij and Tween series surfactants, and ii) Various concentrations of Tween 80 surfactants 115

Figure 31. The generation of final products H^+ and Cl^- during the photodegradation of 0.028 mmol/L DR in Tween 80 surfactant solutions at 253.7 nm. The HPLC analysis and Visible spectrometric analysis (color) of the DR is also compared 116

Figure 32: Reaction rates of DR photodecay at different initial pH levels 117

Figure 33: The rate enhancement of photodegradation of DR in the presence of hydrogen source, $BNaH_4$ 118

Figure 34: The rate enhancement of photodegradation of DR in the presence of acetone 119

Figure 35: The photodegradation of Disperse Red (DR) within Tween 80 micelles with various initial concentration of soil extracted materials (SEM) 128

Figure 36: The photodegradation of Disperse Red (DR) within Tween 80 micelles with various initial Aldrich humics (Ha) concentration 129

Figure 37: Photodegradation of DR at low concentration of soil extracted materials (SEM): A plot of $1/\phi$ against 1/[H] for the DR photodegradation within 10 mM Tween 80 micelle and various "SEM" concentrations 130

Figure 38: Photodegradation of DR at low concentration of Aldrach humics (Ha): A plot of $1/\phi$ against 1/[H] for the DR photodegradation within 10 mM Tween 80 micelle and various humic concentrations 131

Figure 39: Photodegradation of DR at high concentration of Soil Extracted Material (SEM): A plot of $1/\phi$ against [H] for the DR photodegradation within 10 mM Tween 80 micelle and various SEM concentrations 132

Figure 40: Photodegradation of DR at high concentration of Aldrich humics (Ha): A plot of $1/\phi$ against [H] for the DR photodegradation within 10 mM Tween 80 micelle and various humic concentrations 133

CHAPTER 1: INTRODUCTION

1.1. Advanced Chemical Oxidation (ACO) Treatment of Dye Wastewater.

Textile industries consume large amount of water and chemicals in the finishing and dyeing processes. The use of dyes and their chemical structures vary enormously. Colour Index (1971, 1987) has listed over 8000 chemicals that can be used in dyeing process. Dyes used today are of synthetic origin, and some of them have complicated aromatic structures that resist degradation in conventional treatment processes due to their stability to sunlight, oxidizing agents, and microorganisms (Mishra G. and Tripathy M., 1993).

The removal of dyes from industrial effluent is a major concern of the textile industry for several reasons: First, the government legislation becomes increasingly stringent; Second, dyes in the textile wastewater are not readily removed by conventional wastewater treatment processes; and Third, some of the dyes might cause the carcinogenic and/or teratogenic effects. Dye wastewater usually consists of a number of contaminants, including acids, bases, dissolved solids, toxic compounds, and dye's colour (Michelsen D.L. *et al.*, 1992). Comparing with the other pollutants, dye's colour is the most noticeable contaminant to the public even at very low concentration and needs to be removed or decolourized from the wastewater before being discharged into surface waters.

Dyes and pigments are released into the industrial effluent either as a dispersion or as a true solution. Previous studies showed that conventional treatment processes such as trickling filter, activated sludge, chemical coagulation and carbon adsorption processes can remove certain categories of dyes to about 90% (Poon C. and Vittimberga B.M., 1981 & Woldman M. L. and Weston R.F., 1974). However, activated carbon does not adsorb some vat dyes, disperse dyes, and pigment dyes while coagulation does not remove acid dyes and reactive dyes of very low molecular

weights. Likewise, physical methods such as hyper-filtration and reverse osmosis are not quite practicable because of their high running costs and the generation of concentrated waste. Therefore, colour materials may still remain in the effluent or reside in the sludge even after conventional secondary treatment processes. (Mishra G. and Tripathy M., 1993 & Eckenfelder W. W., 1994)

An affordable and easy-operated control technology without the formation of sludge is needed to comply with today's demanding legislation. One choice is Advanced Chemical Oxidation (ACO) like Ozonation & UV irradiation. Ozonation & UV irradiation for dyes removal might be a promising process for the following reasons: 1) no chemical sludge is left in the treated effluent; 2) the potential to accomplish both color removal and organic reduction in one step; 3) less space is required, and it is easily installed on site; 4) it is less dangerous, since no stock hydrogen peroxide or other chemical is required on site; 5) it is easily operated; and 6) all residual ozone can be easily decomposed to oxygen. Therefore, ACO technique including Ozonation and UV-irradiation were explored for dye wastewater treatment in this part of research:

Ozonation process: This part of study was to examine the ozonation of six purified selected Aromatic Dyes with various chromophores. This includes quantitatively determining the ratio of direct/indirect oxidation by 1) studying the kinetics of ozonation of the purified aromatic dye materials with different assorted chromophores and different physical properties by adjusting the dye/ozone ratio; 2) determining the effect of pH on the dye's degradation; and 3) investigating the impact of free radical scavengers, such as carbonate, which may be found as one of the components in the actual dyeing wastewater.

Photodegradation process: This part of study was consisted of a preliminary test and a further photodegradation test. The preliminary test was to examine the basic photodegradaton of sixteen commercial dyes while the further photodegradation test was to explore the reaction pathways and the decay rates of six purified Aromatic Dyes under different conditions. These conditions were aimed at studying including: 1) the effect of initial pH; 2) the effect of pH buffer; 3) the quenching effect in the

presence of free-radical scavenger; and 4) the effect of presence of photosensitizer.

1.2. Remediation of Chlorianted Aromatic Dyes (CADs) Polluted Soil by Surfactant Micellar/UV system.

Hydrophobic dyes such as Chlorinated Aromatic Dyes (CADs) are one of the widely used dyes in dyeing industry today (Mishra G. and Tripathy M., 1993). In general, Hydrophobic compounds like CADs are slightly soluble to water in nature and readily sorbed onto soil or sediment in the disposal sites (Edwards D.A. *et. al.*, 1994 & Liu Z. and Shondali L., 1991 & Miyamoto J. T., 1979). The remaining dyes escaping from treatment system may be discharged to rivers or harbours and eventually deposited in the sediment. Therefore, contamination of soils and sediments by CADs is an environmental concern.

Chu W. and Ma C.W. (1997) & Yang Y. *et al.*, (1998) stated that the solubility of dyestuff was the dominant factor to determine the rate of photodegradation in solution. Therefore, the limited solubility of hydrophobic CAD like disperse dye can hinder the efficiency of photodegradation. Moreover, Chu W. and Tsui S.M. (1999) demonstrate that the photodegradation of azo dye was enhanced in aqueous ketone solution, indicating that the indirect photodegradation by using additional hydrogen source is a useful approach to overcome the low performance of direct photolysis for hydrophobic CADs. Since photoreduction reaction is found to be one of the dominant mechanisms for dye photodegradation, it is possible that photodegradation of CADs can be further enhanced if an additional hydrogen source (i.e. electron donors) or sensitizer is co-existent in the solution.

Several researches have justified that surfactant solutions can not only use as rinsing agents to effectively desorbing hydrophobic organic pollutants from soil (Edwards D.A. *et al.*, 1994 & Liu. Z., 1991 & Kile D.E. and Chiou C.T., 1988), but also act as catalysts in photochemical decay reaction of chlorinated organic compounds (Chu W.

and Jafvert C.T., 1994). To remove the sorbed contaminants from soils followed by photolytic destruction may be a promising soil remediation strategy (Risk Reduction Engineering Laboratory., 1991). Nevertheless, very few researches were concentrated to the remediation of CADs sorbed on soils, especially the effect of CAD's photodegradation in the presence of soil washed humic substance. Therefore, the information regarding photochemical reactions of CADs in surfactant solutions is very limited.

The tasks of this part were: (a) to explore the photodegradation of CADs in aqueous solutions containing various selected surfactants; (b) to investigate the reaction kinetics, reaction rates; (c) to find out the reaction pathways; (d) to explore the various possible ways to enhance the photodegradation by using hydrogen source (i.e. electron donor) or sensitizing agent in the surfactant micellar system and (e) to find out the effect of humic materials, which extracted from surfactant soil washing, in CAD's photodegradation.

CHAPTER 2: THEORY AND LITERATURE REVIEW

2.1. Dyes and wastewater treatment system

2.1.1. Dyes

Each dye has an organic structure called Chromophore, which undergoes the mechanism of light absorption to give the colour of the dyes. Most of these light absorbing structures have multiple bonds such as carbon-carbon double or triple bonds, nitrogen-nitrogen double bonds, 6-carbon member aromatic rings and heterocyclic compounds containing oxygen, nitrogen and/ or sulphur in the ring. A double or triple bond consist of 2σ electron and 2 or 4 π electrons; the π electrons can be delocalized, or convey electron density along a chain of atoms linking alternately with single and multiple bonds. This phenomenon allows a molecule to convey electron density throughout the entire section of the structure. The resulting delocalization of electron lowers the energy of molecule and shifts the light absorption to longer wavelengths, i.e. causes visible colour. (Nebel C., 1975)

a. Azo dyes: This is the largest single group of dyes, accounting for over 50% of the total number of dye structures currently being manufactured. They contain one or more azo group (-N=N-) in their molecules and are described as mono, bi, tri, tetra, etc. Azo dyes may be further classified in various ways depending on the structure. For example, Anionic Azo Dye and Metallized Azo Dyes:

- Anionic Azo Dyes: this group of azo dyes are characterised by the presence of one or more water-solubilising ionisable substituents, most often the readily available sulphonic acid group. Normally, the presence of such anionic group can increase the solubility of the dyes.
- Metallized Azo Dyes: this group of azo dyes usually composed of a chromium or cobalt ions. The colour produced is dependent on the combination of a metal ion with a ligand which may be a constituent of the azo group itself or a substituent such as -

OH, $-NH_2$ or $-COO^-$ in the aromatic nucleus. Bi- or poly-functional ligands can occupy two or more co-ordination sites of the metal ion and form a cyclic complex known as a chelate.

b. Anthraquinone Dye: Although Anthraquinone molecules that shown in scheme IV is not a dye itself, it is the parent structure on which this class of dyestuffs is based. Dyestuffs belong to this class of dye contain 2 keto or carbonyl groups in a conjugated system. Anthroaquinone itself exhibits only a faint yellow colour since the λ_{max} absorption was around 327 nm in dichloromethane. The introduction of electron-donating substituents into the molecule changes the λ_{max} to visible region very drastically; the extent of the shift depends on the position of the substituent and its electron-donating strength. (Mishra G. and Tripathy M., 1993)

2.1.2. Review of the treatments for dye removal from wastewater

There is no general or economically feasible method yet for dye removal. Most textile wastewater was treated by some types of biological oxidation (e.g. lagoon, oxidation pond, tricking filter, activated sludge) prior to discharge to streams or rivers. Biological treatments include aerobic and anaerobic treatment. Bioaeration is ineffective in removing the dye from dye wastewater and is mainly used because of its efficiency in reducing the Biological Oxygen Demand (BOD) from textile effluents. Preliminary clarification methods including screening, sedimentation and floatation are not effective for the dye removai without a simultaneous chemical treatment. Treatment processes such as membrane-filtration, electrokinetic coagulation, ion-exchange methods, adsorption and chemical oxidation techniques are used industrially. (Mishra G. and Tripathy M., 1993)

a. Membrane filtration: This technique can remove all types of dyes from the wastewater. However, the filtration process leaves a concentrated dye solution which must be disposed by some other methods. High capital cost and the possibility of clogging the membrane with dye are also the disadvantages of this technique.

b. Electrokinetic coagulation: This technique is an economically feasible method and it has been shown that ferrous sulphate and ferric chloride give excellent dye removal with direct dyes but poor results with acid dyes. In any case, the optimum coagulant concentration has to be determined including zeta potential measurement for each effluent type. Zeta potential refers to the static charge developed to a substance in an aqueous medium. Another disadvantage of electrokinetic method is that it is difficult to recycle the coagulants from treated sludge.

c. Ion-exchange method: The wastewater is passed over the ion exchange resin until the available exchange sites are saturated. The process can remove both the dye cations and dye anions from the effluent. However, this process is less effective in removing disperse dyes.

d. Adsorption method: Activated carbon is one of a common adsorption method, which involved the transport of the dyes form the bulk solution and simultaneously the diffusion of the dye molecules into adsorbent pores. The performance of activated carbon depends on the type of carbon and wastewater characteristics. Although carbon has been found effective in removing certain categories of dyes, it is ineffective in removing some disperse, vat and pigment dyes. Moreover, activated carbon is expensive and regeneration of activated carbon results in 10-15% loss of the sorbent.

e. Chemical Oxidation: Chlorine and chlorine dioxide frequently gives rise to a colour shift to a strong yellow or orange colouration. In addition, the use of chlorine in particular is unlikely to be used because of the possible formation of toxic chlorinated organics. The use of hydrogen peroxide catalysed by ferrous iron at acid pH (Fenton's reagent) for dye degradation involved the dosing of four or five chemicals and the production of considerable quantities of sludge. (John H. C., 1994) Some researches also found fenton's reagent may not effective for dye colour removal. (Hung Y.S., 1995).

By application of Advanced Chemical Oxidation (ACO), the dye degradation by ozonation and photodegradation can overcome the main drawback of fenton's treatment, which can eliminate the formation of sludge. Actually, dye colour removal via ACO can be obtained by the chemical oxidative cleavage of the conjugated chains i.e. chromophore. Such cleavage shifts the absorption of light from the visible portion of the spectrum to either invisible ultraviolet range or infrared region, which cannot be detected by human eyes. Therefore, Advanced Chemical Oxidation including ozonation and photodegradation is a promising technique for dye degradation.

2.2: Ozonation

2.2.1. Ozone and its decomposed free radicals

Ozone (O_3), an allotrope of oxygen, is a very unstable electrophilic and oxidizing agent. In the past decade, the use of ozone is more popular than chlorine in wastewater treatment. The short life of ozone in water (about 20 min) and the low pressures (1-2 atm) during ozone generation make it more safe to prevent from causing hazards to environment in case of accidental ozone leakage (Carriere J. *et al.*, 1991). Moreover, ozone does not form any toxic chlorinated compounds even after the reactions with organic compounds and unreacted ozone decompose quickly without environmental risk (Lin S.H., 1993).

Table 1: Physical Properties of ozone (American Chemical Society, 1956):

Molecular weight	47.998 g/mol
Boiling point	- 111.3 °C
Melting point	- 192.5 °C
Density (gas at 0°C, 760 mm Hg)	2.14 kg/m3
Density (liquid)	1352 kg/m3
λ_{max} in the absorption spectrum	255 nm

The oxidation potential of ozone (2.07 volts) is 1.52 times higher than that of chlorine (shown in Table 2). The high oxidation potential allows it to degrade most organic compounds. In fact, ozone is able to oxidize inorganic and organics to their highest oxidation states, depending on the molecular selectivity and decay rates (Hung Y.S. *et al.*, 1994). Theoretically, the oxidizing ability of ozone is derived from the ozone molecule and it's decomposed product, hydroxyl radical (Alton G., 1983). Ozone and hydroxyl radicals (·OH) generated in the aqueous solution is able to open the aromatic rings. Typically, ozonation rarely produces complete mineralization to CO_2 and H_2O, but leads to partial oxidation products such as organic acids, aldehydes, and ketones where oxygen is introduced into many of the carbonaceous sites within the product molecules (Ruppert G. and Rupert B., 1994). The decomposition rate of ozone is affected by pH, temperature and ozone concentration.

Table 2: Oxidation potential of various Oxidation Agents (Lin S.H., 1993)

Compounds	Oxidation potential [volts]	Relative power of chlorine
Flourine	3.06	2.25
Hydroxyl radical (·OH)*	2.80	2.05
Atomic oxygen (·O)*	2.42	1.78
Ozone	2.07	1.52
Hydrogen peroxide	1.77	1.30
Perhydrroxyl radical	1.70	1.25
Permanganate	1.67	1.23
Chlorine oxide	1.50	1.10
Hypochlorous Acid	1.49	1.10
Chlorine	1.36	1
Bromine	1.09	0.80
Iodine	0.54	0.40
Oxygen	0.4	0.29

* These ions are formed during ozone decomposition.

In general, ozone reacts with organic compounds dissolved in water through either direct ozone attack or indirect free radical attack. The hydroxyl radicals are generated by ozone decomposition in aqueous solutions and especially catalyzed by hydroxide ions (*i.e.* higher pH) or intermediate products of ozonation with decomposition-promoting properties, such as formic acid (Jurgen B., 1995). The predominance of the oxidation reactions by molecular ozone at a lower pH has already been established, while beyond some critical pH level, hydroxyl radicals might become the predominant oxidizing species. The critical pH is expected to differ for different chemical composition in the aqueous phase (Mirat D.G. and Vatistas R., 1987). During the ozonation process, dyes lose their colour by the oxidative cleavage of the chromophores. The cleavage of carbon-carbon double bonds and other functional groups, which have high electron densities, will shift the absorption spectra of the molecule out of the visible region.

2.2.2. The stability of ozone in aqueous solution

The decomposition rate, measured in the presence of excess radical scavengers is expressed by a pseudo first-order kinetic equation of the following equation 1: (Bruno L. *et al.*, 1991)

$$-\left(\frac{d[O_3]}{dt}\right)_{pH} = k'[O_3]^1 \qquad (1)$$

where k' is the pseudo first-order rate constant for a specific pH value.

The pseudo first-order constant is linear function of pH, this evolution reflects the fact that the ozone decomposition rate is first order with respect to both ozone and hydroxide ions, resulting in an overall equation of the following form

$$-\left(\frac{d[O_3]}{dt}\right) = k'[O_3][OH^-] \qquad (2)$$

Ozone decomposition occurs in alkaline aqueous solution that can be represented by the following fundamental reactions:

$O_3 + OH^- \xrightarrow{k_1} HO_2 + O_2^-$	$k_1 = 7.0 \times 10\ M^{-1}s^{-1}$ HO_2 : hydroperoxide radical	(3)
$HO_2 \overset{k_2}{\leftrightharpoons} O_2^- + H^+$	k_2 (i.e.ionization constant) = $10^{-4.8}$ O_2^-: superoxide radical ion	(3')
$O_3 + O_2^- \xrightarrow{k_{2'}} O_3^- + O_2$	$k_{2'} = 1.6 \times 10^9\ M^{-1}s^{-1}$ O_3^- : ozonide radical ion	(4)
$O_3^- + H^+ \underset{k_{3'}}{\overset{k_3}{\leftrightharpoons}} HO_3$	$k_3 = 5.2 \times 10^{10}\ M^{-1}s^{-1}$ $k_{3'} = 2.3 \times 10^2\ s^{-1}$	(5)
$HO_3 \xrightarrow{k_4} OH + O_2$	$k_4 = 1.1 \times 10^5\ s^{-1}$	(6)

The hydroxyl radical ($^{\cdot}OH$) generation from decomposition of ozone in alkaline pH mainly depends on the hydroperoxide free-radical initiating step (rate-determining step) in the chain reaction and the regeneration of the superoxide radical ion O_2^-.

2.2.3. Ozonation of Aromatic Dye:

Up to now, no unique doctrine was concluded from previous researchers upon the pH effect on ozonation of some aromatic dyes. Green J.M. and Sokol C. (1985) explored the efficiency of ozonation in wastewater containing acid, disperse and direct dyes. The author found that the efficiency of dye removal was increased when the pH was lowered. Namboodri C.G (1994) also supported this doctrine. He concluded that ozonation can quickly and completely decolourized disperse, direct, acid and reactive dyes while lowered the pH and increased the conductivity of the solutions.

Hung Y.S. (1995) & Huang C.R. *et al.* (1994) tried to use ozone to decolour the dyeing effluent containing Direct Black and Blue dyes. The author found that the efficiency of colour removal was highest at neutral pH 6.45 but not at alkaline pH. Nevertheless, Carriere J. *et al.* (1991) concluded that the decolouration of some commercial dyes occurred faster at higher temperature and higher pH.

Schultz G. (1992) concluded that the amount of ozone required for decolouration depend on the dye hydrolysate concentration. Higher dye hydrolysate concentrations required lower specific ozone usage. Decolouration even took place in the presence of dying auxiliaries. Ozonation can also improve the Chemical Oxidation Demand (COD), Total Organic Carbon (TOC), Biological Oxygen Demand (BOD) and nitrogen content of the effluent. TOC remains unchanged after ozonation since larger part of organic carbon remains in the effluent which oxidized to higher number of carbon especially carbonic acids.

Spadaro J.T. *et al.* (1994) proposed that the ozonation of dye was mainly undergone via Hydroxyl free radical ($^{\cdot}OH$) attack shown in scheme I: The author explored the use of Fe^{3+} & H_2O_2 treatment to degrade Disperse Yellow 3, Solvent Yellow 14 and Disperse Orange 3. He found that some benzene would be generated from Azo dye and suggested that when $^{\cdot}OH$ (the dominant oxidation agent of ozonation at high pH) added to the azo linkage bearing a hydroxyl or an amine-substituted ring. The resulting $^{\cdot}OH$ adduct breakdown to produce phenyldiazene and a phenoxy radical. Phenyldiazene is extremely unstable; $^{\cdot}OH$ or molecular oxygen can readily oxidize it by one electron to yield a phenyldiazene radical. The latter intermediate is also unstable and cleaves homolytically to generate a phenyl radical and molecular nitrogen. The phenyl radical might abstract a hydrogen radical from $^{\cdot}OOH$ to produce benzene. The phenyl radical is not likely to be scavenged by molecular oxygen since it reacts sluggishly with oxygen. On the other hand, the other intermediate phenoxy radical, might further react with $^{\cdot}OH$ and oxygen leading to the aromatic ring degradation to produce carbon dioxide.

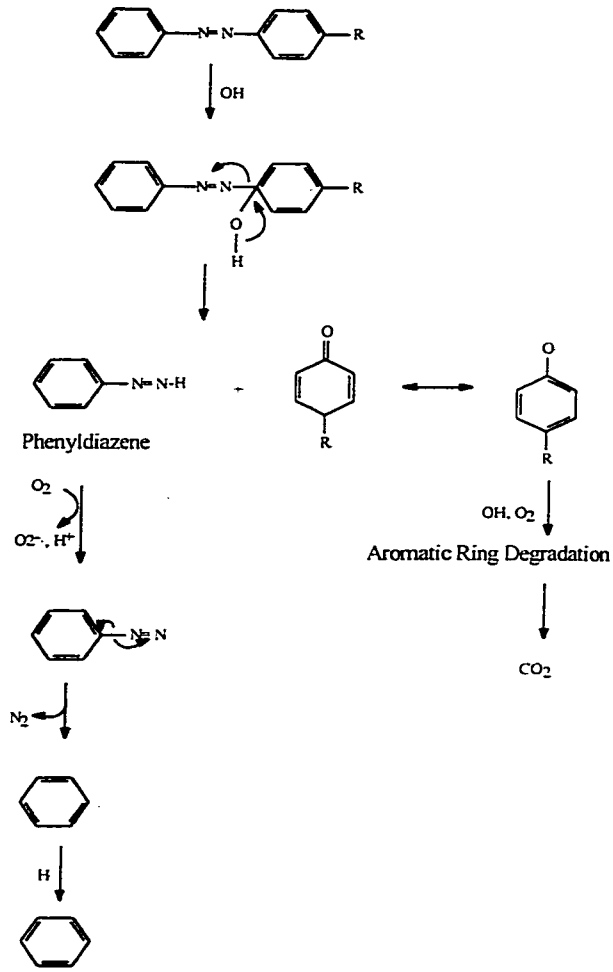

Scheme I: Ozonation reaction of Disperse Dye via Hydroxyl free radical (·OH) reaction.

2.2.4. Ozonation system

Ozonation system consists of the following sections: a. feed-gas treatment; b. ozone generation; c. ozone-water contact mechanism; and d. destruction unit (Lin S.H., 1993). The use of ozonation in preliminary treatment is not economic effective even it can decrease the soluble organic. Therefore, it is better to implement Ozonation in tertiary treatment for effectively colour removal of the residual dyes.

a. Feed gas treatment: Impurities of the feeding gas (ambient air or oxygen is used) such as particles, aerosols moisture and hydrocarbons should be removed. All particles larger than 0.3 μm diameter and 95% of those larger than 0.1 μm diameter should be removed by pressurizing the feed gas to about 2 atm. then filtering and drying it before they reach the generator.

b. Ozone generation: The generation of ozone, the triatomic modification of oxygen, involves the intermediate formation of atomic oxygen radicals, which can react with molecular oxygen to form ozone molecule. The required energy of ozone generation can be provided by either a high voltage electrical discharge or ultraviolet radiation. The instability ozone makes it more suitable for waste treatment applications.

c. Ozone-water contact mechanism: When a gas stream containing ozone-mixture is contacted with a dyeing wastewater, below phenomena will be occurred: (Roth J.A., 1991)

- Mass transfer of ozone from the gas phase to aqueous phase.
- Diffusion in the aqueous phase to pollutant species.
- Self-decomposition of the ozone at certain pH and temperature.
- Reaction of the ozone or free radical with the pollutant.
- Further oxidation of the daughter products of the original pollutants.
- Simultaneous removal of volatile organics by gas stripping.

By applying relatively simple reaction mechanisms and using the two-film theory, rate expressions can be developed by the following regimes which very slow and slow reaction in bulk liquid; moderately fast reaction; and fast reaction in the diffusion film. The fast reaction in the diffusion film may be pseudo first order in which case the rate of absorption is an apparent half order with respect to the dye concentration.

Since the pressure of the feeding gas is usually low, dissolving large quantities of ozone in water is time consuming. Moreover, the content of the wastewater can also reduce the solubility of the ozone. In order to obtain the maximum possible area of contact between the effluent and ozone, the application of counterflow design is important.

d. Ozone destruction unit: Unreacted residual ozone gases in the contactor vessel should be destructed before being released to the atmosphere. Ozone destruction units can be catalytic, thermal-catalytic or activated carbon.

2.3. Photochemical Reaction of Aromatic Azo Dyes

Ultraviolet is a form of electromagnetic radiation or energy. Its magnitude varies from substrate to substrate, UV photons at 180 to 400 nm can provide 72 to 155 kcal mol^{-1} energy (Leaver I.H., 1980) that are able to produce excited-state species of some reactants. When dye molecules absorb photons, the energy of UV will be transferred to the dye molecules and the electronic structures of dyes will be excited to their singlet or triplet states (existence $<18^{-8}$ sec). Dyes in such excited states are extremely unstable and short lived and will either decay back to their ground states losing their excitation energy in some physical ways or undergo chemical reactions and form new species. This self-rearrangement of the dye molecule, which varies widely with the dye structure, depends on the photosensitivity and the ease of dye reactivity. The decolourization of dye mainly depends on the latter property.

Up to now, photochemical studies are still confined to the reactions of simple azobenzene compounds, such as those derived by coupling a phenol or aromatic amine with a diazotised aniline. Azobenzene is isoelectronic with stilbene, its derivatives undergo facile trans $\leftrightharpoons$ cis photoisomerisation reactions in a manner analogous to that of stilbene. Azo dyes which possess a hydroxyl or amino substitutent ortho or para to the azo group

are often unstable in the cis form, and they usually adopt the lower energy trans configuration at room temperature. Exposure to light can bring about a reversible change in the colour of the dye due to the photointerconversion of trans and cis isomers. This phenomenon called photochromism. (Leaver I.H., 1980)

2.3.1. Photooxidation

The light-induced decolourization of dyes in the presence of air (i.e. oxygen) usually entails photooxidation. It has been reported that hydroxyl and hydroperoxyl radicals will be generated when UV is absorbed by water in the presence of oxygen (Mirat D.G. and Vatistas R., 1987). For most azo dyes, photooxidation is generally associated with oxidative cleavage of the azo linkage.

Some researcher reported that photofading behaviour of a series of disperse azo dyes in polyester and nylon films may involve the initial oxidation of dye to the azoxy form, followed by a Wallach photorearrangement (Leaver I.H., 1980) to give an o-hydroxyazo dye (see scheme II):

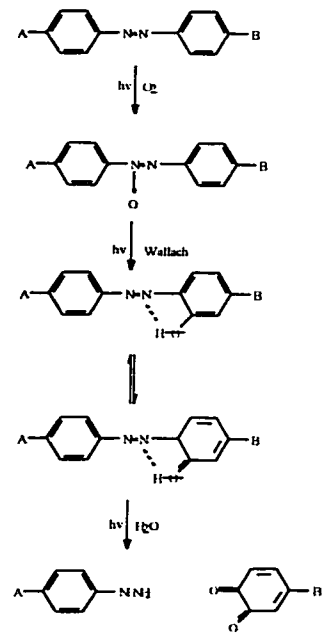

Scheme II: Photooxidation of disperse azo dyes involved the formation of the azoxy form and Wallach photorearrangement

The ketohydrazone tautomer of this intermediate dye can then undergo photohydrolysis to give the expected photo decayed products – a phenylhydrazine and an o-quinone.

On the other hand, Daryner A. *et al.* (1977) explored the photodegradation of some reactive azo dyes in cellophane films. He believed that the first step in the fading reaction involves either photoionisation of an upper excited singlet state of the dye:

$$DH \xrightarrow{hv} {}^{1}DH^{*} \rightarrow DH^{\cdot +} + e^{-} \qquad (7)$$

or photodissociation to form a dye radical and a hydrogen atom:

$$DH \xrightarrow{hv} {}^{1}DH^{*} \rightarrow D^{\cdot} + H^{\cdot} \qquad (8)$$

The ions and radicals that formed may recombine to restore the original dye, or they may undergo further reactions with oxygen, water or undergo self-disproportionation to form colourless end products.

Hirashima T. (1973) also believed that the ions and radicals pathways were involved in the photooxidation. He revealed that some kind of diazonium ions is produced during the photodegradation of amino-substituted azobenzene (see scheme III). He also found that an envisaged reaction scheme in which preferential cleavage occurs at the C-N bond adjacent to the aromatic ring containing the substituent of lower electronegativity. This results mainly in the formation of the diazonium ion, which contains the more electronegative component. (Leaver I.H., 1980)

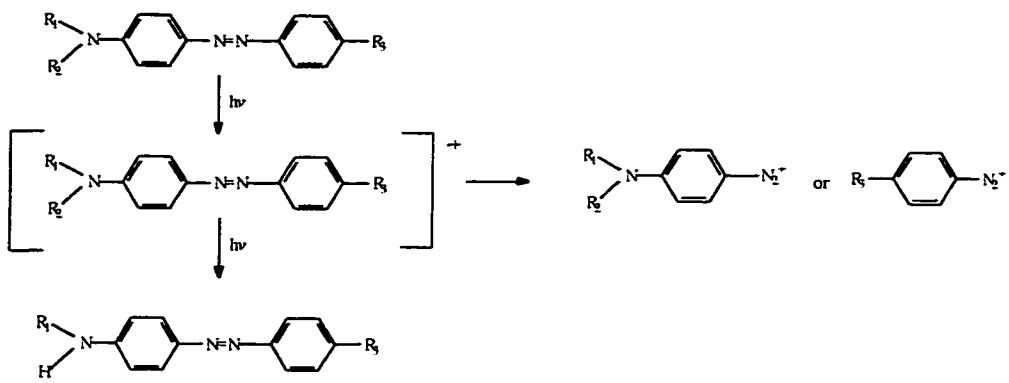

R_1, R_2 and R_3 = alkyl groups

Scheme III: Photooxidation of amino substituted azo benzene dye to produce diazonium ions

2.3.2. Photoreduction

The photodegradation reactions involve not only the photooxidation, but also the photoreduction. For example, Chu W. and Javert C.T. (1994) reported a photoreduction reaction for aromatic compounds in the presence of hydrogen sources in which high reaction quantum yields were observed. Many dyes are also noted for their ease of decolourization in the absence of oxygen when a suitable electron donor or hydrogen source is present. For example, in the scheme IV, formation of colourless leuco-form of anthraquinone dye is observed after photo-reduction that the main structural integrity of the dye molecule retains (Rys P. and Zollinger H., 1972).

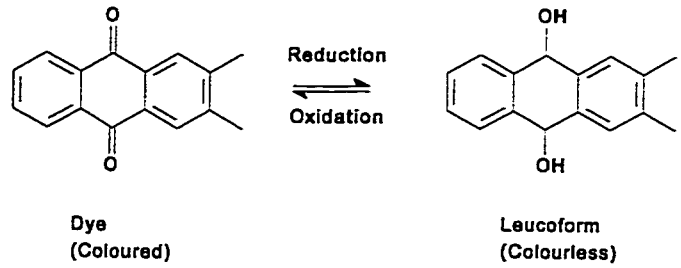

Scheme IV: Photoreduction of anthraquinone dye to produce the colourless leuco form

Blaisdell B.E. (1949) investigated the photoreductive processes of azobenzene and 4-amino-4-nitroazobenzene in isopropanol and isooctane, he concluded that the main products were hydrazobenzene and aniline derivatives after photodisproportionation.

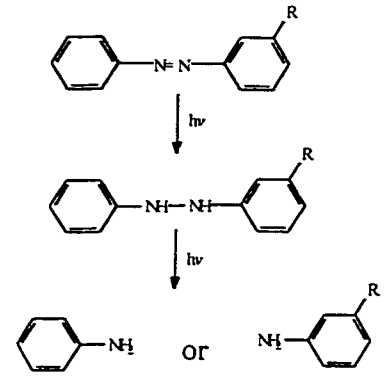

R =alkyl group, H, halogen

Scheme V: Photoreduction of azo benzene to produce hydrazobenzene and amine derivatives

A photoreductive scheme was proposed in which the triplet state of the ketone (^3B) first abstracts a hydrogen atom from the solvent or from a hydrogen donor (YH_2) to give a ketyl radical ($BH^{\cdot}$). Hydrogen atom transfer from the ketyl radical to the azo linkage of the dye (D) leads to the formation of a hydrazl radical ($DH^{\cdot}$), which is finally reduced to the colourless hydrazobenzene (DH_2) as follow:

$$B \xrightarrow{hv} {}^1B^* \rightarrow {}^3B \quad (9)$$

$$^3B \rightarrow B \quad (10)$$

$$^3B + YH_2 \rightarrow 2BH^{\cdot} \quad (11)$$

$$BH^{\cdot} + D \rightarrow DH^{\cdot} + B \quad (12)$$

$$DH^{\cdot} + BH^{\cdot} \rightarrow DH_2 + B \quad (13)$$

$$DH^{\cdot} + BH^{\cdot} \rightarrow D + BH_2 \quad (14)$$

This scheme predicts a linear relationship between the reciprocal of the quantum yield for fading and the reciprocal of hydrogen donor concentration.

2.3.3. Photochemical reaction of chlorinated aromatic halides

The main photochemical reaction for chlorinated aromatic halides in aqueous systems is photoreduction. More specifically, the photoreduction of these compounds is primarily through photodechlorination by way of free radical chain reactions.

a. Singlet and Triplet: It's well established that during photolysis many aryl halides undergo homolysis to generate aryl radicals and halogen atoms. There had been some debate whether the excited singlet or triplet state or indeed both excited states are responsible for reaction. Bunce N.J. *et al.* (1978) claimed that the singlet is an energy-wasting intermediate rather than a reactive one, since the halogen substituents on the aromatic rings increase intersystem crossing, which is consistent with the higher

decay rate of the more chlorinated aryl halides. Additionally, for some Polychlorinated Benzene, the quantum yields for dechlorination are often larger than the quantum yields for fluorescence. Hence, one may anticipate that the triplet state of aryl halides will be efficiently populated and therefore this state is a likely candidate that responsible for the homolysis reaction, i.e. the free radical reaction. Accordingly, the following mechanism may be proposed, in which upon absorption of light, ArCl produces the singlet excited state, ^{1}ArCl, which through intersystem crossing (ISC) gives the triplet, ^{3}ArCl, which upon dissociation produces the aryl radical, Ar$^\cdot$, and chlorine atoms, Cl$^\cdot$.

$$\text{Ar-Cl} \xrightarrow{h\nu} {}^1\text{Ar-Cl} \xrightarrow{ISC} {}^3\text{Ar-Cl} \tag{15}$$

$${}^3\text{Ar-Cl} \rightarrow \text{Ar}^\cdot + \text{Cl}^\cdot \tag{16}$$

Aryl halides, unfortunately, also may undergo an electrocyclic reaction in which higher ring products are generated. From an environmental standpoint, this is a reaction that should be avoided. The ability of electrocyclic reaction to compete with homolysis reactions depends upon the relative energies of activation for these two processes and the reaction conditions. The energies of activation depend upon steric effects and the strength of the carbon-halogen bond (see Table 3), among other factors, whereas the reaction conditions include such variables as the solvent and additives. Davidson R.S. *et al.* (1984) has shown that when benzene is used as the solvent, the chlorine on chlorobenzens is replaced by a phenyl group, while a hydrogen donating solvent such as methanol, however, leads to reductive dechlorination.

Table 3: Bond Dissociation Energies for Carbon-Halides (Egger K.W. and Cooks A.T., 1973)

Bond	Kcal/mole
Ar-Cl	94.5
Ar-Br	79.2
CH_3CH_2-Cl	80.8
CH_3CH_2-Br	67.6

2.3.4. Quenching mechanism: Stern-Volmer Plots

A substance, which accelerates the decay of an electronically excited state (singlet and/or triplet) to the ground state or a lower state, is described as a quencher. Quenching processes can be induced by a variety of compounds including oxygen, humic acids, nitrobenzene, butylhydroxy-toluene, dodecanethiol, and methyl iodine. Hawari J. *et al.* (1992) reported that some aryl chloride like Arochlor 1254 extracted from soil by alkaline 2-propanol was dechlorinated in 20 hours on exposure to sunlight, and in 2 hours at 350 nm (ϕ = 0.28). This photoreaction was totally quenched by oxygen and nitrobenzene (0.1M), which indicated that a free radical reaction was occurring. Pure O_2 generally can significantly quench free radical reactions, however, only small retarding effects were observed if a mixture is exposed to the atmosphere (Po_2 = 0.21 atm).

In fact, quenching effects can be evaluated and linearized through classic Stern-Volmer plots. Rate constants responsible for dechlorination, decay of triplets, and quenching can be estimated according to a proposed mechanism. A Stern-Volmer analysis of photochemical kinetics postulates that a reaction mechanism involves a competition between unimolecular decay of pollutant in the excited state, D^*, and a bimolecular quenching reaction involving D^* and the quencher, Q (Turro N.J., 1978). The kinetics are modeled with the steady-state approximation, where the excited intermediate is assumed to exist at a steady-state concentration:

$$d[D_1^*]/dt = 0 \quad (17)$$

for example, the possible mechanism occurred during the photodegradation:

Process	Rate		
Photon absorption	fI	$D_0 + h\nu \rightarrow D_1^*$	(18)
Deactivation of singlet	$k_{d1}[D_1^*]$	$D_1^* \rightarrow D_0 + \text{heat}$	(19)
Fluorescene	$k_f[D_1^*]$	$D_1^* \rightarrow D_0 + h\nu'$	(20)
Intersystem crossing	$k_{isc}[D_1^*]$	$D_1^* \rightarrow D_3^*$	(21)
Phosphorescence	$k_p[D_3^*]$	$D_3^* \rightarrow D_0 + h\nu''$	(22)
Deactivation of triplet	$k_{d3}[D_3^*]$	$D_3^* \rightarrow D_0 + \text{heat}$	(23)
Quenching of triplet	$k_q[D_3^*][Q]$	$D_3^* + Q \rightarrow D_0 + Q_3^*$	(24)
Photochemical reaction	$k_r[D_3^*][H]$	$D_3^* + [H] \rightarrow \text{Products}$	(25)

Photochemcial reaction, in fact involved several complex reaction. However, several assumptions may be made based on earlier observations or hypotheses regarding the specific mechanisms of transformation, resulting in consideration simplification of the kinetic expression. Nevertheless, if the singlet state is responsible for the reaction, a simpler mechanism may be proposed:

	Rate		
Photon absorption	fI	$D_0 + h\nu \rightarrow D_1^*$	(26)
Fluorescence	$k_f[D_1^*]$	$D_1^* \rightarrow D_0 + h\nu'$	(27)
Radiationless deactivation	$k_d[D_1^*]$	$D_1^* \rightarrow D_0$	(28)
Fluorescence Quenching	$k_q[D_1^*][Q]$	$D_1^* + Q \rightarrow D_0 + Q_1^*$	(29)

results in the change of D_1^* (singlet) as,

$$d[D_1^*]/dt = fI - k_f[D_1^*] - k_d[D_1^*] - k_q[D_1^*][Q] = 0 \quad (30)$$

where I is the illuminating intensity, f is the efficiency of light absorption, k_f is the rate of fluorescene processes, k_d is the rate of all deactivation processes, and k_q is the rate of bimolecular quenching processes. Further information can be obtained by utilizing the concept of quantum yields. For the purpose of discussion, fluorescence may be used (although similar expression for all other processes may be derived), in which the quantum yield is defined as the ratio of the process responsible for fluorescence to the initial illumination. That is,

$$\phi = \frac{k_f[D_1^*]}{fI} = \frac{k_f[D_1^*]}{(k_f + k_d + k_q[Q])[D_1^*]} = \frac{k_f}{k_f + k_d + k_q[Q])} \tag{31}$$

In the absence of quencher this reduced to,

$$\phi_0 = \frac{k_f}{k_f + k_d} \tag{32}$$

the ratio of the above two equations has come to be known as the Stern-Volmer kinetic treatment. If the proposed mechanism is correct , a plot of quencher concentration verses ϕ_0/ϕ will give a straight line with a slope of $k_q/(k_f+k_d)$ and an intercept of 1 as below,

$$\frac{\phi_0}{\phi} = \frac{k_f + k_d + k_q[Q]}{k_f + k_d} = 1 + \frac{k_q}{k_f + k_d}[Q] = 1 + k_q\tau[Q] \tag{33}$$

where the ratio $1/(k_f+k_d)$ is the lifetime of the fluorescent state, τ; ϕ and ϕ_0 are the quantum yields with and without quencher, and [Q] is the concentration of the quencher. The slope of the plot gives the product $k_q\tau$, where k_q is the rate constant of the quenching process (about 10^{10} L/ mole/ sec in water when the process is controlled by diffusion.)

2.3.5. Hydrogen source/Electron donor

In the presence of hydrogen sources and electron donors, the reaction mechanisms for photodechlorination of aryl halides may follow two general mechanisms, i.e., homolysis and electron transfer processes. In the homolysis process, C-Cl bond photolytic cleavage is the primary reaction, forming an aryl radical, which abstracts a hydrogen from the hydrogen source, and gives the product ArH.

$$\text{Ar-Cl}^* \rightarrow \text{Ar}^{\cdot} + \text{Cl}^{\cdot} \xrightarrow{\text{R-H}} \text{ArH} + \text{HCl} \qquad (34)$$

while in the electron transfer process, the donor molecule may donate an electron to the excited aryl chloride, forming an unstable aryl radical anion, which cleaves to form the aryl radical and the chloride ion.

$$\text{D} + \text{ArCl}^* \rightarrow \text{D}^{\cdot+} + \text{ArCl}^{\cdot-} \rightarrow \text{Cl}^{\cdot} + \text{Ar}^{\cdot} \xrightarrow{\text{R-H}} \text{ArH} \qquad (35)$$

Hawari J. *et al.* (1992) reported that aryl halides are photo-dehalogenated in the presence of the hydrogen source, 2-propanol (in the presence of ionic metal alkaoxides) through the radical chain reaction illustrated below,

$$\text{Ar-Cl} \xrightarrow{hv} {}^1\text{Ar-Cl} \xrightarrow{\text{ISC}} {}^3\text{Ar-Cl} \qquad (36)$$

$${}^3\text{Ar-Cl} \rightarrow \text{Ar}^{\cdot} + \text{Cl}^{\cdot} \qquad (37)$$

$$\text{Ar}^{\cdot} \text{ or } \text{Cl}^{\cdot} + (\text{CH}_3)_2\text{CHOH} \rightarrow (\text{CH}_3)_2\text{C}^{\cdot}\text{OH} + \text{ArH or HCl} \qquad (38)$$

$$(\text{CH}_3)_2\text{C}^{\cdot}\text{OH} \rightarrow (\text{CH}_3)_2\text{CO}^{\cdot-} + \text{H}^+ \qquad (39)$$

$$\text{Ar-Cl} + (\text{CH}_3)_2\text{CO}^{\cdot-} \rightarrow (\text{CH}_3)_2\text{CO} + \text{Ar}^{\cdot}\text{-Cl} \qquad (40)$$

$$\text{Ar}^{\cdot-}\text{-Cl} \rightarrow \text{Ar}^{\cdot} + \text{Cl}^{-} \qquad (41)$$

Upon irradiation, eq 36 is the initiation step for free radical formation, while in later steps, 2-propanol has been used as both hydrogen source (eq 38) and an electron donor (eq 40). Upon inspection, eqs 36, 37 and 38 represent the homolysis process, and eqs 38, 39, 40 and 41 represent at the electron transfer process mentioned previously.

2.3.6. Photosensitization

A sensitizer is a substance that absorbs light energy (UV), transforms it into chemical energy, and under favorable conditions transfers this energy to other photochemically inert substances. Indirect photochemical reactions of hazardous compounds can occur through reaction with sensitizers directly or through reactions with secondary products of sensitizer reactions. Photo-sensitizers are often added to enhance the rate of photodechlorination reactions. Carboxylic compounds such as acetone (A) is one of the examples, which can be used as a photo-sensitizer because of their high triplet energy and their ability to transfer energy to a singlet ground state of dye molecule (D). This mechanism can be formulated as eq. 42, where ^3D is able to carry out further chemical reaction and eventually loses its colour. Acetone can be reused after it is decayed back to ^1A state (Jacques K., 1993).

$$^1A + D \xrightarrow{UV} {}^3A + {}^1D \rightarrow {}^1A + {}^3D \qquad (42)$$

Rygalov L.N. and Chibisov A.K. (1971) proposed a photooxidation scheme involving electron transfer between semioxidized form ($S^{\cdot+}$) and a molecule of the dye (D) to give a semioxidized azo dye radical ($D^{\cdot+}$) and a molecule of the sensitizer.

$$S \rightarrow {}^1S^* \rightarrow {}^3S \qquad (43)$$

$$^3S + S \text{ (or } {}^3S) \rightarrow S^{\cdot+} + S^{\cdot-} \qquad (44)$$

$$S^{\cdot+} + D \rightarrow S + D^{\cdot+} \qquad (45)$$

where S is the sensitiser, $^1S^*$is the sensitiser singlet and ^3S is the sensitiser triplet.

2.4 Photochemical Reaction within Surfactant Micelle:

2.4.1. Surfactant micelles

Each surfactant molecule possesses both polar (or ionic) and non-polar, (generally, a straight chain hydrocarbon with 8 – 18 carbon atoms) functional groups. Surfactants are termed amphiphilic (i.e. loving both), hence they may dissolve in water as monomers, adsorb at interfaces, or become incorporated with other surfactant molecules as part of a micelle. The term micelle refers to an aggregation of surfactant molecules in solution, arranged such that their polar groups associate with the aqueous phase, and their non-polar groups self associate.

Micelle formation begins or becomes appreciable over a narrow range of surfactant concentration, through a process somewhat analogous to precipitation. The concentration of monomers in solution at this point is termed the critical micelle concentration (cmc). The cmc value of a surfactant depends upon the hydrocarbon chain length, chain structure, valence and nature of the counterions, temperature, and often the presence of non-electrolytes. Micellar aggregates typically consist of 20 to 100 monomers with either spherical, distorted spherical, ellipsoidal, disk-like, or rod-like configuration, with a radius of approximately 15 – 30 Å. Generally, few micelles are present below the cmc; as the concentration of surfactant increases above the cmc, the change in monomer concentration is small enough to be negligible. In other word, for micelle-forming surfactants, the cmc is approximately the monomeric solubility.

The most widely accepted physical model for the micelle, originally developed by Hartley. (1938), consists of a roughly spherical configuration with three dissimilar phases, and is described in Figure 1. The "core" is a liquid like hydrocarbon interior from which

water is excluded with the polar or charged head groups located at the surface of this core. The "Stern layer" consists of a large fraction of the counterions (in the case of ionized surfactants) and exists in the aqueous phase immediately in contact with the head groups. The "Gouy-Chapman layer", also called the diffuse double layer, surrounds the Stern layer and extends up to several hundred angstroms into the aqueous solution. This layer contains the remaining counterions. The life-time of a single surfactant molecule within a micelle at room temperature is estimated to be in the range of $1 - 100$ μsec (Whiten D.G. *et al.*, 1982). Hence, micelles generally are considered dynamic structures, which are in equilibrium with the solution phase monomers. Micelles behave similarly to organic colloids, in that they may increase the mobility of contaminants in the subsurface.

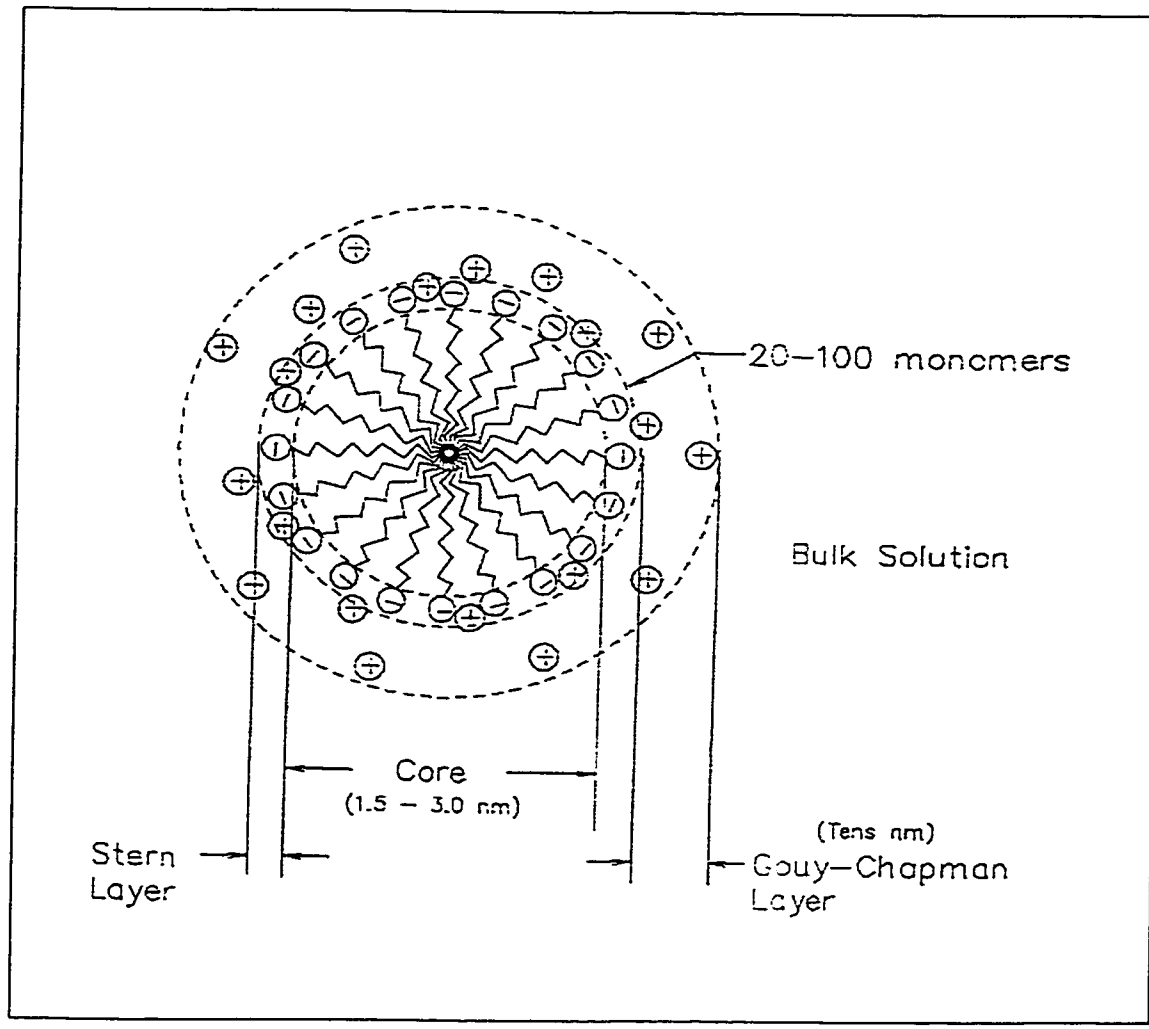

Figure 1: Basic Structure of an Anionic Surfactant Micelle

2.4.2. Enhanced solubility

One of the most relevant properties of aqueous micelles is their ability to solubilize compounds whose water solubility is limited. Because the size of the hydrophobic core of micelle is about 15 – 30 Å, this solubilization process allows the organization of solutes on a molecular scale. Hazardous materials solubilzed by micelles undergo similar processes as those of the surfactant monomers, i.e. rapid exchange takes place between micelles and the bulk solution. The solute, on the average, may spend most of its time within a micelle, with residence times approaching 10^{-3} sec being reported. Water penetration of two to four carbon atoms from the head group or surface of the micelle is often cited (Thomas J.K., 1980).

The location occupied by a solute within a micelle depends upon the structure and hydrophobicity of the solute as well as the charge of both the surfactant and the solute (Mittal K.L., 1977). A solute bearing a charge may associate tightly to an oppositely charged micelle surface, be confined to a region close to the surface, or exist in the bulk phase. A neutral solute may be solubilized within the micelle interior, close to the surface, "in" the surface, or "on" the surface. For those solutes with dimensions that are comparable to that of the micelles, a specific micellar location may not exist. However, two operational positions may be defined: (a) within the micelle or close the surface and (b) on the surface, in close proximity to the aqueous bulk phase. Thomas J.K. (1980), for example, suggested that several aromatic molecules are solubilized on, or at the surface of cetyl trimethyl ammonium bromide (CTAB) micelles.

The solubility of an organic compound in a micelle depends on the surfactant structure and chemical properties, micelle geometry, ionic strength and composition, temperature, and solute structure and properties. Almgren M.A. *et al.* (1979) and Jafvert C.T. (1991) have shown that for hydrophobic compounds solubilized within micelles, a Poisson distribution is obeyed; that is the solubilization of one molecule does not affect the solubilization of another. Solubilization of compounds generally is initiated at the cmc and is proportional to the surfactant concentration beyond this point. Kile D.E. and Chiou

C.T., (1988) extended this simple model to account for solubility enhancement due to both micelles and monomers.

$$\frac{S^*_w}{S_w} = 1 + X_{mon}K^k{}_{mon} + X_{mic}K^k{}_{mic} \tag{46}$$

where (S^*_w/S_w) is the ratio of the total aqueous phase concentration of chemical in solution to its intrinsic water solubility at a given temperature, X_{mon} and X_{mic} are concentrations (g/mL) of surfactant as monomers and micelles. respectively, and $K^k{}_{mon}$ and $K^k{}_{mic}$ are the partition coefficients to surfactant monomers and micelles, respectively (mL/g). Alternatively, solubilization of hydrophobic pollutants by micellar surfactant can be described by an analogous micelle-water partition coefficient, K_m, which has the different units of M^{-1},

$$K_m = \frac{[P]_{mic}}{[P]_w[S]_{mic}} \tag{47}$$

where $[P]_w$ is the concentration of solute in the water (mol/L), $[P]_{mic}$ is the concentration of hydrophobic pollutants in the micelles (mol/L of water), $[S]_{mic}$ is the concentration of surfactant in micellar form (mol/L).

Kile D.E. and Chiou C.T., (1988) have compared their $K^k{}_{mic}$ values for different surfactants and found solubility to correlate better to length of hydrocarbon chain and accessibility to the inner core than to micellar size. For micelles composed of ionic surfactants, hydration at the charged sites may obscure portion of the inner core and thus reduce partitioning to the micelles. In general, the magnitude of solubiliztion of nonpolar organic solutes by micelles follows the surfactant order: nonionic > cationic > anionic, for similar nonpolar chain lengths.

Based on this model, the estimated K_m values for the CAD (Disperse Red - DR) solubilized by various surfactants interest to this research are listed in Table 4.

Table 4: Enhanced solubility of DR at different non-ionic surfactants

Type of surfactant	K_m value (l/M)
Tween 20	1179.25
Tween 60	1365.78
Tween 80	1035.97
Brij 52	139.342

2.4.3. Catalytic effect of micelles

Quite large enhancements in the rate of photochemical reaction have been observed in heterogeneous environments such as those that occur in aqueous micelle solutions or surface semiconductors (Cooper W.J. and Herr. F.L., 1987). The ways that micelles may influence solute chemical reactivity have been summarized below. These influences include cage, localization-compartmentalization, microviscosity, polarity, pre-orientation, counterion and local electric field effects.

a. Cage effects: Cage effects involve the ability of micelles to hold two reactive intermediates long enough in a restricted space for reaction to occur. This effect may be important for hydrophobic solutes as their partition to the micelles may be significant. Organic molecules may be isolated in the hydrophobic core for time periods ranging from 10^{-3} to 10^{-6} sec. For radical reactions, the probability of occurrence of spin correlated events (e.g. intersystem crossing and recombination of singlets) is increased by this effect, because diffusive separation of the radical fragments, the local occurrence of spin uncorrelated free radicals is inhibited (Ramnath N. *et al.*, 1985).

b. Localization and Compartmentalization Effects: The localization and compartmentalization effects result from the unusually high or low concentration of solutes which exist in the restricted space of each micelle, this phenomenon can be explained by the Poisson model (Neter J. *et al.*, 1988) for solute distribution in the micelles (Turro N.J. *et al.*, 1985):

$$P(n) = \frac{S^n{}_{mean}}{n!} e^{-S_{mean}} \tag{48}$$

where P(n) is the probability of finding a micelle with n solute molecules and S_{mean} is the "mean occupancy number" (ratio of the bulk concentration of solute molecules to the bulk concentration of micelles). Depending on the magnitude of S_{mean}, two possible situations may arise:

- At high mean occupancy (e.g. S_{mean} =3), the probability of multiple occupancy of micelle is large. This lead to localization of the reactants and hence the production of extremely high local concentrations – a favorable condition for bimolecular reactions. Thus localization effects have been observed for many bimolecular photochemical reactions with enhancements up to 1000 times that in homogeneous solutions.

- At low mean occupancy (e.g., S_{mean} =0.1), the substrate concentration is such that most of the micelles are "empty" at any given instant, which leads to compartmentalization of the reactants and hence the production of extremely low local concentrations - a favorable condition for unimolecular reactions. This phenomenon not only leads to the "protection" of the excited singlet or triplet from quenching processes, but also prevents the formation of dimer products. In the photodechlorination of chlorinated benzenes, this effect may help to inhibit the formation of the more toxic polychlorinated biphenyls.

c. Microviscosity Effects: These effects result from the fluidity of the environment (the micelle) that the probe molecule sees. This phenomenon may alter or result in variation of the photochemical mechanisms if they are sensitive to viscosity. The microviscosity inside a micelle is generally higher (15 cp to 100 cp) than the overall viscosity of an aqueous solution (Ramnath N. *et al.*, 1985).

d. Polarity Effects: A micelle is less polar than the aqueous phase and more polar than most hydrocarbon solvents. The polarity experienced by a solute will be a time averages value due to the various locations which each solute experiences. Therefore the average location of a solute or the polarity it experiences within a micelle can be quite different for solutes with different hydrophobicities. Reactions influenced by solvent polarity, obviously will have different reaction rates in micelllar systems compared to those in pure aqueous or organic solvent systems.

e. Pre-orientation effects: A pre-orientation effect is the tendency of solubilized molecules to become spatially oriented in the ordered micelle environment. Aromatic molecules such as benzene, for example, and higher arenes are mildly surface active and resident at the micellar surface or the interface of ionic micelles near the head groups; alkyl- substituted benzene, alkyl-naphthalene and simple alkanes (similar in structure to the surfactant hydrophobic chains) show an increasing tendency to reside in the micellar core with increasing length of the alkyl chain (Fendler J.H., 1975). The potential of pre-orientation provides a pathway to achieve regio-selective dimerizations.

f. Counterion Effects: Counterion associate with the charged shell of anionic, cationic or mixed micelles. Chemical reactivity often can be altered by carrying the charge on the micelles or by changing the counterion. This effect has been utilized to accelerate or retard reactions between micelle solubilized substrates and ionic reactant in the aqueous phase. Depending on whether the charge on the surfactant results in the

repulsion of reacting species or organization through attraction, a retardation or acceleration of the reaction results. This phenomenon is often important when charged intermediates exist. Such effects have been explored in photoinduced substitution reactions or aromatic compounds, and in reactions involving organic substrates and metal ions.

g. Local Electric Field Effects: This is a unique property of micelles composed of ionic surfactants and occurs at the micelle-water interface. The local electric field at the surface of ionic micelles can be as large as 10^6 V/cm, which may significantly affect the transition state of a reaction. (Thomas J.K., 1980)

2.4.4. Photochemical reaction mechanism within micelles

Based on the knowledge of micellar catalytic effects, an exclusive photochemical reaction mechanism in micellar solution possibly may be "expected" or "designed" to fulfill each particular environmental problem. Thomas J.K. (1980) proposed four possible photochemical reaction mechanisms that might exist in micellar system (see Figure 2).

a. Mechanism I: Two reactants, A and B reside primarily within the micelles due to hydrophobicity. Usually, enhanced rates of A reacting with B are observed in this case (over pure solvent rates). Most free radical reactions are influenced by this process.

b. Mechanism II: The hydrophobic reactant, A, is dissolved within the micelle while hydrophilic reactant, B, is in the water phase. In order to react, excited A* must have a long lifetime (>> 10^{-6} sec) and may exit the micelle to the bulk phase and react with B, or vice versa. Many examples of this process involve triplet state reactant, because triplet states generally have long lifetimes (10^{-9} sec to seconds). If A's lifetime is short and does not easily leave the micelle, retardation is observed. Therefore, A* may be protected from reaction with impurities (such as C). This effect is readily observed if C and the micelle have the same charge.

c. Mechanism III: If reactant B is only weakly solubilized in the micelle, excitation may yet lead to electron transfer between A and B. Significant exclusion of B ion from the micelle, then leads to efficient separation of A ions and B ions, preventing back neutralization. Exclusion is enhanced if the micelle charge is the same as that of B ion. Through this process, light energy is often converted into chemical energy and stored in micelles.

d. Mechanism IV: This is a variation of Mechanism III in which the electron acceptor, now B, is in the bulk solution. Excitation by light leading to photoionization results in hydrated electrons in the aqueous phase, e_{aq}^-. This process is particularly efficient for anionic micelles, where energy required for photoionization, generally, is reduced.

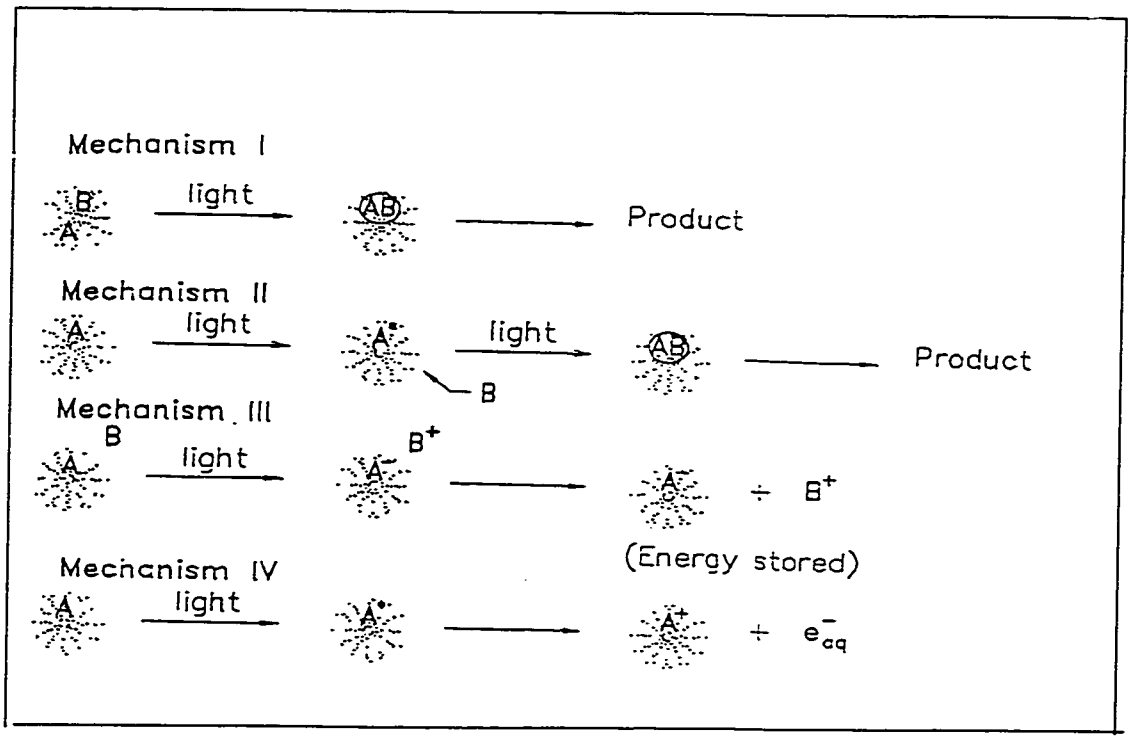

Figure 2: Reactions in Micelles (after Thomas J.K., 1980)

2.5 Soil Washing with Surfactant Micelles

2.5.1. Soil washing

Surfactant micelles can strongly enhance the apparent solubility of hydrophobic compound and assist the remediation of contaminated soils and sediments, especially for anionic and nonionic surfactants (Jafvert C.T. *et al.*, 1994 & Edwards D.A. *et al.*, 1991 & Kile D.E. and Chiou C.T., 1988 & Liu Z. and Shonali L., 1991). Some investigators have studied surfactants in the past decade for their ability to act as soil-washing agents and as facilitators of subsurface remediation of hydrocarbon spills; West C.C. and Harwell J.H. (1992) has reviewed the use of surfactant as soil-washing agents. For in-situ soil washing, Wayt H.J. and Wilson D.J. (1989) reported that the concentration of hydrophobic contaminants (such as 1,4-DCB, naphthalene, and biphenyl) solubilized in surfactant solutions is a linear function of the total surfactant concentration, providing the critical micelle concentration (cmc) is reached.

Vigon B.W. and Rubin A.J. (1989) evaluated surfactant selection and dose optimization through evaluation of parameters such as surface tension, cmc. extent of hydrophilic-hydrophobic balance, solubilizaton efficiency, and partition coefficient. Chu W. and So W.S. (2000) has studied the surfactant aided soil washing of some contaminated non-chlorinated aromatic dyes. They concluded that dye concentration increased slightly until the surfactant monomers in the bulk solution was saturated; the washing performance was 1:1 proportional to the monomer concentration. Above the effective critical micelle concentration (as the result of the sorption of surfactant monomer onto soil), the soil-washing performance increased linearly with increasing available surfactant micelles in the aqueous phase.

Based on these studies, the utilization for surfactants as a soil-washing agent appears to be a promising strategy for many future site remediations. Figure 3 illustrates three conceptual systems that will aid the description of the physicochemical concepts of CAD partitioning in the systems of soil and micellar surfactant solution.

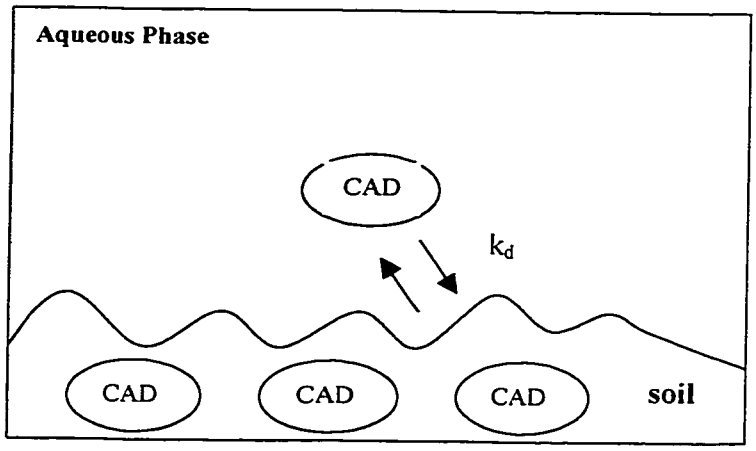

Fig 3a: A two-phase soil/aqueous system in the absence of surfactant.

The CAD molecules dissolved in the solution at concentrations up to the water solubility limit exist in the equilibrium with CAD molecules that are sorbed onto soil. If CAD sorption is directly proportional to the aqueous-phase CAD concentration, the equilibrium soil/aqueous CAD partitioning of the CAD can be described by the coefficient K_d, which is defined as the ratio of the number of moles of sorbed CAD per gram of soil to the number of moles of CAD in the aqueous phase per liters of solution.

$$k_d = \left(\frac{n_{sorb}}{w_{soil}}\right)\left(\frac{v_{aq}}{n_{aq}}\right) \tag{49}$$

Where n_{aq} is the equilibrium number of moles of CAD in solution; n_{sorb} is the equilibrium number of moles of CAD sorbed onto soil; w_{soil} is the weight of the soil in grams and v_{aq} is the volume of the aqueous solution in liters. The unit of k_d is liters per gram.

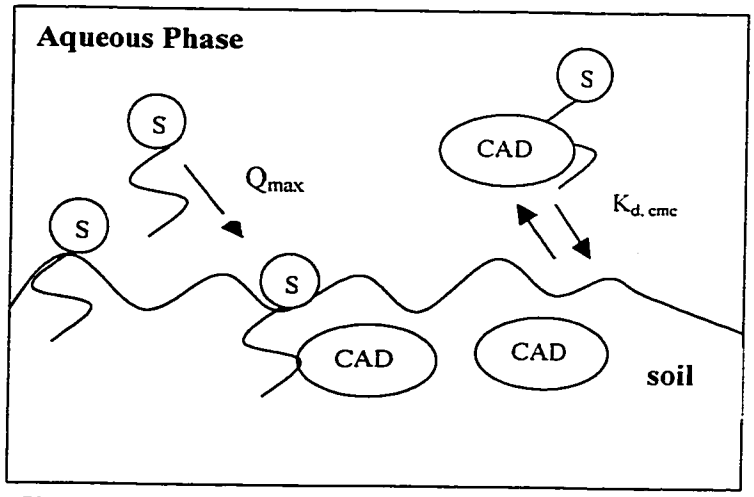

Figure 3b: A system after nonionic surfactant added to the aqueous phase.

Figure 3b illustrates the other system when just enough non-ionic surfactant added for the surfactant CMC to be attained in the aqueous phase. This is also a two-phase system. In this system, the surfactant monomer concentration in the aqueous phase is at a maximum. The addition of surfactant in excess of that needed to attain this critical value would result in the formation of surfactant aggregates or micelles. Sorbed surfactant is present on the soil, with Q_{surf} denoting the number of moles of surfactant sorbed per gram of soil. Several experiments described the values for Q_{surf} may be constant over a range of bulk solution surfactant values greater than the CMC. If so, then the particular value of Q_{surf} at the CMC may be referred to Q_{max} in fig. 3b. The presence of both dissolved and sorbed surfactant molecules at equilibrium modifies the relative affinity of the soil for CAD, CAD partitioning between the sorbed phase and the aqueous phase is characterized for this type of system by the parameter $k_{d,cmc}$, the ratio of the number of moles of CAD sorbed per gram of soil to the number of moles of CAD dissolved per litre of monomeric solution at the CMC:

$$k_{d,cmc} = \left(\frac{n_{sorb,cmc}}{w_{soil}}\right)\left(\frac{v_{aq}}{n_{aq,cmc}}\right) \tag{50}$$

Where $n_{aq,cmc}$ is the equilibrium number of moles of CAD in surfactant solution at the CMC; and $n_{sorb,cmc}$ is the equilibrium number of moles of CAD sorbed onto soil at the surfactant CMC.

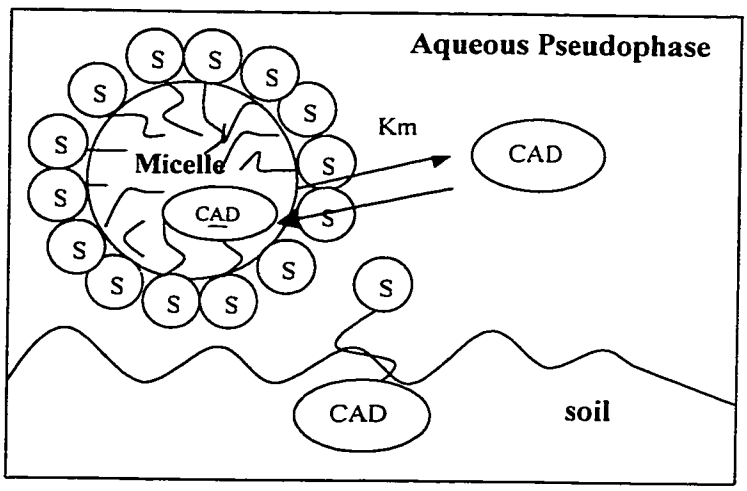

Figure 3c: A system consists of soil, CAD and nonionic surfactant micellar solution

Figure 3c illustrates a system of soil, CAD and nonionic surfactant micellar solution. In this system, sufficient surfactant has been added such that the liquid phase now has a bulk surfactant concentration, C_{surf}, that is greater than the CMC. As a result, micelles are present in the system, necessitating the use of the term pseudophase to describe each of the contrasting compartments for CAD partitioning in the bulk solution: the hydrophobic micellar pseudophase, which has a micellar surfactant concentration equal to C_{surf} less the

CMC, and the hydrophilic aqueous pseudophase, which has a monomeric surfactant concentration equal to the CMC. Dissolved CAD is present in the aqueous pseudophase, and solubilized CAD is present in the micellar pseudophase. The equilibrium CAD partitioning between the sorbed phase and the aqueous pseudophase is still characterized by $K_{d,\,cmc}$; and the equilibrium CAD distribution between the micellar pseudophase and the aqueous pseudophase can be characterized by a partition coefficient, K_m, which represents the ratio of X_m, the mole fraction of CAD in the micellar pseudophase, to X_a, the mole fraction of CAD in the aqueous pseudophase. (Edwards D.A. *et al.*, 1994)

$$k_m = \frac{x_m}{x_a} \tag{51}$$

2.5.2. Extraction of naturally occurring humic material

Humic materials, a complex mixture of polymeric phenolic macromlecules, are known to be extracted from soils by surfactants. Humic materials substances consist of a heterogeneous mixture of compounds for which no single structural formula will suffice. Humic materials are operationally classified by their aqueous solubility. This classification is arbitrary because solubilities of Humic materials depend on their molecular weight, their state of aggregation and their metal and mineral contents. Basically, humic substances can be classified into three categories (see Figure 4) (Davies G. and Ghabbour E.A., 1998).

Humic acids - the fraction of humic substances that is not soluble in water under acidic conditions (pH < 2) but is soluble at higher pH values. They can be extracted from soil by various reagents and which is insoluble in dilute acid. Humic acids are the major extractable component of soil humic substances. They are dark brown to black in color.

Fulvic acids - the fraction of humic substances that is soluble in water under all pH conditions. They remain in solution after removal of humic acid by acidification. Fulvic

acids are light yellow to yellow-brown in color.

Humins - the fraction of humic substances that is not soluble in water at any pH value. On this basis, humins include any humic-type material that is dissolved in non-aqueous solvents after the soil has been exhaustively extracted with basic aqueous solvents. Humins are often considered to consist mainly of humic materials strongly associated with the soil inorganic colloids.

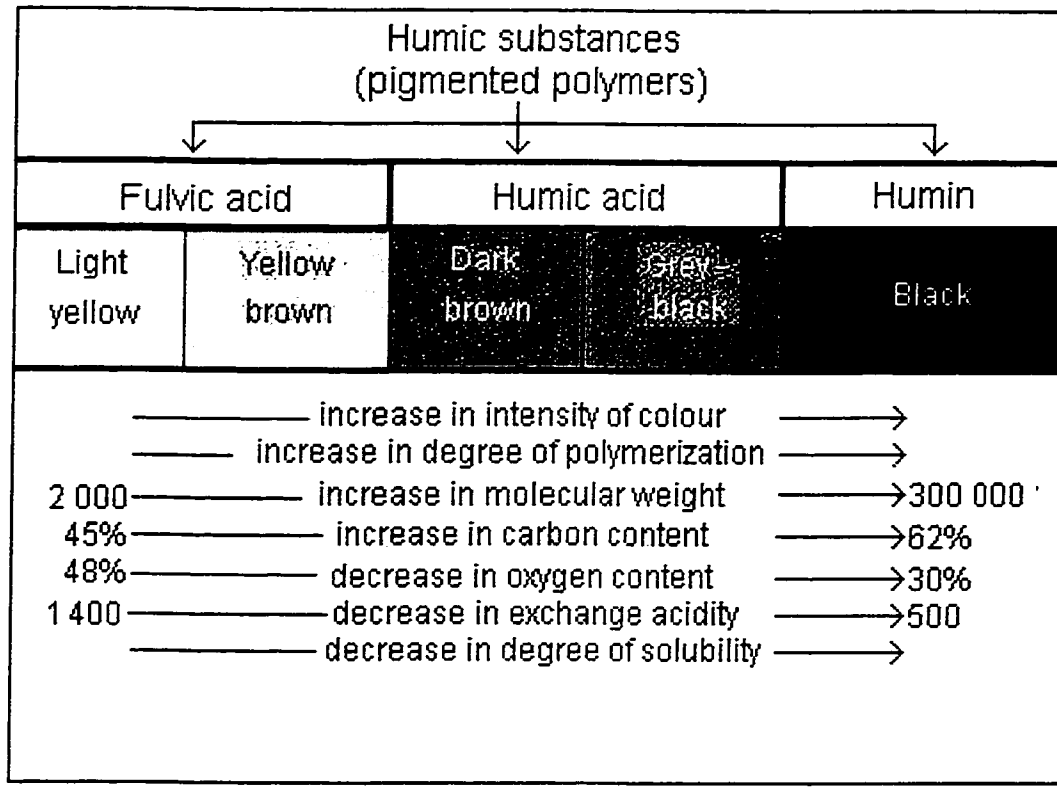

Figure 4: Chemical properties of humic substances (Stevenson F.J., 1982)

Humic acids are thought to be complex aromatic macromolecules with amino acids, amino sugars, peptides, aliphatic compounds involved in linkages between the aromatic groups. The hypothetical structure for humic acid, shown in Figure 5, contains free and bound phenolic OH groups, quinone structures, nitrogen and oxygen as bridge units and COOH groups variously placed on aromatic rings. (Stevenson F.J., 1982)

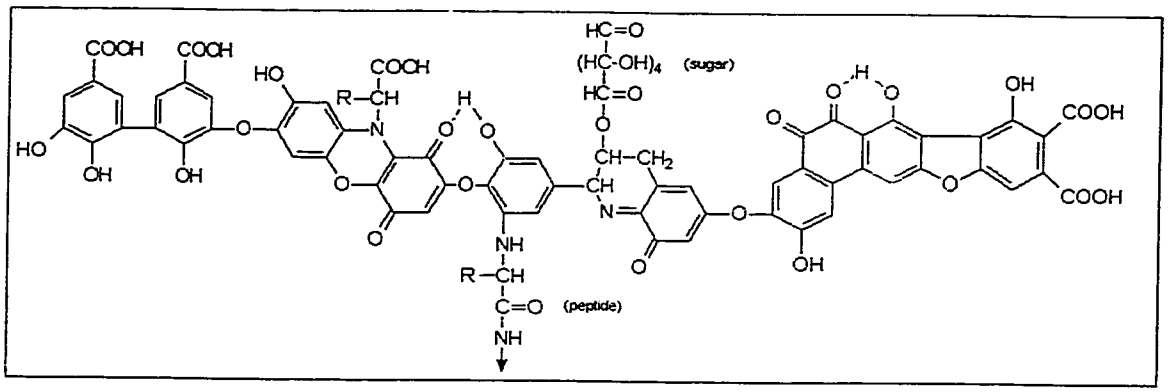

Figure 5: Model structure of humic acids (Stevenson F.J., 1982)

The hypothetical model structure of fulvic acids (Buffle's model) (shown in Figure 6) contains both aromatic and aliphatic structures, both extensively substituted with oxygen - containing functional groups.

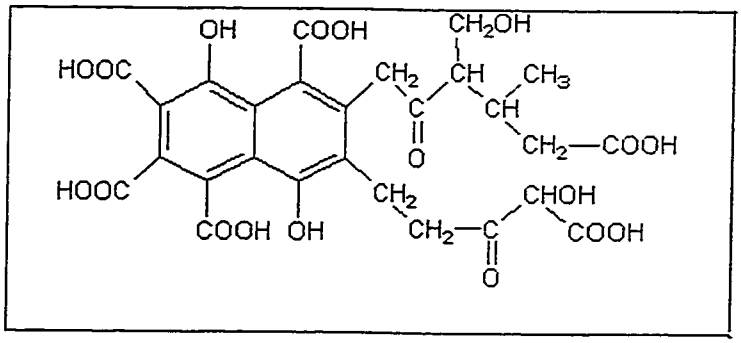

Figure 6: Model structure of fulvic acids (Buffle J.A.E., 1977)

2.5.3. The humic acids / fulvic acids ratio

The percentage of the humus, which occurs in the various humic fractions, varies considerably from one soil type to another. In fact, the humus of forest soils is characterized by a high content of fulvic acids while the humus of peat and grassland soils is high in humic acids (see Figure 7). Usually, the humic acids / fulvic acids ratio usually, but not always, decreases with increasing depth. (Stevenson F.J., 1982)

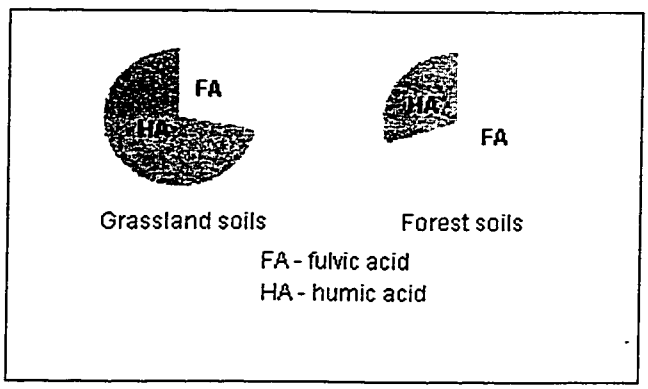

Figure 7: Distribution of humus forms in grassland and forest soil

2.5.4. Effect of humic materials in photodegradation

Some researchers pointed out that extracted humic materials might cause problems for the extraction and photolysis of probe (pollutant) molecules. First, the extraction efficiency may decrease, and second, humics are known to quench photochemical reaction. For example, Zepp R.G. *et al.* (1975) suggested that phenolic humic substances present on most inland waters could inhibit free radical chain reactions. Thus, quantum yields for direct photolysis of chlorinated compounds in the aquatic environment are not likely to exceed unity.

On the other hand, some researchers had another doctrine toward the effect of humics during photodegradation. They pointed out that humic materials can not only increase the photodegradation by increasing the solubilities, reactivities, and mobilities of environmental chemical, but also increase the photosensitization ability to absorb solar energy and generation radical species, which may attack chemicals in the environments and initiate their degradation. (Zepp R.G. *et al.*, 1981 & Choudhry G.G., 1984 & Frimmel F.H. *et al.*, 1987 & Cooper W.J. and Herr F.L., 1989 & Frimmel F.H., 1994). For example, Mamoru K. (1998) pointed out that rate of photodegradation of organophosphosphrous pesticides depends on the radical generation abilities of humic substances. He also suggested that the sensitization action of humic acids depends on binding affinities of pesticide to the radical generation source of humic acids.

CHAPTER 3: MATERIALS AND METHODS

3.1. Experimental Approach

Based on the evidences from literature review in Chapter 2, the optimal scientific and engineering approaches to remove Aromatic Dyes are still unclear. The optimal pH, sensitizer, oxidant concentration for Advanced Chemical Oxidation by UV-irradiation and ozonation were needed for further exploration. Moreover, there is still an unknown for the possible use of surfactants as facilitators of soil remediation, as both extracting agents and as a medium (i.e. micelle) in which to carry out photochemical decay within micellar solution of the solubilized Chlorinated Aromatic Dyes (CADs). More specifically, there is only little information in the photochemical decay of CADs at such micellar medium. In addition, the potential quenching or catalytic effect of humic materials in photochemical decay of CADs at micellar medium is still an unknown. Hence, in this research, the tasks were focused on the following areas:

3.1.1. Advanced Chemical Oxidation (ACO) treatment of dye wastewater.

a. Ozonation of Aromatic Dyes

Six selected Aromatic Dyes with various chromophores were reacted with ozone by adjusting the pH and dye/ozone ratio of the reaction mixture. The concentrations of the dyes were determined by HPLC. The kinetics of the ozonation and the ratio of direct/indirect oxidation were studied quantitatively from the results.

Ozonation at high pH was mainly via the hydroxyl free radical ($^{\cdot}OH$). This kind of ozonation may be diminished in the presence of some radical scavenger. Free radical scavengers - carbonate, which may be found as one of the components in the actual dyeing wastewater, was selected in order to determine the effect of the free radical scavenger.

b. Photodegradation of Aromatic Dyes:

- Preliminary test: Sixteen commercial dyes were used to explore the fundamental performance of dye photodegradation.

- Further test: Six selected Aromatic Dyes with various chromophores were UV-irradiated at λ = 253.7 nm to explore the reaction pathways and decay rates of photo-degradation under different initial pH levels and pH buffers. The concentrations of the dyes during photodegradation were determined by HPLC.

Photodegradation may be contributed by some free radicals attack like hydroxyl & hydroperoxyl radicals. Therefore, free-radical scavenger – carbonate was added to determine it's effect on photodegradation.

In order to enhance the photodegradation rates, Acetone was also selected to determine its photosensitization effect.

3.1.2. Remediation of Chlorianted Aromatic Dyes (CADs) polluted soil by surfactant micellar/UV system.

a. Photodegradation of Chlorinated Aromatic Dyes (CADs) in micelle

Surfactant solutions containing the selected Chlorinated Aromatic Dyes (CADs), i.e Disperse Red (DR) were UV-irradiated at λ = 253.7 nm to determine the reaction pathway. The surfactants were four non-ionic surfactants: Tween 20, Tween 60, Tween 80 and Brij 52. The rates of decayed DR were determined by HPLC. In order to determine the rate of dechlorination, the pH and chlorides ions were quantified by pH meter, HPLC and Ion Chromatography (IC).

A hydrogen source (sodium borohydride) and a photosensitizer (acetone) were investigated for their ability to enhance the reaction rate of DR solubilized within surfactant micelles. The enhancements were defined by comparison of the relative reaction rate constants.

The impact of pH to DR photodegradation within micelle was examined. pH of the system is another important factor for photochemical reactions. It may affect these reactions in a number of ways.

b. Photodegradation of Chlorinated Aromatic Dyes (CADs) in micelle with the presence of humic materials

The effect of humic materials on the photolytic micellar system was evaluated in DR's photodegradation. DR solubilized within Tween 80 micellar solution with or without humic materials was determined. In order to calculate the quantum yield, the molar absorptivity of DR was determined by spectrophotometry. The determination of the quantum yield and reaction rates was examined through a pseudo first-order decay rate expression. Quenching and catalytic effects resulting from the humic substances were examined through Stern-Volmer analysis. A reaction mechanism of photolytic decay of DR solubilized within surfactant micelles in the presence of various amount of humic materials was proposed for this purpose. The effect of high and low concentration of humic materials has been accounted for by a designed model.

3.2. Chemical and Reagents

3.2.1. Selection of dyes

a. Preliminary test: Sixteen different commercial dyes without purification were used in the preliminary test including 4 anthraquinone dyes, 7 azo dyes, 2 metal containing (Copper and Chromium) azo dyes, 2 cyanine dyes and 1 stilbene azo dye. The chemical structures of these dyes are shown in Figure 8. Also, their physical and/or chemical properties are given in Table 5.

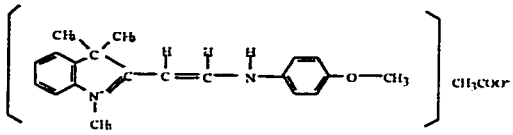

Sample 1: Cyanine (Basic yellow 13)

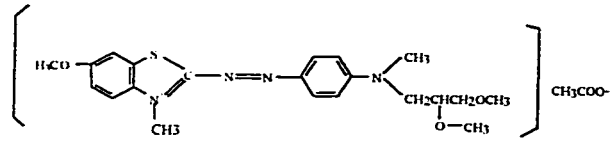

Sample 2: Thiocyanine (Basic blue 41)

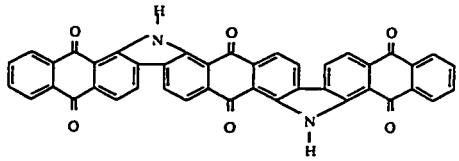

Sample 3: Anthraquinone (Vat orange 11)

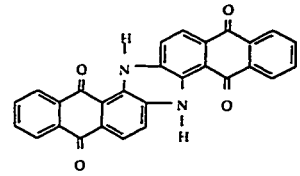

Sample 4: Anthraquinone (Vat blue 4)

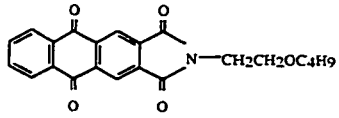

Sample 5: Anthraquinone (Disperse blue 143)

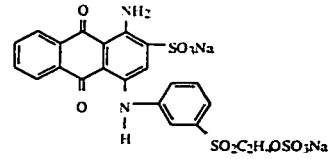

Sample 6: Anthraquinone (Reactive blue 19)

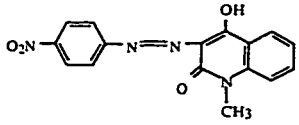

Sample 7: Monoazo (Disperse yellow 79)

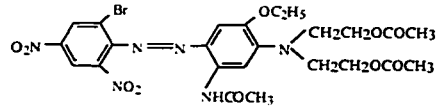

Sample 8:Monoazo (Disperse blue 142)

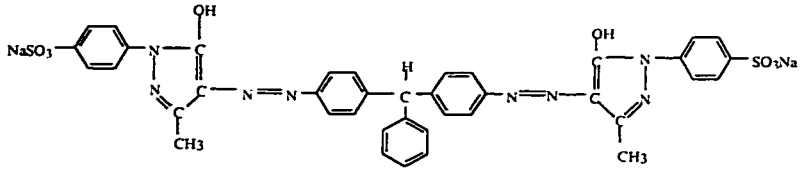

Sample 9: Triarylmathane (Acid Yellow 117)

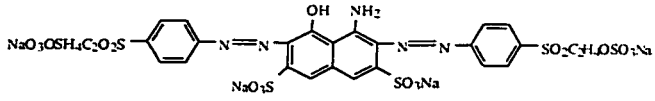

Sample 10:Diazo(Reactive black 5)

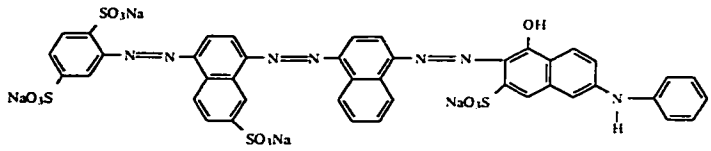

Sample 11: Triazo (Direct blue 78)

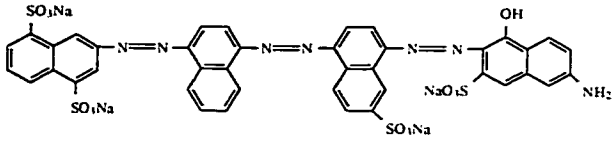

Sample 12: Triazo (Direct blue71)

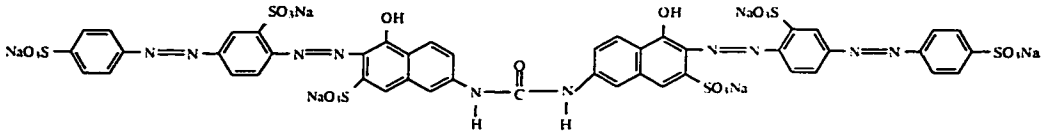

Sample 13: Polyazo (Direct red 80)

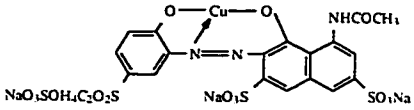

Sample 14: Cu containing Monoazo (Reactive violet 5)

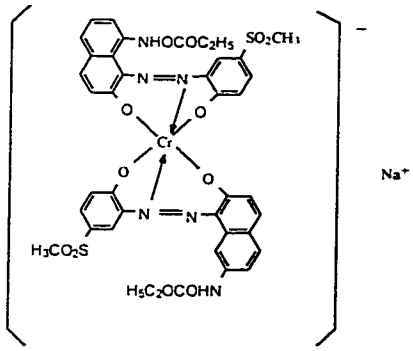

Sample 15: 1:2 Cr Metal complex (Acid black 58)

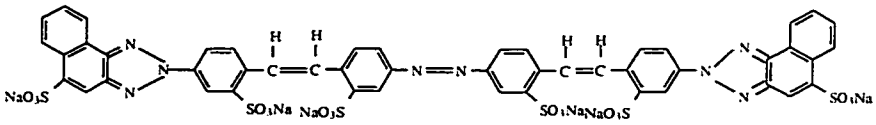

Figure 8: Chemical structures of sixteen commercial dyes in preliminary test

Table 5: physical and/or chemical properties of 16 commercial dyes

Exp. no	Chromophore	Dye class*	Solubility (g/L)	λ_{max} (nm)
1	Cyanine	Basic	5	412
2	Thiocyanine	Basic	80	607
3	Anthraquinone	Vat	< 1	415
4	Anthraquinone	Vat	< 1	613
5	Anthraquinone	Disperse	< 1	688
6	Anthraquinone	Reactive	100	589
7	Monoazo	Disperse	< 1	409
8	Monoazo	Disperse	< 1	550
9	Monoazo	Acid	80	412
10	Diazo	Reactive	100	598
11	Triazo	Direct	20 ~ 30	604
12	Triazo	Direct	20 ~ 30	589
13	Polyazo	Direct	20 ~ 30	529
14	Cu Monoazo	Reactive	100	559
15	Cr Monoazo	Metal-complex	60	595
16	Stilbene	Direct	20 ~ 30	400

* Based on the substitute groups added to the dye molecules.

b. Further test and ozonation: Since most commercial dyes used today are mixtures of dye and other additives such as surfactants, salts, inorganic diluents, side products and impurities from synthetic process, the actual decay rates of the dyes themselves may be interfered by these additives. The dye purification by either N,N-dimethylforamide acetone method and/or ethanol extraction method (David M.H. and Warren S.R., 1971) was adopted. The selections of dyes were based on the variation of chromophores. Since anionic and non-ionic dyes are mostly azo groups or anthraquinone types (Mishra G. and Trypathy M., 1993), totally 6 different dyes with assorted chromophores were used in further test and ozonation test. These include two anthraquinone dyes, three azo dyes, and one copper azo dye. The chemical structures of these dyes are shown in Figure 9. Also, their physical and/or chemical properties are given in Table 6.

Table 6: The physical and/or chemical properties of six purified dyes (Colour index 1971, 1987)

Code	Class	C.I. Name	C.I. Number	Molecular mass	Solubility (g/L)	Purification method
A1	Anthraquinone	Reactive Blue 19	61200	610	100	DMF/Acetone extraction
A2	Anthraquinone	Disperse violet 28	61102	307	< 1	DMF/Acetone extraction
AZ2	Disazo Vinylsulphonate	Reactive black 5	20505	976	100	Ethanol extraction
AZ3	Triazo	Direct green 26	34045	1286	10	DMF/Acetone extraction
AZ5	Polyazo	Direct blue 86	35780	1373	10	DMF/Acetone
AM1	Monoazo (Cu Vinylsulphonate)	Reactive violet 5	18097	797	100	DMF/Acetone extraction

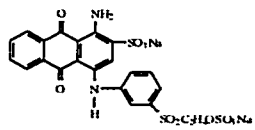

A1: Anthraquinone (Reactive blue 19)

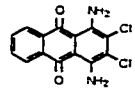

A2: Anthraquinone (Disperse violet 28)

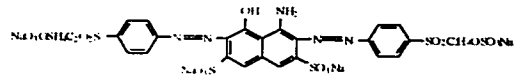

AZ2: Diazo (Reactive black 5)

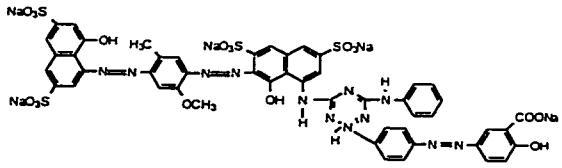

AZ3: Triazo (Direct green 26)

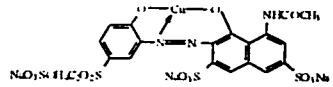

AM1: Cu containing Monoazo (Reactive violet 5)

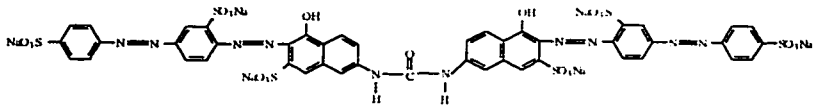

AZ5: Polyazo (Direct red 80)

Figure 9: The chemical structure of the six selected dyes used in photodegradation and ozonation.

c. Photodegradation of CADs in micelle: A mono-Chlorinated Aromatic Dye - Disperse Red 13 was purchased from Aldrich (purity > 98%). DR, one of the typical hydrophobic dyes that used in today's dye house, was selected as the probe compound in the test of photochemical reactions in micelle. Its chemical structure is shown in Figure 10.

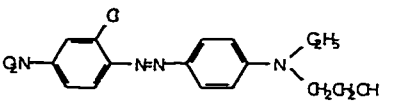

Disperse Red 13
C.I. 11115

Figure 10: The chemical structures of the Chlorinated Aromatic Dye (CAD) - DR
2-chloro-4-nitroaniline → 2-(N-ethylanilino) ethanol

All dyes used in this research were tested by spectrophotometer to ensure that no distinguish λ_{max} shifting was observed at different pH levels. In all experiments, spectrometric analysis was conducted before the UV irradiation to ensure all selected dyes would not have significant shift of the λ_{max}.

3.2.2. pH & pH buffer

The pH values of the solution were adjusted by sulphuric acid or sodium hydroxide. Whereas the buffer tests were prepared by 0.08 M sodium di-hydrogen phosphate/0.12 M di-sodium hydrogen phosphate (buffer solution of pH 7) or sodium tetraborate/sodium hydroxide (buffer solution of pH 10).

3.2.3. Surfactants

Due to the positive charge present on most soils, application of surfactants in proposed soil washing schemes is largely restricted to neutral and anionic types. Non-ionic surfactant may have several further advantages over anionic and cationic surfactants with respect to certain aspects of engineered remediation of contaminated soils. These advantages result from their lower Critical Micelle Concentration (CMC) values, reduced toxicity and greater biodegradability. Some surfactants (non-ionic and anionic) were investigated as extracting agents, as the extraction of humic materials from the soil varies with surfactant properties. Some physical and chemical characteristics of the surfactants chosen for this study are shown in Table 7. All the surfactants were obtained from the China National Chemicals Import & Export Corporation and Aldrich. It should be noted that the surfactants are homologue mixture (i.e. not reagent grade) and used without further purification.

Table 7: The characteristic of the non-ionic surfactants (Fendler J.H., 1975)

Surfactant	Chemical Formula and/or name	F.W.	cmc $(M)^2$
Tween 20	Polyoxyethylene (20) sorbitan monolaurate	1227	3.0×10^{-6}
Tween 60	Polyoxyethylene (20) sorbitan monostearate	1312	
Tween 80	Polyoxyethylene (20) sorbitan monooleate	1310	9.9×10^{-6}
Brij 52	Polyoxyethylene Certyl ether	331	

3.2.4. Soil & humic materials

Two different humic materials were used in this study for comparison, a well-defined soluble humic material (Ha) that purchased from Aldrich, and a soil extracted material (SEM) that prepared by soil washing with surfactant. The soil samples of the latter were undistributed, subhumid soil collected from Tai Mei Tuk, Hong Kong. The soil samples were air-dried and screened through U.S. standard No. 10 mesh (2mm) sieve to remove coarse fragments. The fractions of organic carbon in the soil samples were determined to

be 1.039% by Shimadzu Total Organic Carbon Analyzer (model TOC-5000A). Only non-ionic surfactant (Tween 80) was used in this study due to the cationic adsorption capacity present in most soils and the advantages of using non-ionic surfactants: lower toxicity, greater biodegradability (Attwood D. and Florence A.T., 1983), and lower cmc value (1.0×10^{-5} mol/L) in field applications. The preparation of SEM was to add 50 mL of 10 mM of Tween 80 to the tube containing pre-weighted soil sample. The tube was then sealed with a Teflon-lined screw cap, and shaken in a mechanical rotary shaker at 20°C for 24 hrs. After the partitions reached equilibrium, the suspensions were centrifuged for 1.5 hrs at 2500 rpm to separate the solid particles from the soluble materials. The supernatant (surfactant-soluble humic material, which hereafter defined as "soil extracted material (SEM)") was collected and used in the experiments by expressing its concentration as "weight of dehydrated total solid of supernatant/volume of solution".

Humic materials substances consist of a heterogeneous mixture of compounds for which no single structural formula will suffice. In fact, extracted humic materials are different from place to place. Therefore, no unique exact value could be represented the molecular weight of the extracted humics. Some researcher (Stevenson F.J., 1982) proposed that the molecular weight of humics are ranged from 2000 (fulvic acids) to 300000 (humins). Based on this point, a medium value of 150000 was used as the molecular weight in our quenching calculation.

3.2.5. Other chemical

Acetone, methanol and acetonitrile were HPLC grade, used without further purification and purchased from Aldrich. Sodium carbonate and sodium borohydride were prepared by dissolving defined amount of powder in distilled/deionized water.

3.3. Experiments and Dye's Quantitative Analysis:

3.3.1. Ozonation of Aromatic Dyes:

All experiments were carried out in a 500 mL cylindrical contact tower (300 mm x 170 mm ID), as shown in Figure 11. The ozone was generated from the ozone generator Dwyer Model-2001 (manufactured by the Jelight Co. Ltd. CA, USA) and driven by an air pump with adjustable flow rates. The ozone-oxygen mixture was then fed into the contact tower through a porous plate gas sparer located at the tower's base. 500 mL of dye solution was used during each batch ozonation. A mechanical stirrer worked with the gas diffuser to achieve sufficient recirculation of the dye solution, so a favorable gas transfer rate was expected (Lin S.H., 1993).

Different purified dye concentrations (14.4, 7.2, and 3.6 x 10^{-2} mmol/L) and saturated ozone concentrations in excess (by adjusting air-flow rate) were applied to investigate the reaction kinetics of dye ozonation. Samples were collected from the contact tower at times of 0, 5, 15, 30, 60, 120 and 180 minutes, then the residual dyes were analyzed by HPLC for quantification. Three initial pH values of 4, 7 and 10 adjusted by sulphuric acid or sodium hydroxide were used to examine the consequence of the initial pH values on the overall reaction rates.

Free radical scavengers - carbonate was selected in order to determine the effect of the free radical scavenger. Therefore, 0.5 M of sodium carbonate (Na_2CO_3) was added to the reaction mixture for quenching test.

All of the samples were analyzed by HPLC, comprising a pump, a 150 mm x 4.6 mm ID Supelcosil LC-SAX (5 micron) column, and a WATERS 486 UV/VIS detector, which is capable of measuring the absorbance of light, ranging from 200 to 600 nm. The mobile phase was 65% acetonitrile with 35% water (for hydrophilic dyes) and 80% methanol with 20% water (for hydrophobic dyes). In addition, a spectrophotometer Spectronic

Genesys™ was also used to scan the dye spectra (at 3 nm intervals) and determine the ozone concentration of the samples.

a. Ozone quantitative analysis

Ozone concentration, or more precisely the total oxidants in the ozonation system, were investigated. The dissolving of ozone into water was found to be kinetically controlled. Fast zero-order dissolution was observed before the system reached a saturated ozone concentration (O_{sat}). The changing of the ozone concentration and the final O_{sat} in a clean water system under various pH values at different air flowrates were determined by the idometric method based on the spectrometric method proposed by Hana S. (1973).

- Calibration curve: The calibration curve is a standard curve of absorbance against iodine (or ozone) concentration and is plotted from readings of a series of freshly prepared standards. The iodine reagent was prepared by obtaining a solution of iodine 4×10^{-5} N (1mL = 0.96 μg ozone). Different portions of this solution are transferred to test tubes and diluted with 5% (w/w) neutral potassium iodide reagent to 10 mL final volume. After the mixing, reading of absorbance at 352 nm was taken immediately by using distilled water as the reference.

- Ozone measurement: Ozone reacts with the neutral potassium iodide solution and liberates iodine and in an excess of potassium iodide, iodine is in the complex triiodide form. The concentration of triiodide liberated was determined spectrophotometrically at a wavelength of 352 nm. By adding 5 mL of sample into a sample vial with 5 mL of 2% neutral potassium solution, a yellow colour was developed. After 30 minutes, measurement of the absorbance at 352 nm was compared with calibration curve to obtain the aqueous ozone concentration.

3.3.2. Photodegradation of Aromatic Dyes:

a. Preliminary test:

Photodegradation of sixteen commercial aromatic dyes: Experiments were carried out with a Rayonet™ photochemical reactor RPR-200 with a merry-go-round apparatus, manufactured by The Southern New England Ultraviolet Company. A schematic of this reactor is given in Figure 12. The merry-go-round rotates at a speed of 5 rpm, so that all the cuvettes could receive the same intensity of photons. Phosphor-coated low pressure mercury lamps emitting monochromatic light at 253.7 nm were used in all experiments. In this preliminary test, only six lamps were applied (power consumption is 17.5 watt), and the light intensity at 1.5 inches from the lamps was about 10500 μ watt/cm^2 (Light intensity: 1.2 x 10^{-5} Einstein$L^{-1}s^{-1}$) (Rabek J.K., 1982).

The stock solution of each dye was prepared as 20 mg/L except those insoluble ones. All the samples were put into the rotating merry-go-round in which they were exposed to same amount of UV light. 2 ml samples were removed from each quartz tube at pre-determined time. The samples were analyzed under the respective absorption λ_{max} for each dye by a Milton Roy UV-Visible spectrophotometer, model Spectronic Genesys-2.

b. Further test

Photodegradation of six purified aromatic dyes: All experiments were carried out in 10 mL cylindrical quartz cuvettes also placed in an RPR-200 Rayonet photochemical. Light sources were twelve 253.7 nm phosphor-coated low-pressure mercury lamps with a total power consumption of 400 watts. The light intensity at 1.5 inches from the lamps was about 21000 μ watt/cm^2 (Light intensity: 2.4 x 10^{-5} Einstein $L^{-1}s^{-1}$) (Rabek J.K., 1982). The purified dyes were prepared at 50 mg/L, and were placed into the rotating merry-go-round photoreactor in which the cuvettes were exposed to same amount of UV light during the reaction. Samples were collected from each quartz cuvette at time 0, 15, 30, 60, 150, 240. 300 and 360 minutes, and then they were analysed by HPLC and/or UV-

Visible spectrophotometer for quantification.

All the samples were analysed by a HPLC comprising a pump, a 250 mm x 4.6 mm ID Supelcosil LC-SAX (5 micron) column, and a ISCO V^4 Variable Wavelength UV/VIS detector which is capable of measuring the absorbance of light ranging from 190 to 750 nm. The mobile phase was 65% acetonitrile with 35% water (for hydrophilic dyes) and 80% methanol with 20% water (for hydrophobic dyes). In addition, a spectrophotometer Spectronic (R) Genesys TM was also used to scan the spectra of the tested samples at 3 nm intervals.

3.3.3. Photodegradation of Chlorinated Aromatic Dyes (CADs) in micelle

The CAD in the surfactant micelle was prepared by spreading 1 mL of 1 mmol/L dye solution (prepared in acetone) to each 50 mL Pyrex glass tube and air-dried so that the dye was evenly coated onto the tube wall. Various amounts of stock surfactant solution and additives (if any) were added to each tube and diluted by distilled and deionized water to a predetermined concentration with a final volume of 25 mL. Samples were then mixed with the solution, sealed with a Teflon-lined screw cap, and shaken in a mechanical rotary shaker at 20°C for 24 hrs. Different initial pH levels were adjusted by sulphuric acid or sodium hydroxide so that the consequence of initial pH to the overall reaction rates can be realised.

All photolysis experiments were carried out in 10 mL cylinderical quartz cuvettes placed in an RPR-200 Rayonet photochemical reactor. The light intensity at 1.5 inches from the lamps was about 21000 μwatt/cm^2 (Light intensity: 2.4×10^{-5} Einstein $L^{-1}s^{-1}$). (Rabek J.K., 1982) The prepared DR samples were placed into the rotating merry-go-round photoreactor in which the cuvettes were exposed to same amount of UV light during the reaction.

Samples were collected from each quartz cuvette at time 0, 2.5, 5, 15, 30, 45, 60, 90, 120 minutes, and then they were analysed by a HPLC comprising a pump, a 250 mm x 4.6

mm ID Supelcosil LC-SAX (5 micron) column, and a WATERS 486 UV/VIS detector, which is capable of measuring the absorbance of light, ranging from 200 to 600 nm. The mobile phase was 80% methanol with 20% water. In addition, a spectrophotometer Spectronic (R) Genesys TM was also used to scan the spectra of the tested samples and the decolouration of the sample at 3 nm intervals. Moreover, chloride ion released from the photoreduction of DR was also analysed by HPLC with 150 mm Allsap Arison Column connected with a conductivity detector Alltech ERIS™ 1000HP Autosuppressor to determine chloride ion concentrations of the aqueous samples. The eluant was 0.85 mM $NaHCO_3$/0.9 mMNa_2CO_3.

3.4. Data Analysis

In order to quantitatively characterize the photochemical reaction, several mathematical procedures were performed. These included 1) Determination of pseudo first-order rate constants and quantum yields and 2) Stern-Volmer analysis of photochemical kinetics (quenching and rate enhancement study by humic materials).

3.4.1. Quantum yield determination

For photo-dechlorination of DR in micellar systems, pseudo first-order decay of DR is generally observed at constant temperature, light intensity, and illumination wavelength:

$$P_t=P_o e^{-kpt} \qquad (52)$$

where P_t= the concentration of DR at time t, mol/L

P_o = the concentration of DR at time zero, mol/L

k_p = the first order decay rate constant, s^{-1}

The quantum yield for decay using a monochromic light source, therefore, can be calculated from the experimental first order decay rate constant (Choudhry G.G. and Webester C.R.B., 1987):

$$\phi_p = \frac{k_p}{2.303 I_{\lambda o} \varepsilon_{p\lambda} I} \tag{53}$$

ϕ_p = quantum yield for the disappearance of DR molecules.

$I_{\lambda o}$ = intensity of the incident light at wavelength λ, Einstein $L^{-1}s^{-1}$.

$\varepsilon_{p\lambda}$ = molar absorptivity of DR at wavelength λ, L/mole-cm.

l = cell path length within the reactor, cm.

3.5. Summary of Experiments

The experiments conducted in this research are summarized from Table 8 to Table 12 and all experimental data are listed in the Appendix A, B, C and D.

3.5.1. Ozonation of Aromatic Dyes:

Table 8: Ozonation of Aromatic Dyes:

Exp. No	Probe compound	(mg/L)	Dye/Ozone Ratio	pH	Additive	Remark
O1-1	A1	44.98	0.42	4		pH effect
O1-2	A1	97.91	0.80	7		Dye/ozone effect
O1-3	A1	45.98	0.40	7		pH & Dye/ozone effect
O1-4	A1	21.99	0.20	7		Dye/ozone effect
O1-5	A1	44.68	0.38	10		pH effect
O2-1	A2	22.30	0.42	4		pH effect
O2-2	A2	22.21	0.40	7		pH effect
O2-3	A2	22.69	0.38	10		pH effect
O3-1	AZ2	70.32	0.42	4		pH effect
O3-2	AZ2	140.00	0.80	7		Dye/ozone effect
O3-3	AZ2	69.98	0.40	7		pH &Dye/ozone effect
O3-4	AZ2	35.23	0.20	7		Dye/ozone effect
O3-5	AZ2	68.99	0.38	10		pH effect
O4-1	AZ3	92.62	0.42	4		pH effect
O4-2	AZ3	180.23	0.80	7		Dye/ozone effect
O4-3	AZ3	93.05	0.40	7		pH & Dye/ozone effect
O4-4	AZ3	47.02	0.20	7		Dye/ozone effect
O4-5	AZ3	91.89	0.38	10		pH effect
O5-1	AZ5	98.84	0.42	4		pH effect
O5-2	AZ5	97.89	0.40	7		pH effect
O5-3	AZ5	98.59	0.38	10		pH effect
O5-4	AZ5	97.90	0.38	11	Na_2CO_3 (0.5M)	quenching effect
O6-1	AM1	57.83	0.42	4		pH effect
O6-2	AM1	57.45	0.40	7		pH effect
O6-3	AM1	56.98	0.35	10		pH effect

A1: Soluble Anthraquinone
A2: Insoluble Anthraquinone
AZ2: Disazo Vinylsulphonate
AZ3: Triazo
AZ5: Polyazo
AM1: Monoazo (Cu Vinylsulphonate)

3.5.2. Photodegradation of Aromatic Dyes: Preliminary test

Table 9: Photodegradation of Aromatic Dyes (Preliminary test)

Exp. No	Probe compound	concentration (g/L)	Dye class
P1	Cyanine	20	Basic
P2	Thiocyanine	20	Basic
P3	Anthraquinone	≈ 5	Vat
P4	Anthraquinone	≈ 5	Vat
P5	Anthraquinone	≈ 5	Disperse
P6	Anthraquinone	20	Reactive
P7	Monoazo	≈ 5	Disperse
P8	Monoazo	≈ 5	Disperse
P9	Monoazo	20	Acid
P10	Diazo	20	Reactive
P11	Triazo	20	Direct
P12	Triazo	20	Direct
P13	Polyazo	20	Direct
P14	Cu Monoazo	20	Reactive
P15	Cr Monoazo	20	Metal-complex
P16	Stilbene	20	Direct

3.5.3. Photodegradation of Aromatic Dyes: Further test

Table 10: Photodegradation of Aromatic Dyes (Further test)

Exp. no	Probe compound	(mg/L)	pH	Additive (M)		Remark
UV1-1	A1	50	4			pH effect
UV1-2	A1	50	7			pH effect
UV1-3	A1	50	10			pH effect
UV1-4	A1	50	7	acetone	0.05	photosensitization
UV2-1	A2	50	4			pH effect
UV2-2	A2	50	7			pH effect
UV2-3	A2	50	10			pH effect
UV2-4	A2	50	7	acetone	0.05	photosensitization
UV3-1	AZ2	50	4			pH effect
UV3-2	AZ2	50	7			pH effect
UV3-3	AZ2	50	10			pH effect
UV3-4	AZ2	50	7	acetone	0.05	photosensitization
UV4-1	AZ3	50	4			pH effect
UV4-2	AZ3	50	7			pH effect
UV4-3	AZ3	50	10			pH effect
UV4-4	AZ3	50	7	acetone	0.05	photosensitization
UV5-1	AZ5	50	4			pH effect
UV5-2	AZ5	50	7			pH effect
UV5-3	AZ5	50	10			pH effect
UV5-4	AZ5	50	7	acetone	0.05	photosensitization
UV5-5	AZ5	50	10	sodium carbonate	0.1	quenching effect
UV6-1	AM1	50	4			pH effect
UV6-2	AM1	50	7			pH effect
UV6-3	AM1	50	10			pH effect
UV6-4	AM1	50	7	acetone	0.05	photosensitization
UV7-1	AZ2	50	pH 7 buffer	0.08M sodium dihydrogen phosphate & 0.12M di-sodium hydrogen phosphate		pH buffer effect
UV7-2	AZ2	50	pH 10 buffer	sodium tetraborate/sodium hydroxide		pH buffer effect

A1: Soluble Anthraquinone AZ2: Disazo Vinylsulphonate AM1: Monoazo (Cu Vinylsulphonate)
A2: Insoluble Anthraquinone AZ3: Triazo AZ5: Polyazo

3.5.4. Photodegradation of Chlorinated Aromatic Dyes (CADs) in micelle

Table 11: Photodegradation of Chlorinated Aromatic Dyes (CADs) in micelle

Exp. no	Probe compound (mg/L)		Surfactant	Additive concentration (M)		Remark
S1-1	DR	12.337	Tween 20	pH 7		Surfactant type
S1-2	DR	10.838	Tween 60	pH 7		Surfactant type
S1-3	DR	10.838	Tween 80	pH 7		Surfactant type
S1-4	DR	1.458	Brij 52	pH 7		Surfactant type
S1-5	DR	1.044	D.I water	pH 7		Control
S2-1	DR	5.863	Tween 80	pH 7		solute concentration
S2-2	DR	18.674	Tween 80	pH 7		solute concentration
S-3	DR	10.838	Tween 80	pH 5.6		H^+ & Cl^- analysis
S4-1	DR	10.695	Tween 80	pH 5.5		pH effect
S4-2	DR	11.621	Tween 80	pH 10		pH effect
S5-1	DR	11.445	Tween 80	hydrogen source ($NaBH_4$)	0.001	Hydrogen source
S5-2	DR	12.769	Tween 80	hydrogen source ($NaBH_4$)	0.01	Hydrogen source
S5-3	DR	12.031	Tween 80	hydrogen source ($NaBH_4$)	0.05	Hydrogen source
S5-4	DR	11.953	Tween 80	hydrogen source ($NaBH_4$)	0.1	Hydrogen source
S6-1	DR	12.949	Tween 20	acetone	0.034	Photosensitization
S6-2	DR	13.275	Tween 20	acetone	0.68	Photosensitization
S6-3	DR	13.004	Tween 20	acetone	2.04	Photosensitization
S6-4	DR	13.389	Tween 20	acetone	3.5	Photosensitization
S6-5	DR	14.024	Tween 20	acetone	4.5	Photosensitization
S6-6	DR	13.473	Tween 20	acetone	6	Photosensitization

3.5.5. Photodegradation of Chlorinated Aromatic Dyes (CADs) in micelle with the presence of humic materials

Table 12: Photodegradation of Chlorinated Aromatic Dyes (CADs) in micelle with the presence of humic materials

Exp. No	Probe compound (mg/L)		Surfactant	Additive concentration (μmol/L)		Remark
H1-2	DR	10.338	Tween 80	soil extracted material	0.40	effect of soil extracted material
H1-3	DR	10.278	Tween 80	soil extracted material	0.65	effect of soil extracted material
H1-4	DR	10.19	Tween 80	soil extracted material	1.19	effect of soil extracted material
H1-5	DR	10.18	Tween 80	soil extracted material	1.98	effect of soil extracted material
H1-6	DR	9.677	Tween 80	soil extracted material	2.97	effect of soil extracted material
H1-7	DR	9.598	Tween 80	soil extracted material	3.96	effect of soil extracted material
H1-8	DR	9.26	Tween 80	soil extracted material	4.94	effect of soil extracted material
H1-9	DR	9.216	Tween 80	soil extracted material	5.93	effect of soil extracted material
H1-10	DR	9.175	Tween 80	soil extracted material	6.59	effect of soil extracted material
H2-1	DR	10.283	Tween 80	humic acids	0.017	effect of humic materials
H2-2	DR	10.797	Tween 80	humic acids	0.027	effect of humic materials
H2-3	DR	10.701	Tween 80	humic acids	0.033	effect of humic materials

H2-4	DR	10.608	Tween 80	humic acids	0.044	effect of humic materials
H2-5	DR	10.711	Tween 80	humic acids	0.089	effect of humic materials
H2-6	DR	10.271	Tween 80	humic acids	0.177	effect of humic materials
H2-7	DR	10.097	Tween 80	humic acids	0.440	effect of humic materials

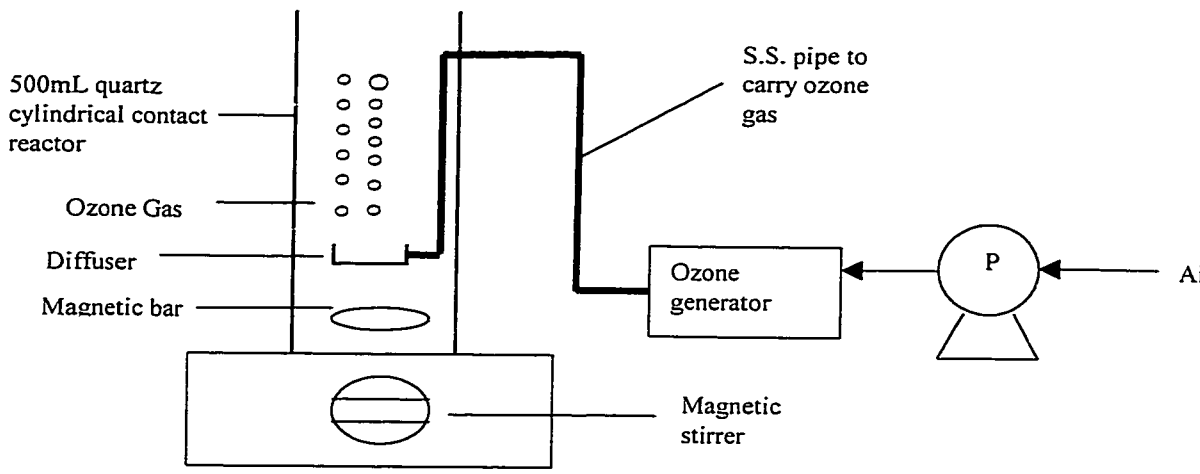

Figure 11: Diagram of ozonation system

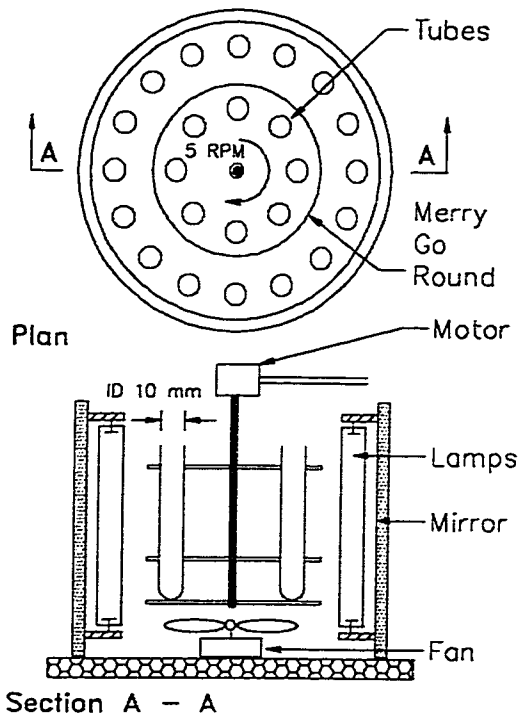

Figure 12. The Rayonet photochemical reactor

CHAPTER 4: RESULTS & DISCUSSION
ADVANCED CHEMICAL OXIDATION (ACO) TREATMENT OF DYE WASTEWATER – OZONATION OF AROMATIC DYES

4.1. Ozonation of Aromatic Dyes:

4.1.1. The Mass Transfer of Ozone

Saturated ozone concentrations in excess were applied to investigate the reaction kinetics of dye ozonation. Three initial pH levels of 4, 7 and 10 adjusted by sulphuric acid or sodium hydroxide were used to examine the consequence of the initial pH levels to the overall reaction rates.

Ozone concentrations, or more precisely the total oxidants in the ozonation system, were investigated. The dissolving of ozone into water was found to be kinetically controlled. Fast zero-order dissolution was observed before the system reached a saturated ozone concentration (O_{sat}). The changing of ozone concentration and final O_{sat} in a clean water system under various pH values at different air flowrates were reported in Figure 13. The concentration of the ozone in water was determined by the spectrometric method (Hana S., 1973). The over-saturation of ozone in the system was not significant because the reactor was designed as an open system. The rate constant of dissolution (in zero-order), K_{O3} and O_{sat} at various pH levels and air flowrates are demonstrated in Figure 14. In general, the K_{O3} and O_{sat} were proportional to the air flowrate that was pumped into the ozone generator and the reactor. By increasing the flowrate of the supplied air, the K_{O3} and O_{sat} in the system would increase because more ozone was generated and transferred into the reactor. Therefore, higher O_{sat} at steady state resulted in an open system, while the ozone input equals to the output (*i.e.* self-decay plus escape to the atmosphere). The pH of the solution will alter the chemical composition of ozone; for example hydroxyl free radicals were formed from ozone decomposition at high pH, while the molecular ozone remains as the main oxidant at a low pH. Since hydroxyl radicals have a higher oxidizing

ability than that of ozone, higher O_{sat} and K_{O3} were observed at a high pH than with low or neutral pH levels at a constant air flowrate.

4.1.2. Reaction Kinetics of Ozonation

The reaction kinetics of ozonation can be determined after the O_{sat} is reached, and the resistance of the ozone transfer from gas phase to liquid phase becomes insignificant where the concentrations of ozone are uniform in the liquid. In this case, the ozone consumption rate is determined solely by the rate of chemical reaction in the bulk (Charpentier, 1981). The reaction kinetics of dye ozonation, therefore, was studied under this circumstance, and the rate constants of dye decay were determined at various initial dye concentrations and pHs. From Figure 15, the results of dye ozonation at different pHs have shown that the reaction followed a pseudo first-order reaction. Since the oxidizing ability of ozone comes from either molecular ozone or hydroxyl free radicals, the rate of dye disappearance can be formulated as follows:

$$-\frac{d[D]}{dt} = k_o[D][O_3] + k_{OH}[D][\cdot OH] \tag{54}$$

where [D] is the concentration of dye in the solution, $[O_3]$ and $[^{\cdot}OH]$ are the concentrations of ozone and hydroxyl radicals, and k_o and k_{OH} are the respective kinetic rate constants. In this study, since the ozone was offered in excess, the hydroxyl free radicals and ozone concentration in the solution are presumably close to constants (i.e. at steady state). Therefore, eq. 54 can be rearranged to the pseudo first-order equation as eq. 55, where the k is the overall or pseudo first-order rate constant.

$$\frac{d[D]}{dt} = -(k_o[O_3] + k_{OH}[OH\cdot])[D] = -k[D] \tag{55}$$

To verify the involvement of free radical reactions in dye ozonation at a high pH, a quenching test was conducted by the use of carbonate as the free radical scavenger (Hoigen J. and Bader H., 1976). The results of the quenching effect is shown in Figure 16,

where it is seen that the presence of a free radical scavenger can depress the ozonation rate by 40%. This observation confirms the involvement of the free-radical chain mechanism. The pseudo first-order rate constants for soluble Anthraquinone at different initial dye concentrations were therefore determined and demonstrated in Figure 17. Eq. 55 was further studied by changing the dye/ozone ratio. As demonstrated in Figure 17, three different dyes (A1, AZ2 and AZ3) with different initial concentrations (14.4, 7.2 and 3.6×10^{-2} mmol/L) were used to study the effect of initial dye concentration in ozonation. It was found that the pseudo first-order rate constants decreased as the dye/ozone ratio increased; this observation confirmed our assumption in eq. 55. When dye/ozone ratio is increased, the ozone concentration has a lower chance to present in excess, resulting in the term of $(k_o[O_3] + k_{OH}[OH\cdot])$ in eq. 55 being actually reduced. Nevertheless, there is not a linear relationship between the reaction rate constant k and the Dye/Ozone molar ratio. Since some intermediate products of ozonation may also catalyze the formation of hydroxyl free radicals (thus increasing the ozonation reaction), and this effect may be strengthened at high ozone concentration (Carriere J. *et al.*, 1991).

4.1.3. Effect of Initial pH

The ozonation of dyes at various initial pH levels (4, 7 and 10) were also examined, and is shown in Figure 18. The pseudo first-order rate constants of ozonation of all selected dyes varied from 5.2×10^{-4} to 1.2×10^{-4} s^{-1} at pH 4, 1.5×10^{-4} to 5.1×10^{-4} s^{-1} at pH 7, and 1.1×10^{-4} to 6.3×10^{-4} s^{-1} at pH 10, respectively, as shown in Figure 18. The decay rates of azo dyes were found to increase with the increment of the pH, and the solution pH decreased during ozonation. In general, ozone oxidation pathways include direct oxidation by ozone or radical oxidation by ·OH radical. Direct oxidation is more selective and predominates under acidic conditions, while radical oxidation is less selective and predominates under basic conditions. Since the oxidation potential of hydroxyl radicals is much higher than that of the ozone molecule, direct oxidation is slower than radical oxidation.

The increase in solution pH did not show a positive enhancement of the ozone oxidation of the two anthraquinone dyes (A1 and A2); instead, lowering the solution pH can lead to a higher reaction rate. Four possible reasons may be helpful in explanation:

a. It is already known that anthraquinone dye contains a rigid structure that is insensitive to oxidation reaction (Chu W. and Ma C.W., 1998), so the ozonation mechanism may not be the dominant process for the dye's decomposition.

b. Anthraquinone may change to leuco-form (less coloured) in an acidic medium, which will reduce its colour content (Chu W. and Ma C.W., 1997).

c. The amine groups ($-NH_2$) on anthraquinone dyes can be ionized into ($-NH_3^+$) at a low pH, which can promote the solubility of the dye. If we compare the dyes' solubility with their ozonation decay rates from neutral to alkali pH, the order of solubility (from Table 6) exactly matches the order of rates (from Figure 18). That is, insoluble anthraquinone (A2) < triazo (AZ3) < polyazo (AZ5) < soluble anthraquinone (A1) < disazo (AZ2) < Cu monoazo (AM1). The results justify the presumption that the rate of dye decomposition by ozone strongly depended on the solubility of the dyes.

d. In high pH, a sudden drop of decay rate was observed at an initial pH of 10. With respect to the chemical structure of A1 & A2, substituent of an electron-donating group such as $-NH_2$ in the α-positions to the carbonyl group are capable of forming an intramolecular hydrogen bond at high pH levels (Zollinger H., 1961 & Rys P. and Zollinger H., 1972). Therefore, the dye structure of A1 & A2 becomes chemically stable at high pH ranges. The chromophores of A1 & A2 remain intact even after the ozonation and therefore greatly reduce the decay rate.

Therefore, the characteristics of anthraquinone dye (insensible structure for oxidation, leuco-form, and higher solubility) contribute a slightly higher ozonation rate at a low pH.

4.1.4. Quantitative Prediction

By applying the pseudo steady state conditions to the free radicals, the concentration of hydroxyl radicals can be estimated by: (Benitez F.J., 1994)

$$[OH\cdot] = \frac{3k_{OOH}[O_3][OH^-]}{k_{OH}[D]} \tag{56}$$

where k_{OOH} is the kinetic rate constant for the formation of free radical $\cdot OOH^-$ from ozone decomposition at a high pH: (Staehelin J. and Hoigne J., 1982)

$$O_3 + OH^- \rightarrow \cdot OOH^- + O_2\cdot \tag{57}$$

From eq. 56, more hydroxyl radicals are generated by ozone decomposition in aqueous solutions at a high pH because hydroxide ions may act as a catalyst. By substituting eq. 56 to eq. 54, the oxidation rate of dye decomposition can be obtained:

$$-\frac{d[D]}{dt} = k_o[D][O_3] + 3k_{OOH}[O_3][OH^-] \tag{58}$$

Since the source of the hydroxyl radical is coming from the self-decomposition of ozone, the rate of self-decomposition is therefore closely related to the ozone consumed by the dye decomposition reaction. This phenomenon is foreseen by eq. 58, where the rates of dye decay are proportional to the ozone and hydroxyl ion concentrations. Based on our observation, the ozonation of dyes is dominated by the pseudo first-order reaction, so eq. 58 can be restated as:

$$-\frac{d[D]}{dt} = k[D] = k_o[O_3][D] + 3k_{OOH}[O_3][OH^-] = a_1[D] + a_2[OH^-] \tag{59}$$

where k is the overall (pseudo first-order) rate constant, and a_1 and a_2 are coefficients equivalent to $k_o[O_3]$ and $3k_{OOH}[O_3]$. The first term in eq. 59 stands for the pathway of

direct ozone oxidation, and the second term represents the indirect free radical oxidation. As the $[O_3]$ concentration is maintained at a constant, or overdosed at O_{sat} (*i.e.* the situation in this study), the a_1 and a_2 both become constants. By using multiple linear regression and initial rate assumption (*i.e.* initial rate = $k[D]_0$), we can determine the respective coefficients a_1 and a_2 for each selected dye summarized in Table 13. From the ratio of a_1/a_2, we can also figure out the term $3k_{OOH}/k_o$ which indicates the contribution (or weighting) of two parallel pathways (*i.e.* through direct or indirect pathways in eq. 59 in the overall reaction). In general, the decay of all azo dyes (AZ2, AZ3, AZ5, and AM1) at low pH levels is mainly dominated by the direct ozone oxidation, because the ratios of $3k_{OOH}/k_o$ are all less than one, ranging from 0.08 to 0.39. However, at high pH levels, the free radical oxidation may become dominant if the product of a_2 by $[OH^-]$ is higher than that of a_1 by [D]. In addition, the higher overall rates of those dyes carrying higher water solubility were observed. This can be explained by the increment of direct ozonation (i.e. first term in the eq. 59) if the soluble form of the dye (*i.e.* [D]) increases. On the other hand, an increase in pH can improve the dye decay rate because of the associated effects from the $3k_{OOH}$ and the high $[OH^-]$ concentration in the second term, resulting in a significant decay pathway by free radical oxidation. For anthraquinone dyes (A1 and A2), negative values of a_2 are resulted from the analysis of multiple linear regression, as listed in Table 13. The negative sign of a_2 ($3k_{OOH}[O_3]$) indicates that, as the pH increases, the dye decay rate will decrease, which agrees with our observation (Figure 18).

For prediction purposes, the term $\Delta k/\Delta pH$, which was determined from the slopes in Figure 18, has been correlated to the $3k_{OOH}/k_o$ in Table 13, which results in a good linear relationship, as shown in Figure 19. Therefore, The ratio of $3k_{OOH}/k_o$ (*i.e.* the contribution of two parallel pathways) becomes predictable if the change of the overall reaction rate k at various initial solution pHs ($\Delta k/\Delta pH$) is predetermined.

Table 13: The analysis of constants k_o, k_{OOH} and k.
(The initial concentration of all dyes is 0.072 mmol/L)

Dyes	$3k_{OOH}[O_3]$ (s^{-1})	$k_o[O_3]$ (s^{-1})	$3k_{OOH}/k_o$	$\Delta k/\Delta[OH^-]$ ($L\ h^{-1}mol^{-1}$)
AZ2	1.46×10^{-4}	3.80×10^{-4}	0.38	3.85E-05
AZ3	5.95×10^{-5}	1.55×10^{-4}	0.38	1.92E-05
AM1	8.86×10^{-5}	5.33×10^{-4}	0.17	2.05E-05
AZ5	1.80×10^{-5}	2.35×10^{-4}	0.08	4.17E-06
A1	-1.51×10^{-5}	3.41×10^{-4}	-0.04	-5.67E-06
A2	-3.96×10^{-5}	1.75×10^{-4}	-0.23	-1.17E-05

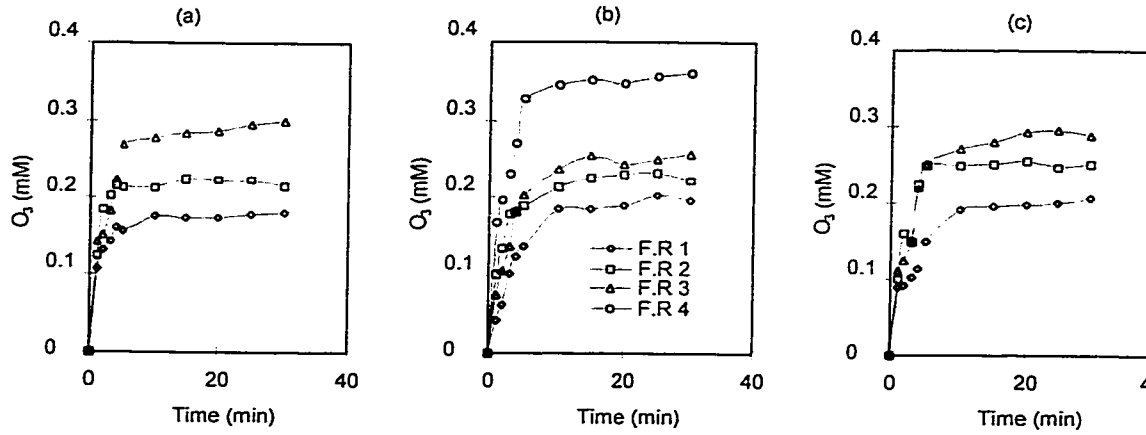

Figure 13: Ozone concentration at different pHs - (a) pH 4, (b) pH 7 and (c) pH 10 under different air input flowrates. F.R. 1, F.R. 2, F.R. 3 and F.R. 4 indicate air flowrate at 1, 2, 3 and 4 L/min, respectively.

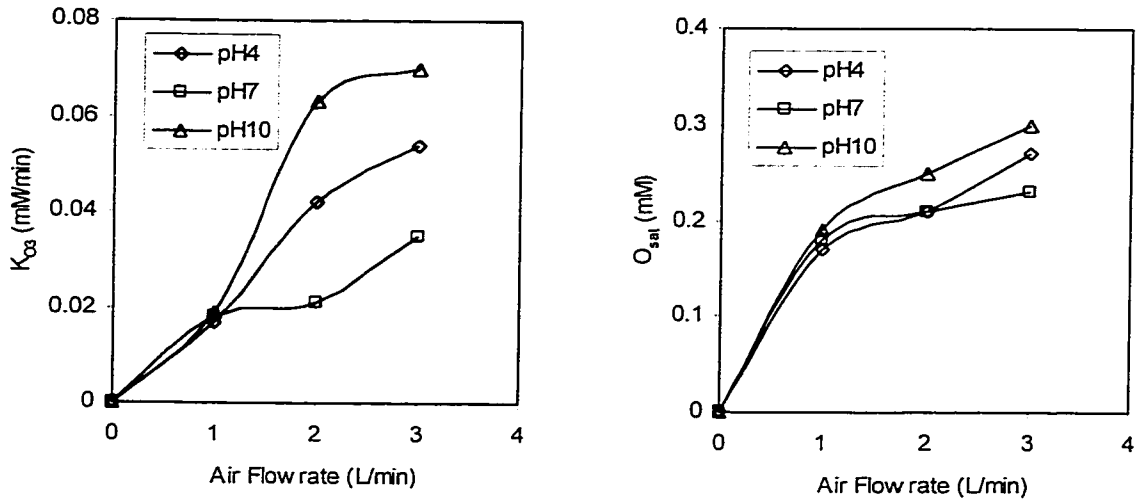

Figure 14: The rate of ozone transfer from the gaseous phase to the aqueous phase (Left); and the amount of the saturated ozone at different pHs and flowrates (Right). Where K_{O3} (in mmol/L/min) is the rate of the ozone transfer from the gaseous phase to the aqueous phase and O_{sat} (in mmol/L) is the saturated ozone concentration.

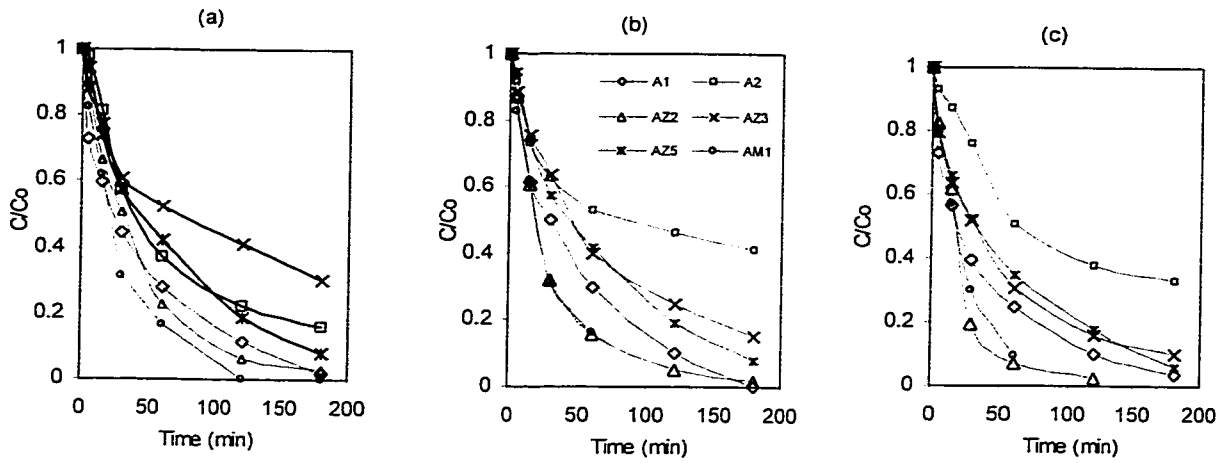

Figure 15: The pseudo first-order decay of dye ozonation at different initial pHs - (a) pH 4, (b) pH 7 and (c) pH10. Six purified dye (initial concentrations - 7.2 x 10^{-2} mmol/L) under saturated ozone concentrations (in excess) were applied to investigate the reaction kinetics.

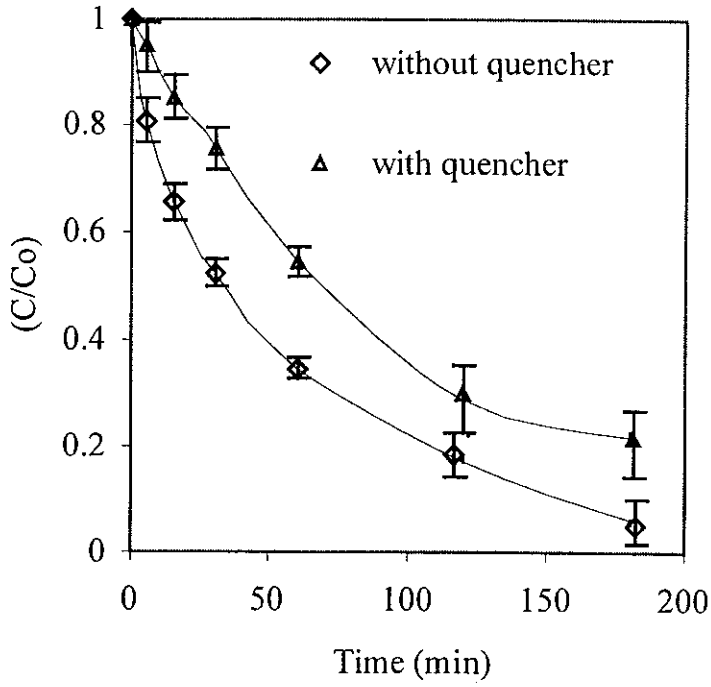

Figure 16: Quenching of free radical reaction in ozonation of Polyazo dye AZ5 (initial concentrations - 7.2 x 10^{-2} mmol/L) at pH 10. A quencher, 0.5 M of sodium carbonate (Na_2CO_3) was added to the reaction mixture.

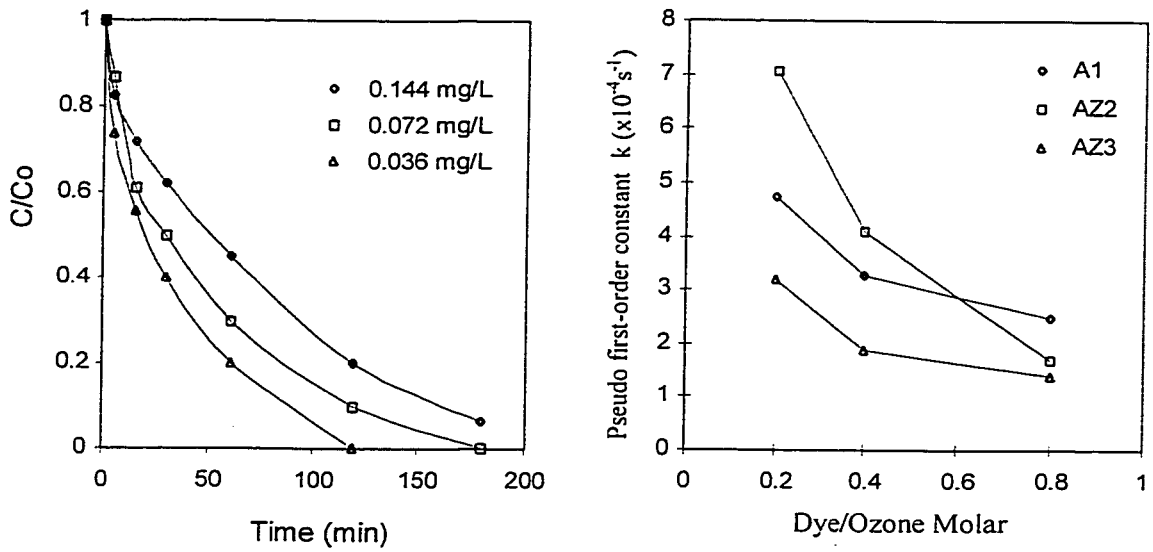

Figure 17: Pseudo first-order decay of A1 at different initial dye concentrations (mmol/L) (Left); Ozonation of three different dyes at various dye/ozone ratios (Right). Three purified dye concentrations (14.4, 7.2, and 3.6 x 10^{-2} mmol/L) under saturated ozone concentrations (in excess) were applied to investigate the reaction kinetics of dye ozonation.

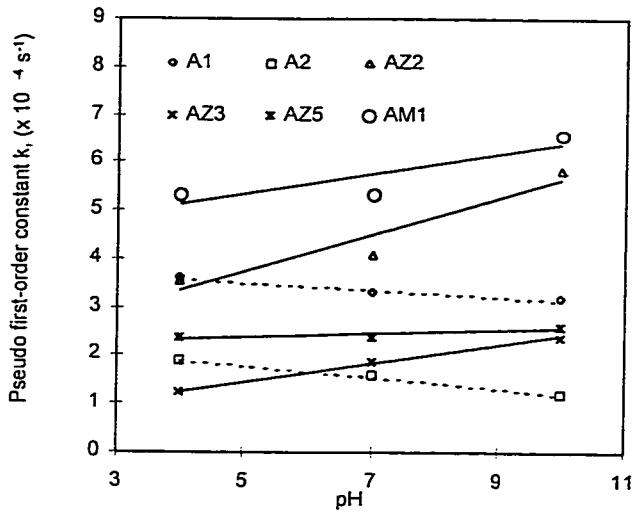

Figure 18: Variation of pseudo first-order rate constants at different pH: Six purified dye concentrations (7.2 x 10^{-2} mmol/L) under saturated ozone concentrations (in excess) were applied to investigate the reaction kinetics of dye ozonation at different initial pH.

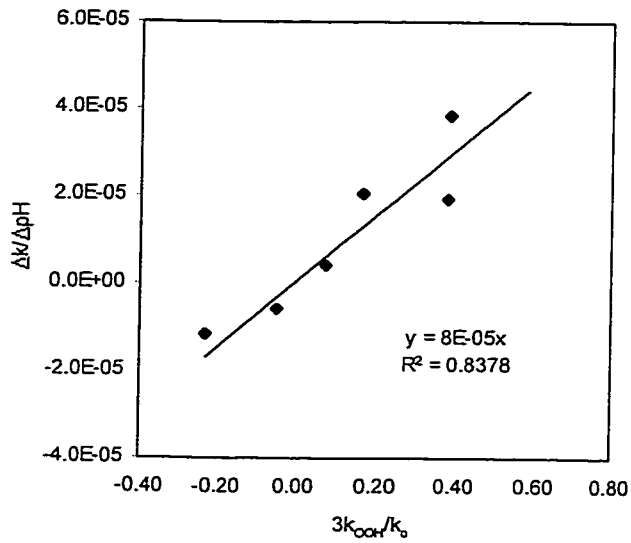

Figure 19: The correlation between $\Delta k/\Delta pH$ vs. $3k_{OOH}/k_o$

CHAPTER 5: RESULTS AND DISCUSSION ADVANCED CHEMICAL OXIDATION (ACO) TREATMENT OF DYE WASTEWATER: PHOTODEGRADATION OF AROMATIC DYES

5.1. Preliminary Test

Totally 16 different dyes were used without purification in this preliminary test including 4 anthraquinone dyes, 7 azo dyes, 2 metal containing (Copper and Chromium) azo dyes, 2 cyanine dyes and 1 stilbene azo dye. Dyes were UV-irradiated under UV light at 253.7 nm.

After 10 hours of UV illumination, almost all the samples (except sample 15) in Figure 8 showed a drop in their colour contents, which were quantified by the absorbance at λ_{max}. From the result, the degrees of the colour removal by the UV-irradiation can be ranked in the following ascending order:

> anthraquinone vat & disperse dye < monoazo disperse dye < Cr containing monoazo dye < anthraquinone reactive dye < Cu containing monoazo dye < monoazo basic dye < cyanine basic dye < stilbene azo direct dye < diazo reactive dye < triazo direct dye < polyazo direct dye

Judging from the colour removal efficiencies indicated in Table 14, the solubility of the dye molecules was the dominant parameter for the photodecomposition. Anthraquinone dyes were UV intact due to their chemical structure (Leaver I.H., 1980). Nevertheless, the results from samples 3 to 6 suggested that the solubility was another critical factor to hinder their UV decomposition. The sulphonate anthraquinone reactive dye (sample 6 in figure 8), for example, had a much greater colour removal rate in the experiment (36.8%)

compared with other anthraquinone dyes (from -35.3% to 8.0%). It was solely due to the high solubility of sulphonate anthraquinone reactive dyes since all the anthraquinone dyes had similar chemical structures. We also found that the cationic dyes (sample 1 and 2 in figure 8) which carried positive charges in a solution could easily be decolourized.

Table 14: The results of colour removal of 16 commercial dyes by UV-irradiation

No	Chromophore	Dye class*	Solubility (g/L)	λ_{max}	Colour removal (%) 5th hour	10th hour
1	Cyanine	Basic	5	412	61.8	70.0
2	Thiocyanine	Basic	80	607	67.9	79.6
3	Anthraquinone	Vat	< 1	415	-3.8	8.0
4	Anthraquinone	Vat	< 1	613	-0.4	1.3
5	Anthraquinone	Disperse	< 1	688	-15.0	-35.3
6	Anthraquinone	Reactive	100	589	26.3	36.8
7	Monoazo	Disperse	< 1	409	3.0	17.9
8	Monoazo	Disperse	< 1	550	-1.5	8.0
9	Monoazo	Acid	80	412	64.8	76.2
10	Diazo	Reactive	100	598	72.0	98.0
11	Triazo	Direct	20~30	604	73.0	88.0
12	Triazo	Direct	20~30	589	72.6	97.5
13	Polyazo	Direct	20~30	529	68.5	97.6
14	Cu Monoazo	Reactive	100	559	43.4	56.6
15	Cr Monoazo	Metal-complex	60	595	12.9	20.0
16	Stilbene	Direct	20~30	400	19.6	84.6

* Based on the substitute groups added to the dye molecules.

The effect of solubility to the photodecolourization rate can be interpreted by free radical mechanisms. The photo-reaction may involve photo-ionization of an upper excited molecule of the dye (D) and photo-dissociation to form a dye radical and a hydrogen atom as shown in equations (60) and (61), respectively. (Poon C. and Vittimberga B.M., 1981)

$$DH + hv \rightarrow DH^{*} \rightarrow DH^{\cdot +} + e^{-} \qquad (60)$$

$$DH + hv \rightarrow DH^{*} \rightarrow D^{\cdot} + H^{\cdot} \qquad (61)$$

In addition, it is possible that the use of commercial dyes allows the impurities in dyes act as electron donors (E) or hydrogen sources, which will make another mechanism possible (Chu W. and Javert C. T., 1994), see equation (62):

$$E + DX + hv \rightarrow E^{\cdot +} + DX^{\cdot -} \rightarrow E^{\cdot +} + D^{\cdot} + X^{-} \qquad (62)$$

The excited ions ($DH^{\cdot +}$, $DX^{\cdot -}$) and/or radicals ($D^{\cdot}$) might either go back to the original dye molecule, or undergo further reactions with other components in water such as dissolved oxygen, free H^{+}/OH^{-}, and other impurities to form colourless end products. The presence of water was used to carry the charged intermediates, which lowered the photo-ionization energy, and therefore facilitated the dye decomposition.

It was observed that certain dyes (sample 3, 4, 5 and 8 in Figure 8) showed enhanced colour contents after the exposure to UV light at the 5th hour then decolourized after a longer UV exposure (10 hours). This change of colour might be due to the low photodecay rates of these dyes (since all these dyes come with low solubilities), and the formation of some reaction intermediates carrying higher extinction coefficients (ε) during photo-reaction (all λ_{max} located in the visible range).

For azo dyes, the efficiencies of colour removal generally increase with the substituted number of azo groups. The higher the number of azo (-N=N-) group substitution in a single dye molecule, the higher the colour removal efficiency being observed (samples from 7 to 13 in Figure 8). This finding may be explained by the higher probability of azo group being attacked by photons.

Stilbene dyes (sample 16 in Figure 8) with a central carbon-carbon double bonds were readily attacked by the singlet oxygen and undergo the photodecomposition. However, Cr containing metal complex dye (sample 15 in Figure 8) could resist the 253.7 nm UV irradiation, as only 20% of colour is removed after 10 hours of irradiation.

5.2. Further Test

From the results of the preliminary test, it can be concluded that photodegradation rate was closely related to the physical and chemical characteristics of dyes. The solubility of the dye molecules was one of the dominant factors to determine the efficiency of photodegradation. The higher the dye solubility, the higher the photodegradation rates. Based on these results, a further exploration of dye photodegradation was continued.

The six selected Aromatic Dyes were irradiated in 10 mL cylindrical quartz cuvettes placed in a RPR-200 Rayonet photochemical reactor under different conditions:

i. Different initial pH of 4, 7 and 10 were used to examine the effect of initial pH to the overall reaction rates.
ii. Different pH's buffer of pH 7 & pH 10.
iii. 0.05 M acetone solution was used as a photo-sensitizer.

5.2.1. Effect of initial pH

Each dye was exposed to the UV-irradiation at initial pH of 4, 7 or 10, respectively. The decay of dye in terms of undecayed fraction C/C_0 (where C is the undecayed dye concentration at specific time interval & C_0 is the initial dye concentration) was shown in Figure 20. The decay rates of dyes are found to increase with the increase of initial pH, and the solution pH will decrease during the photodegradation process. By comparing Figures 20 and 21, the pH descending rates are accompanied by the dye descending rates, i.e. the faster the dye is decayed, the faster the pH declines. This observation implies that the variation of pH is due to the generation of H^+ or some organic acids during the photodegradation. For hydrophilic dyes, the rates of dye degradation decrease simultaneously as the $[H^+]$ concentration increases, which indicates that the acidic products may resist for further degradation. The C/C_0 of all hydrophilic dyes after 6 hours of UV illumination varies from 0.28 to 0.64 at acidic pH and 0.03 to 0.23 at alkaline pH. For the hydrophobic dye (A2), however, no significant dye degradation is observed

although its pH drops significantly. This is likely due to the photo-dechlorination (*i.e.* photoreduction) becomes the main reaction pathway. In the photo-dechlorination reaction (Chu W. and Jafvert C.T., 1994), the chloride on the benzene ring can be substituted by a proton coming from a hydrogen source (*e.g.* the impurity in the system), and hydrochloric acid (H^+/Cl^-) is released as final product, which reduces the pH of solution. During the photo-dechlorination reaction, the chromophores in the dye molecules remain intact and, therefore, slower dye decay can be observed.

5.2.2. Buffer test

Theoretically the photodecay rates of dyes in an alkaline buffered environment should be increased due to the neutralization of the generated H^+ ions in the photodegradation reaction. However, from Figure 22, there is no significant difference of rate constants between buffered and un-buffered solution at pH 7 and 10. The result suggests that the reaction rates are controlled mainly by the initial hydroxide ion concentration; once the hydroxide ions initiate a free radical reaction, the photodegradation will be continued until stable acidic products are formed.

5.2.3. Reaction kinetics of photodegradation

In order to study the reaction kinetics of the dyes' photodegradation, the rate constants of the selected dyes were determined at various pH. Figure 23 shows that the photodegradation of dyes follows pseudo first-order reactions at different initial pH. This implies that the photodegradation reaction is dominated by a similar reaction pathway. Since it is known that hydroxyl and hydroperoxyl radicals will be generated when UV is absorbed by water in the presence of oxygen (Mirat D.G. and Vatistas R., 1987), it is very likely that the photodegradation of dyes are dominated by free radical reaction in which the hydroxyl and hydroperoxyl radicals are involved. Therefore, the rate law of the dye degradation might be expressed as eq. (63)

$$d[D]/dt = -(k_{OH}[^{\cdot}OH] + k_{OOH}[^{\cdot}OOH])[D] \quad (63)$$

where [D] is the concentration of the dye in the solution, [·OH] is the concentration of hydroxyl, [·OOH] is the concentration of hydroperoxyl radicals and k_{OH} and k_{OOH} are the kinetic rate constant of dye decay contributed by the hydroxyl (·OH) and hydroperoxyl radicals (·OOH), respectively.

Since the formation of the free radicals ·OH or ·OOH solely depends on the UV light absorption, the concentration of free radicals in the solution are assumed to be closed to a constant (i.e. at steady state) as excess photons are absorbed by aqueous phase during the reaction. Therefore, the above equation could be simplified to the pseudo first-order equation in eq. 64.

$$d[D]/dt = -k[D] \quad (64)$$

The pseudo-first-order rate constants can be correlated to the initial pH of the solution as shown in the Figure 24. Higher rate constant and shorter half-life are observed as the initial pH of the solutions increase. It is probably due to the high concentration of hydroxide ions which act as precursors for the free radical formation (·OH and/or ·OOH) under the exposure of UV irradiation.

5.2.4. Free radical

To verify the presumption that the free radical reaction is dominant in the UV degradation reaction, a simple test was conducted to identify whether the free radicals are involved during the UV-irradiation. Carbonate is known as one of the effective radical scavengers (Hoigne J. and Bader M., 1976). The results of quench effect by using CO_3^{2-} in the UV-degradation are shown in Figure 25, where the presence of free radical scavenger can greatly depress the photodegradation rate. This observation confirms the

presumption that photodegradation reaction of dye is dominated by free-radical chain reaction.

5.2.5. Chromophore

The efficiency of UV-degradation for different chromophores is pH depended as shown in Figure 20 and Figure 24. At lower pH, the efficiency of dye removal is ranked in the following ascending order: insoluble anthraquinone (A2) < polyazo (AZ5) < soluble anthraquinone (A1) < disazo (AZ2) ≈ triazo (AZ3) < Cu monoazo (AM1). At higher pH, however, the ranking becomes: insoluble anthraquinone (A2) < soluble anthraquinone (A1) < disazo (AZ2) ≈ triazo (AZ3) < Cu monoazo (AM1) < polyazo (AZ5).

From the examination of the two rankings, anthraquinone dyes (A1 and A2) are difficult to be removed in both high and low pH ranges which is due to their intact carboxylic structures may strongly resist the UV irradiation. At high pH, for azo dyes, the efficiencies of dye removal under the UV irradiation generally increase with the substituted numbers of azo groups. The higher the number of azo (-N=N-) substitution in a single dye molecule, the higher the dye removal efficiency. This observation can be rationalized by the higher probability of multi-azo groups being attacked by free radicals and/or photons. Nevertheless, The low ranking of polyazo (AZ5) at acidic pH is quite astonishing compared with its high ranking at high pH. Two mechanisms are proposed for explanation:

a. As the pH is low, the amounts of free radicals ($^{\cdot}OH$ and/or $^{\cdot}OOH$) in the solution are inadequate for the simultaneous multi N=N bond attack within a dye molecule. Thus the photodegradation reaction for each polyazo molecule tends to be incomplete at low pH. On the contrary, this effect will not be noticed at high pH where free radicals are in plenty.

b. Usually, the electrons of the π bonds in the N=N groups are more diffusive and less firmly held to the bonding nitrogen and thus are particularly susceptible to

electrophilic agents. However, at low pH, the H^+ may interfere the conjugated system of polyazo dye by forming positively charged central amine, which will decrease the electron densities of the azo (N=N) groups and thus decrease the reactivity of electrophilic free-radical mechanism as shown in eq. 65

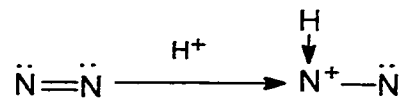

(65)

5.2.6. Solubility

One hydrophilic anthraquinone dye (A1) and one hydrophobic anthraquinone dye (A2) were selected to explore the effect of solubility to the UV-irradiation. From the experimental data, the hydrophilic anthraquinone dye (sulphonate anthraquinone reactive dye) has about twice the dye removal rate than hydrophobic anthraquinone dyes at high pH. Since all the anthraquinone dyes have similar chemical structures and the pH did not show any distinguish effect in dye removal for A2, it is obvious that the rate difference is mainly due to the difference of solubility. The effect of dye's solubility to the photodegradation may be interpreted by the photo-ionization mechanisms proposed by Leaver I.H. (1980). The water can carry the charged intermediates (A1 only), which lower the photo-ionization energy and therefore facilitate the dye degradation.

5.2.7. Photo-sensitization

Acetone is one of the well-known photo-sensitizers with a high triplet energy of 79-82 Kcal/mole (Poon C. and Vittimberga B.M., 1981) and can speed up the energy transfer from UV to dye molecules. Acetone (0.05M) was added in all the reactions at different pH to investigate the photo-sensitization effect to the dye degradation. The results are shown in Figure 20 and Figure 26. All hydrophilic dyes become colourless in 20 minutes of UV-irradiation and 70% hydrophobic dye (A2) decayed in the first 25 minutes. In general, by comparing the half-lives of all samples at pH 7 with/without the presence of

acetone, it shows that acetone can speed up the photodegradation reactions to about 13 to 63 times faster for hydrophilic dye and 139 times for hydrophobic dye. Apparently the addition of acetone can greatly improve the degradation performance through the photo-sensitization mechanism. From the spectrum's analysis the absorption peaks of all decayed dyes shift from visible range to invisible (UV) range after the photo-sensitization as shown in Figure 27.

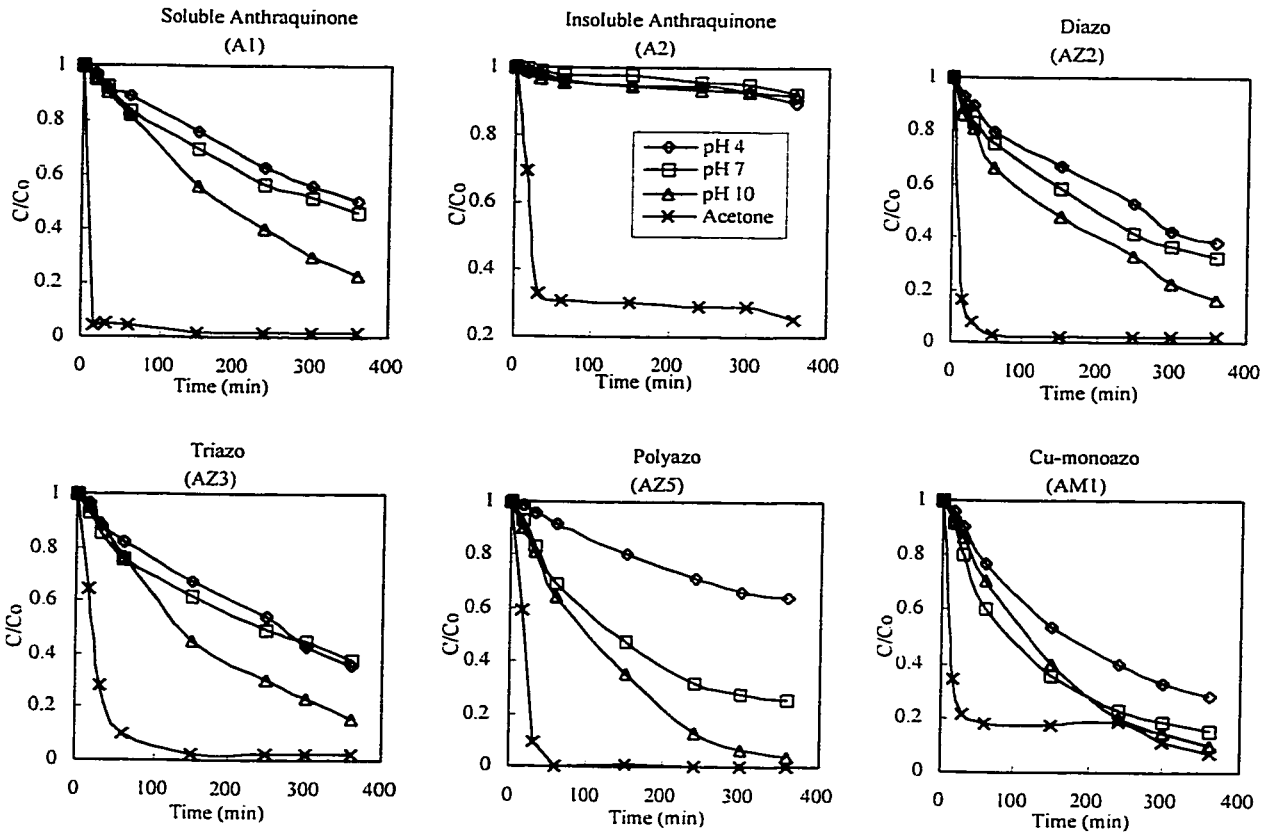

Figure 20: The change of the dye (C/C_0) during photodegradation at different initial pH with and without photosensitizer (0.05 M of acetone) (a) A1, (b)A2, (c) AZ2, (d) AZ3, (e) AZ5 & (f) AM1.

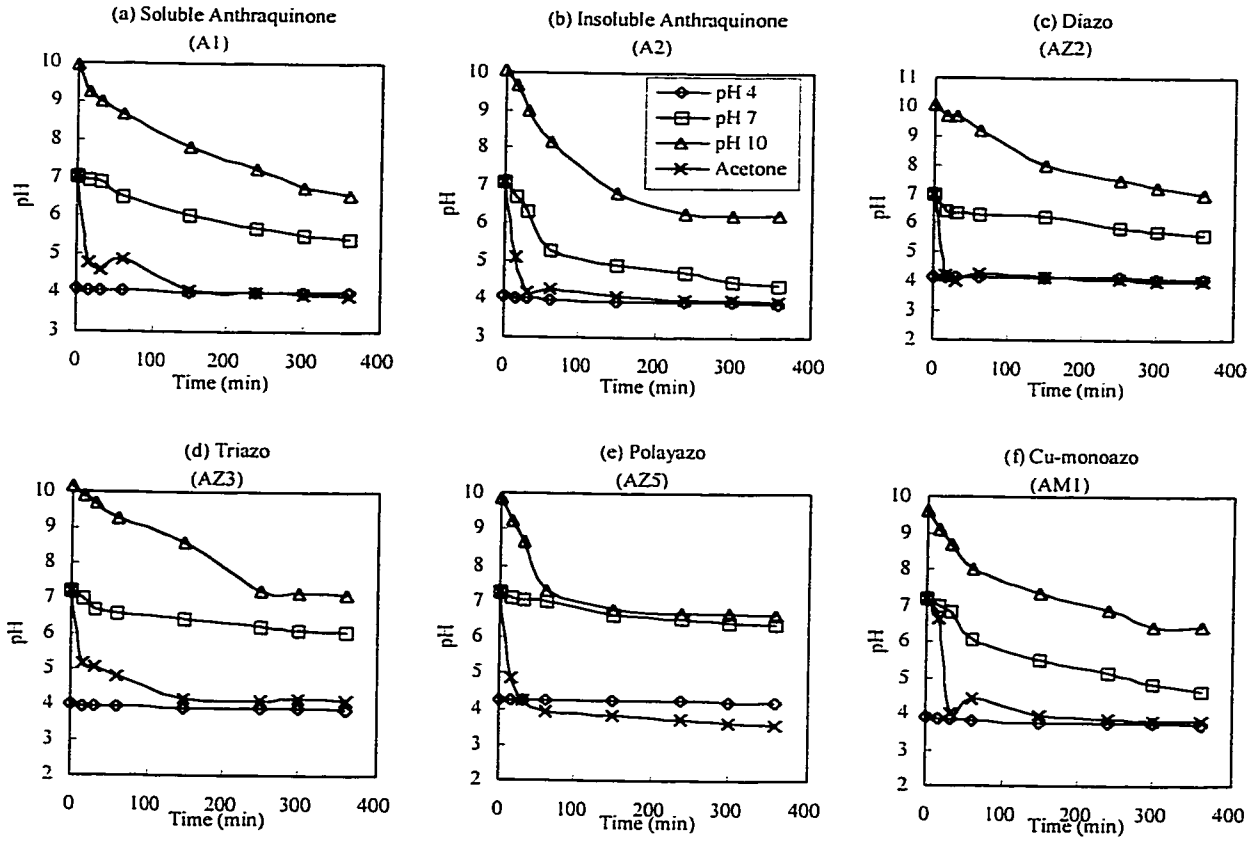

Figure 21: The change of pH during photodegradation at different initial pH with or without photosensitizer (0.05 M acetone) (a)A1, (b)A2, (c) AZ2, (d) AZ3 (e) AZ5 & (f) AM1

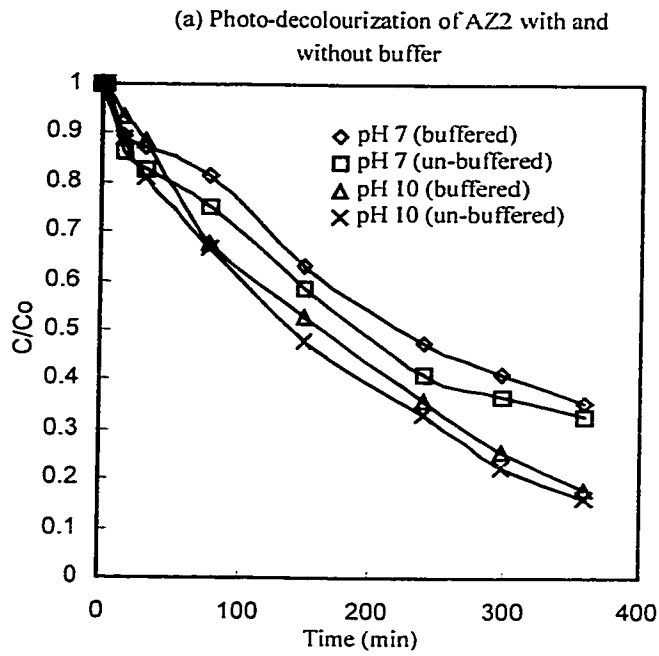

Figure 22: The change of the dye (C/C_0) during UV irradiation at initial pH 7 & 10 and pH buffer 7 & 10.

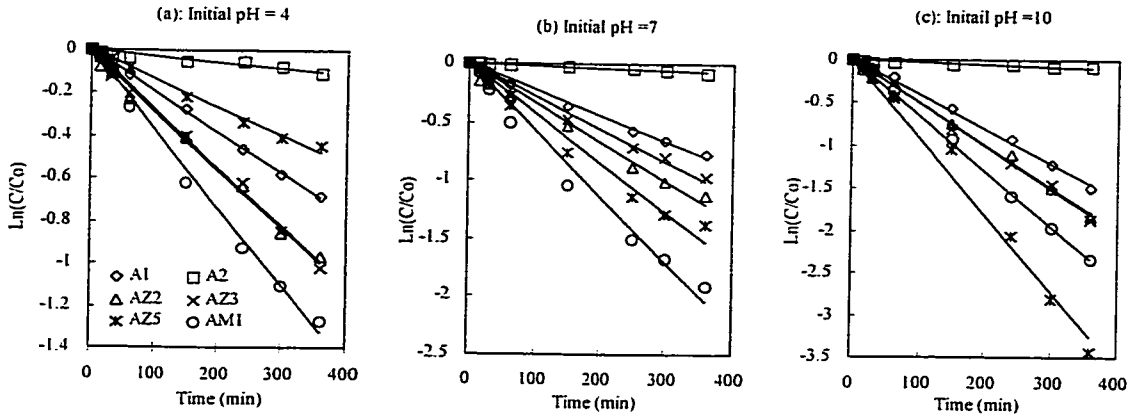

Figure 23: The pseudo first-order photodecay of dyes at initial pH of (a) 4, (b) 7, and (c) 10. [50 mg/L of six purified aromatic dyes were UV-irradiated under 253.7 nm (Light intensity: 2.4 x 10^{-5} Einstein $L^{-1}s^{-1}$)]

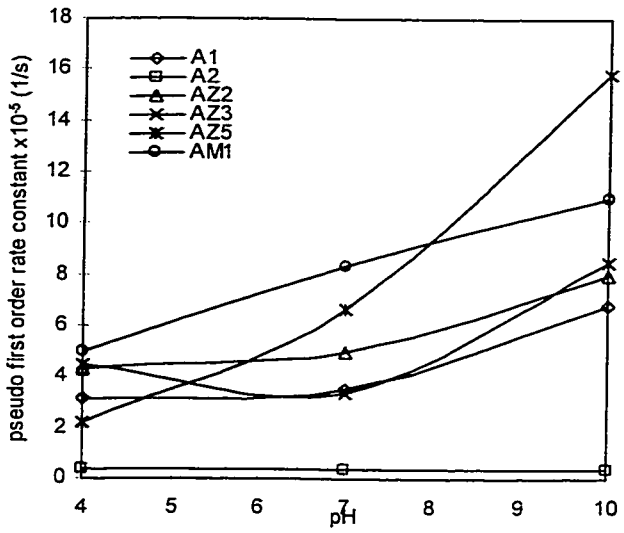

Figure 24: The pseudo first-order constants at different initial pH. [50 mg/L of six purified aromatic dyes were UV-irradiated under 253.7 nm (Light intensity: 2.4×10^{-5} Einstein $L^{-1}s^{-1}$)]

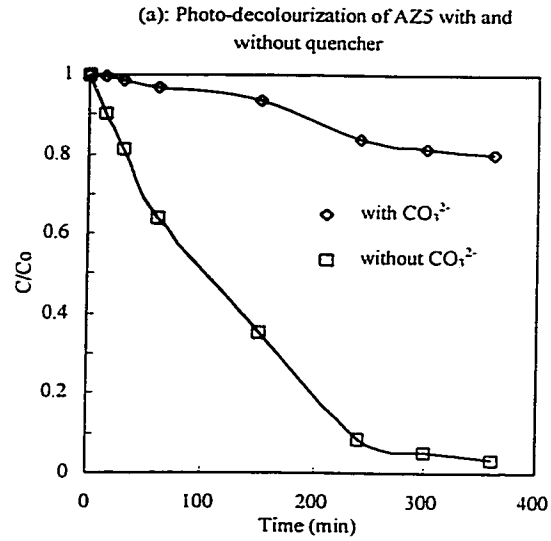

Figure 25: Photodegradation of Polyazo dye (AZ5) with and without quencher (0.1 M carbonate).

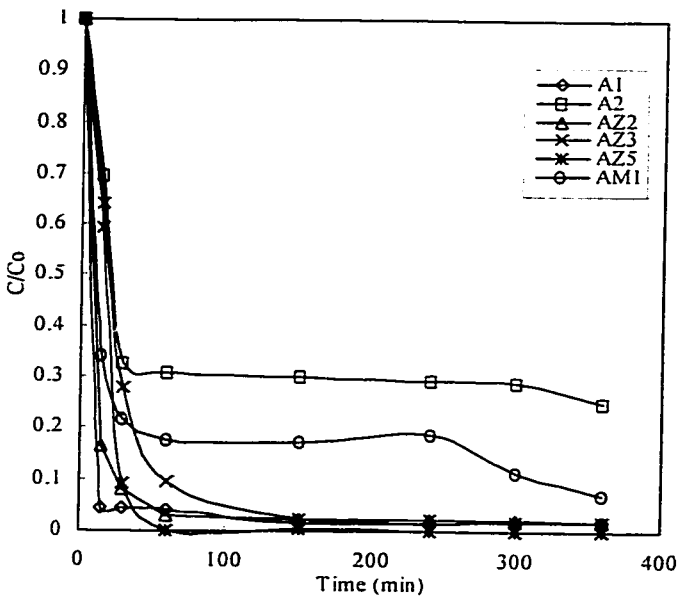

Figure 26: Photosensitization reaction of six purified aromatic dyes. [50 mg/L of six purified aromatic dyes were UV-irradiated under 253.7 nm (Light intensity: 2.4×10^{-5} Einstein $L^{-1}s^{-1}$) with photo-sensitizer (0.05 M acetone)].

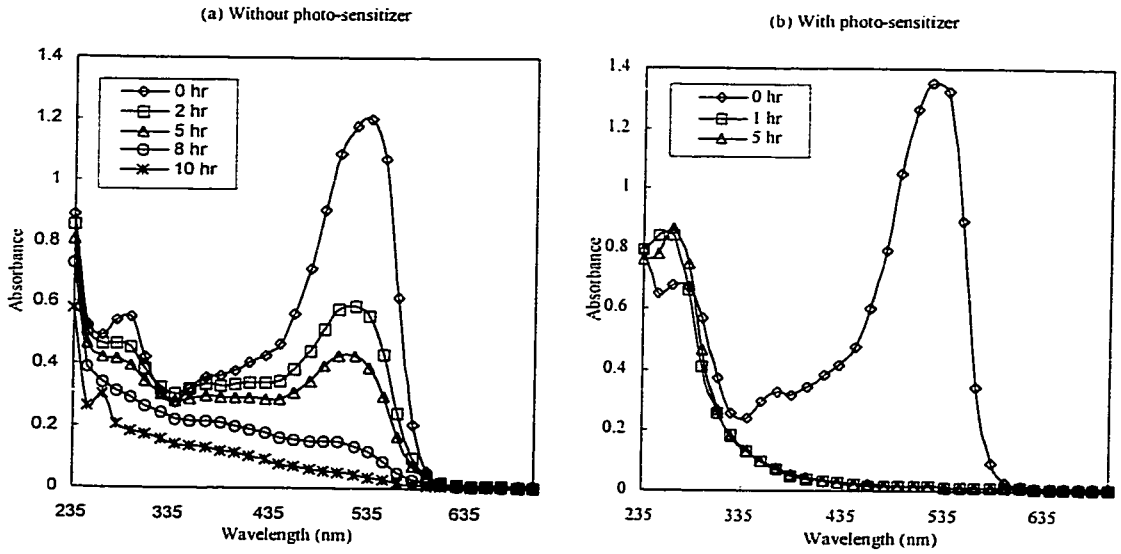

Figure 27: The change of the UV/VIS spectra during the photodegradation reaction of dye AZ5 without (a) and with (b) the acetone (sensitizer) [50 mg/L of Polyazo dye (AZ5) dyes were UV-irradiated under 253.7 nm (Light intensity: 2.4 x 10^{-5} Einstein $L^{-1}s^{-1}$) with photo-sensitizer (0.05 M acetone)].

CHAPTER 6: RESULTS AND DISCUSSION: REMEDIATION OF CHLORINATED AROMATIC DYES (CADs) POLLUTED SOIL BY SURFACTANT MICELLAR/UV SYSTEM

6.1. Photodegradation of Chlorinated Aromatic Dyes (CAD) in Micelle

A Chlorinated Aromatic Dye (CAD) – Disperse Red 13 (DR) in solutions containing the surfactant micelle was UV-irradiated under the UV light at 253.7 nm. Those surfactants used as solubilizing agents were four non-ionic surfactants: Tween 20, Tween 60, Tween 80 & Brij 52.

6.1.1. The Role of Surfactants in the photodegradation of DR

Disperse Red 13 (DR) was irradiated by UV at 253.7 nm in solutions containing different non-ionic solutions. Figure 28 shows the decay curves of DR in water and various surfactant solutions. In general, the photodegradation rates of DR follows pseudo first-order kinetics. The decay rates of DR, therefore, can be determined by the integrated first-order decay expression:

$$P_t = P_0 e^{-kpt} \qquad (66)$$

where P_0 and P_t are the concentration of the parent DR at time zero and defined time at t (mol/L), and k_p is the first-order decay rate constant (s^{-1}), which was determined to be 1.1 $\times 10^{-4}$, 2.0 $\times 10^{-4}$, 2.1 $\times 10^{-4}$, 2.3 $\times 10^{-4}$ and 3.1 $\times 10^{-4}$ s^{-1} for D.I water, Brij 52, Tween 80, Tween 20, and Tween 60, respectively. Obviously, the rate improvement is solely due to the presence of surfactant in the system, and the levels of rate increments depend on the nature of surfactant used, indicating that the performance of this process is strongly dependent on the appropriate selection of surfactant. This presumption can be justified by examining the solubility improvement of DR by those selected surfactants at concentration of 10 mM as shown in Figure 29; we observed about 1.37 (Brij 52) to

13.56 (Tween 60) times of improvement compared with using water alone. Theoretically, the solubilization of hydrophobic compound by surfactant is initiated by surfactant monomer, but much greater and efficient solubilization is observed as the surfactant concentration increases beyond its critical micellar concentration, (CMC). The characteristics of surfactant and its ability to solubilize hydrophobic compounds beyond cmc can be quantified by an analogous micelle-water partition coefficient, K_m:

$$K_m = \frac{[D]_{mic}}{[D]_w [S]_{mic}} \tag{67}$$

where $[D]_w$ is the concentration of dye in the water (mol/L), which could be assumed to be close to its water solubility in common applications, $[D]_{mic}$ is the concentration of dye dissolved in the micelles (mol/L), and $[S]_{mic}$ is the concentration of surfactant in micellar form (mol/L). Therefore, K_m of DR is calculable for the selected surfactants, and they are 139.34, 1035.97, 1179.25 and 1365.78 l/M for surfactants Brij 52, Tween 80, Tween 20, and Tween 60, respectively. The photodegradation rates of DR were correlated to the K_m of each surfactant as shown in Figure 30. The result indicated that the rate of degradation is proportional to the K_m, indicating that the selection of appropriate surfactants in such an application is critical. In general, the higher the K_m of the surfactant, the higher the photodegradation rate. Surfactant micelles can increase both the solubility of CAD in the liquid phase and its photodegradation rate simultaneously. This is likely because the size of the hydrophobic core of a micelle is about 15-30Å, and the solubilization process allows the organization of solute (CAD) on a molecular scale within the core. Secondly, the surfactant micelle has previously been proven to be an effective hydrogen source (Kile D.E. and Chiou C.T., 1988). The combination of the above two features makes a locally high level of hydrogen source and DR in the core, and the chance of molecular collision between them increases.

Since the K_m of a specific solute in a selected surfactant was dependent on the surfactant concentration, various doses of surfactant Tween 80 were therefore used to further examine the connection between photodegradation and the variation of K_m. From Figure

30, a similar trend of photolysis rate improvement was observed compared to that of using different surfactants (with different K_m). Because a difference is noticeable between the two curves (one is the variation of K_m due to varying surfactants, the other is due to varying concentration of a specific surfactant), this suggests that K_m is not the only dominant factor for determining the photodecay rate. The potential of selected surfactant in offering a valid hydrogen source is as important as its concentration.

6.1.2. Three-Stage kinetics

If all the degradation curves in Figure 28 are analyzed in detail, the three stages of DR decay were discovered on every decay curve. In general, they can be classified into the initial lag stage, the rapid decay stage (pseudo first-order), and followed by a retardation stage. The formation of the lag phase can be rationalized by the variation of pH level in the system. It is found that during the photolysis process, the solution pH gradually decreases, as typically shown in Figure 31. It can be seen that the decline in pH is accompanied by a reduction in DR concentration, which suggests that the proton is one of the major end products of the photoreduction reaction of DR. The high proton concentration will generally lower the reaction rate of photodegradation and inhibit the photodegradation process (Chu W. and Ma C.W., 1998 & 2000). This proton effect, however, can be neutralized by OH^- in an alkali medium, resulting in a faster forward reaction (*i.e.* the DR decay) at higher initial pH level, as shown in Figure 32. In addition, hydroxyl and hydroperoxyl radicals are reported to be generated when UV is absorbed by water in the presence of oxygen at higher pH levels (Chu W. and MA C.W., 1998). It is likely that the photodegradation of DR is partly contributed by free radical reaction involving the hydroxyl and hydroperoxyl radicals. Therefore, as the photodegradation is launched, the radical concentration is low in solution and probably inadequate for initiating chain reactions, resulting in a noticeable lag phase.

Similar reasons can also justify the formation of the second stage (the rapid pseudo first-order decay) in the system. After a long enough reaction time (longer than the lag phase),

the system accumulates a higher level of radicals that may be considered as another major parallel reaction (i.e. other than direct photolysis) being created and resulting in the fast pseudo first-order decay. The retardation stage with a gradually reduced decay rate was observed after 70% of DR was removed. The slow-down of the decay rate might be due to the following reasons: 1) the easily-accessible hydrogen source in the solution is about to be depleted; 2) the generated proton can inhibit the reaction; 3) some of the photoproducts may significantly absorb light, performing as a light filter and attenuating the incident UV intensity available for photodegradation; and 4) some of the photoproducts might act as quenchers and compete with the limited free radicals.

6.1.3. Reaction mechanism of photodecay of dye

The photodegradation mechanism of dye is presumably similar to that of any other aromatic compound where photoreduction is the dominant reaction mechanism upon the exposure of aromatic compounds to UV light (Chu W., 1999). However, the study of the dye's photodecay mechanism is even more interesting because colour fading is also observed during the process. Figure 31 shows a typical photodegradation process of DR in Tween 80 surfactant solution, in which Cl^- and H^+ are generated during the photodegradation process. The chloride concentration is observed to increase from zero to 2.54×10^{-5} mol/L after 120 min of light illumination, and the pH level of the solution decreased from 5.6 to 4.6 simultaneously. Assuming close to unity activity coefficients when calculating proton concentrations and assuming insignificant buffer capacity of the solution, the generation of proton and chloride concentrations is 1:1 stoichiometricly matched. This evidence verifies that photoreduction via photodechlorination associated with the generation of HCl (as the product) is the dominant reaction mechanism. However, if we take a closer look at the two decay curves in Figure 31, the decay of DR (detected by HPLC) is not coherent with the fading of colour (detected by Visible spectrophotometer), i.e. more than 50 minutes of time delay is detected. This evidence suggests that photodechlorination is the first step of photodegradation, which leaves the conjugated chromophore in DR intact. After the benzene ring is dechlorinated, the

prolonged exposure to UV light will lead to further bond breaking of the azo group in the dye molecule, leading to decoloration as the second step.

Based on our observation, the proposed photodegradation mechanism of DR was shown in Scheme VI, where a monochloro-substituted azo-benzene is photoreduced in surfactant solution via photodechlorination, in which the surfactant acts as solvent to improve the solubility of DR in aqueous phase and as a hydrogen source to induce photoreduction. The photodechlorination is followed by photodecoloration, which is likely initiated by forming partly reduced hydrazobenzene (-N-NH-), then the colorless hydrazobenzene can be further reduced by prolonged irradiation into aniline, or substituted aniline. Similar results of chromophore reduction were also reported by Leaver I.H. (1980).

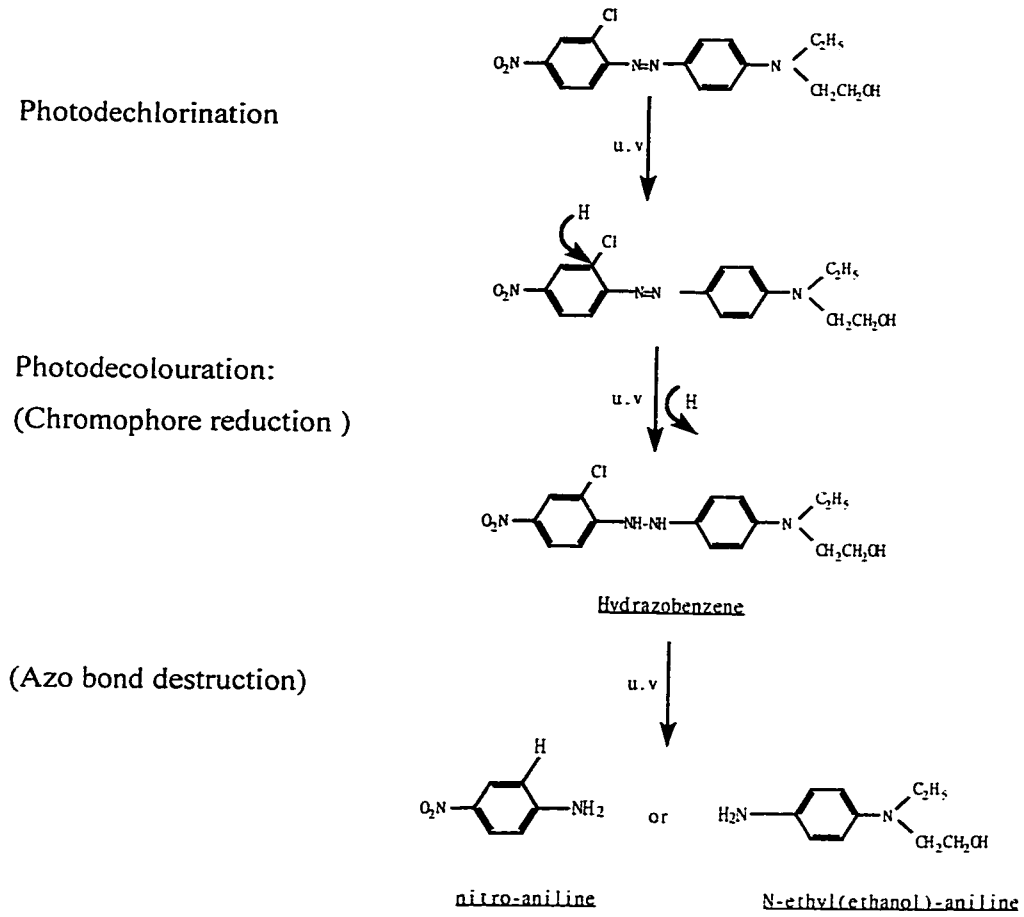

Scheme VI: The proposed photodegradation reaction mechanism involved photodechlorination and photodecolouration (chromphore reduction).

6.1.4. Improvement and inhibition of the reaction

Because photoreduction is determined to be the dominant decay pathway for DR's photodegradation, the property of the hydrogen source becomes critical in determining or improving the degradation rates. The reaction kinetics were therefore further studied by adding an additional hydrogen source. Sodium borohydride ($BNaH_4$) was selected as the hydrogen source and added to the solutions at various concentrations ranging from 10^{-3} mol/L to 10^{-1} mol/L, and the results were shown in Figure 33. Obviously, the presence of

additional hydrogen sources can significantly increase the photodegradation rates by about 2.5 times from $2.08 \times 10^{-4}\ s^{-1}$ (surfactant only without $BNaH_4$) to $5.35 \times 10^{-4}\ s^{-1}$ (surfactant with 0.1 mol/L $BNaH_4$); besides, all the initial lag stages vanished. Though the use of $BNaH_4$ can improve the photodecay rates of DR, an optimal dose of $BNaH_4$ was observed at 5×10^{-2} mol/L. No subsequent improvement could be achieved as the concentration of $BNaH_4$ was further increased, suggesting that this process is limited by another unexpected factor. One proposed explanation is that the molecules of DR reside mostly in the hydrophobic cores of surfactant micelles, yet the ionized borohydride (BH_4^-) either dissolves in the bulk aqueous solution or affiliates on the surface of micelles (which consist of hydrophilic heads of surfactant monomers). The diffusion of borohydride ions from the hydrophilic phases to the hydrophobic core or nearby the DR molecules is likely kinetic controlled due to the barrier between the two dissimilar phases. Therefore, the improvement of photodegradation rates of DR by adding additional $BNaH_4$ does not linearly increase with its concentration.

In addition to the use of an auxiliary hydrogen source, it is possible to improve the photodecay rates of DR by offering another reaction pathway in parallel. Photosensitization is one of the potential reactions that may be useful in this respect. Figure 34 shows the improvement of the photodegradation rates of DR by using acetone as an additive in the surfactant solution, in which case the rate is increased about 3.6 times from $2.28 \times 10^{-4}\ s^{-1}$ (surfactant only without acetone added) to $8.25 \times 10^{-4}\ s^{-1}$ (surfactant with 2.04 mol/L acetone). The rate increment is likely due to two mechanisms. First, the photodegradation efficiency of hydrophobic dyes is generally poor (0~20%), mainly due to their low solubility (Chu W. and Ma C.W., 1997), therefore, the photodegradation of DR can theoretically be enhanced if its solubility is increased. Acetone is a good amphibious solvent, which can increase the solubility of disperse dye in the aqueous phase. Secondly, acetone molecules have high triplet energy of 79-82 Kcal/mole (Poon C. and Vittimerga B.M., 1981), which has great potential to be a photosensitizer and indirectly promotes the energy transfer from UV to dye molecules, especially in the presence of hydrogen sources (Leaver I.H., 1980). In Scheme VII, upon to the UV illumination,

acetone molecule (A) is excited to its triplet state (^3A), which first abstracts hydrogen from hydrogen source SH_2 (i.e. surfactant in our case) and generates a ketyl radical ($AH^{\cdot}$). Hydrogen atom transfers form the ketyl to the azo bond of the dye (D), leading to the formation of a hydrayl radical ($DH^{\cdot}$), which is finally reduced to the colorless hydrazobenzene (DH_2).

$$A \xrightarrow{hv} {}^1A \rightarrow {}^3A$$

$$2\,{}^3A + SH_2 \rightarrow 2AH^{\cdot} + S$$

$$AH^{\cdot} + D \rightarrow A + DH^{\cdot} \text{ (hydrayl radical)}$$

$$DH^{\cdot} + AH^{\cdot} \rightarrow A + DH_2 \text{ (hydrazobenzene, colourless)}$$

Scheme VII: The photosensitization reaction of dye in the presence of hydrogen source

It is also important to note that the rate improvement does not linearly increase with the increment of acetone concentration. This is likely because high concentrations of acetone may act as a light barrier (filter) and will absorb and consume most of the photons without contributing to the sensitization reaction (the molar absorptivity of acetone at 253.7 nm is 11 M^{-1} cm^{-1}), thus indirectly causing the attenuation of light intensity available for dye degradation. To verify this hypothesis, the acetone is overdosed intentionally, and a significant rate decline is observed (Figure 34).

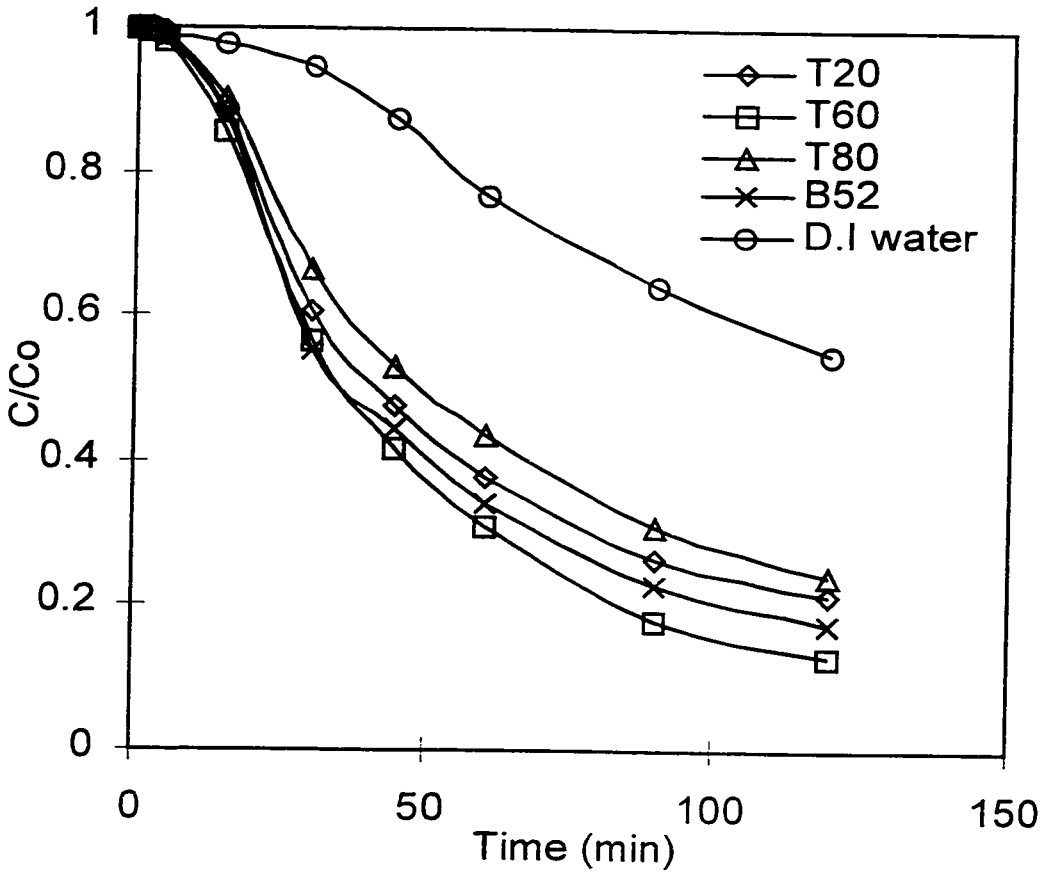

Figure 28: Photodegradation of DR in various non-ionic sufractants solutions. Lag phases were observed for all samples in all cases. Light intensity of the incident light at 253.7 nm was approximately 2.4 x 10^{-5} Einstein $L^{-1}s^{-1}$.

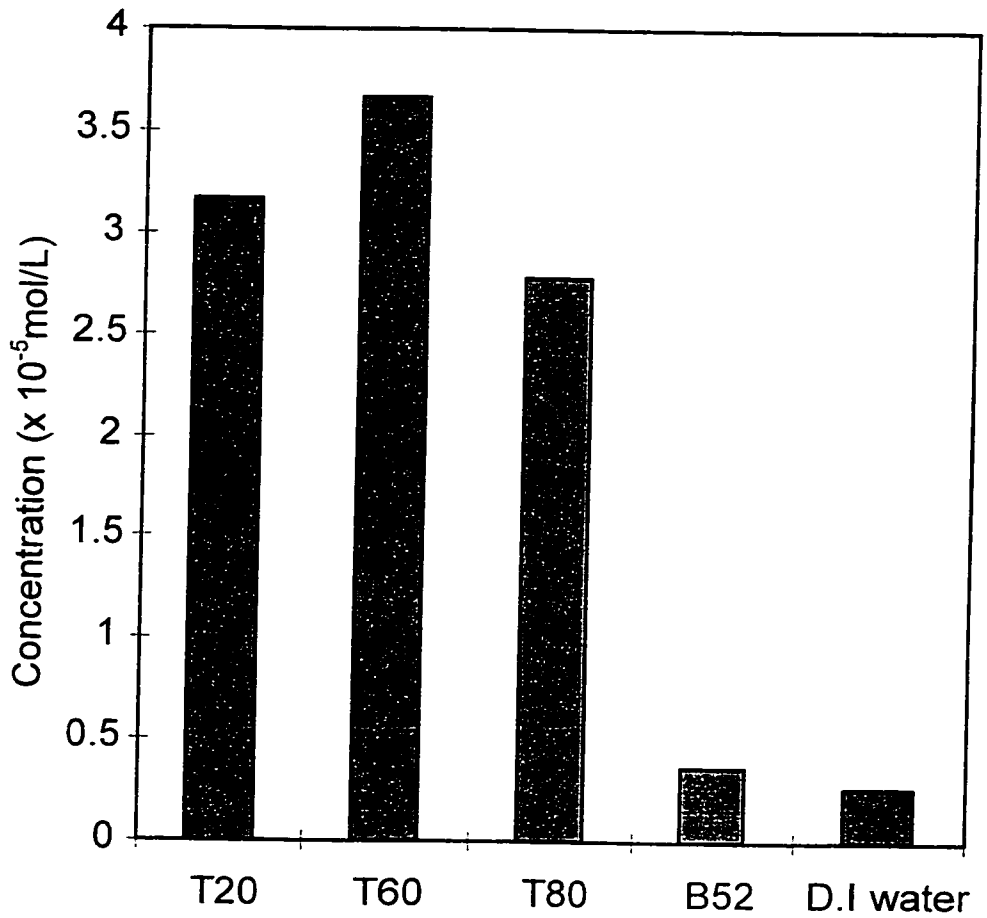

Figure 29: The solubility enhancement of DR at different non-ionic surfactants. In all cases, excess amount of DR was added to the 10 mM of surfactants unit a stable solubilized DR formed.

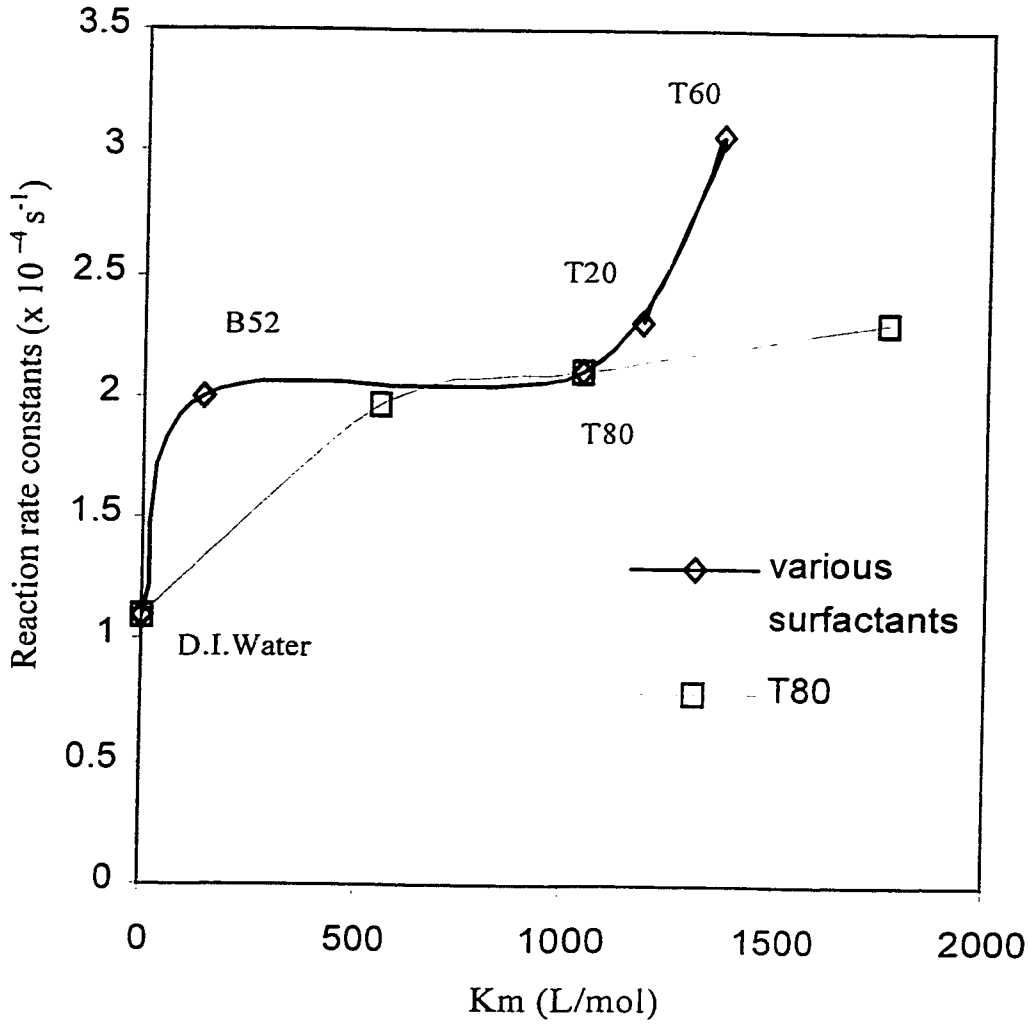

Figure 30: The effect of K_m to the reaction rates of DR: Excess DR was added to the i)10 mM of various surfactants (for inter-surfactant comparison), ii) 5 mM and 20 mM of Tween 80 surfactant (for intra-surfactant comparison).

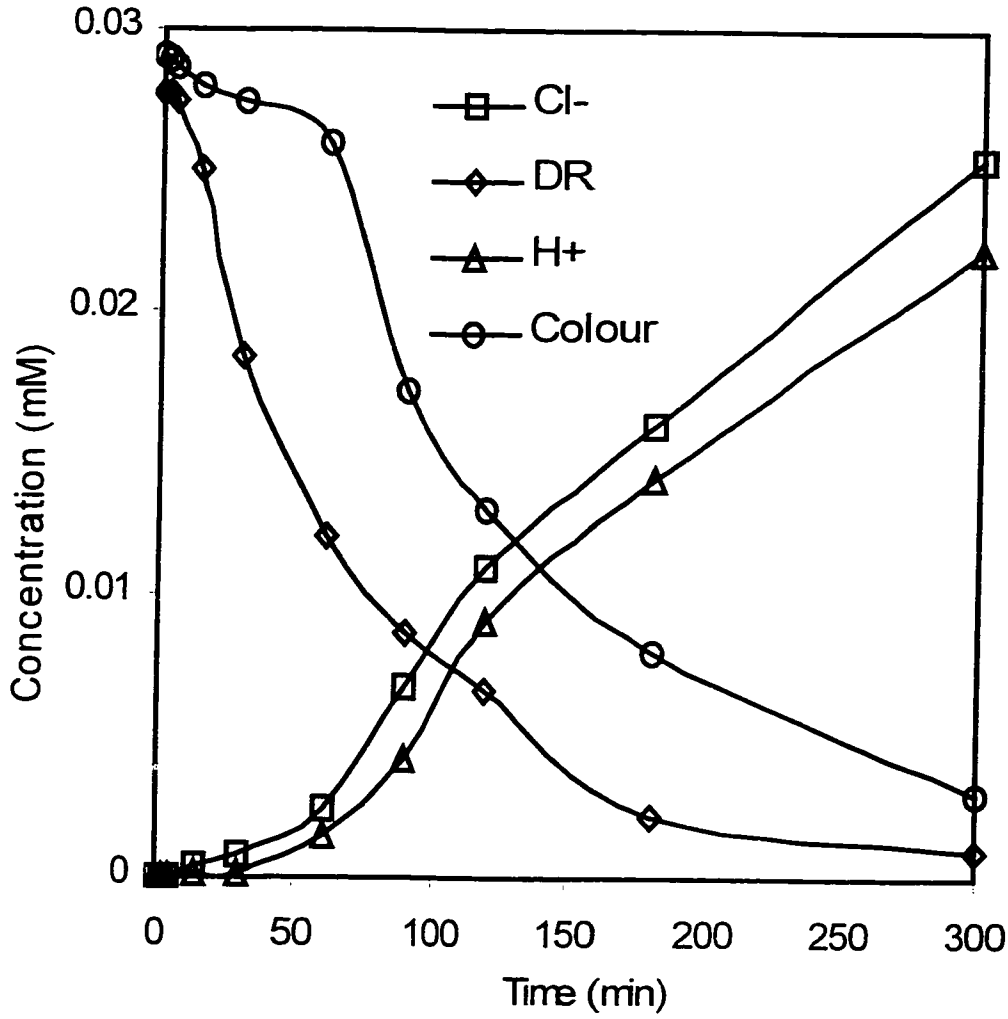

Figure 31: The generation of final products H^+ and Cl^- during the photodegradation of 0.028 mmol/L DR in Tween 80 surfactant solutions at 253.7 nm. The HPLC analysis and UV/Visible spectrometric analysis (color) of the DR is also compared. Photodecolouration occurred with a time delay after the photodechlorination. Generation of proton concentration and chloride concentration is 1:1 stoichiometricly matched.

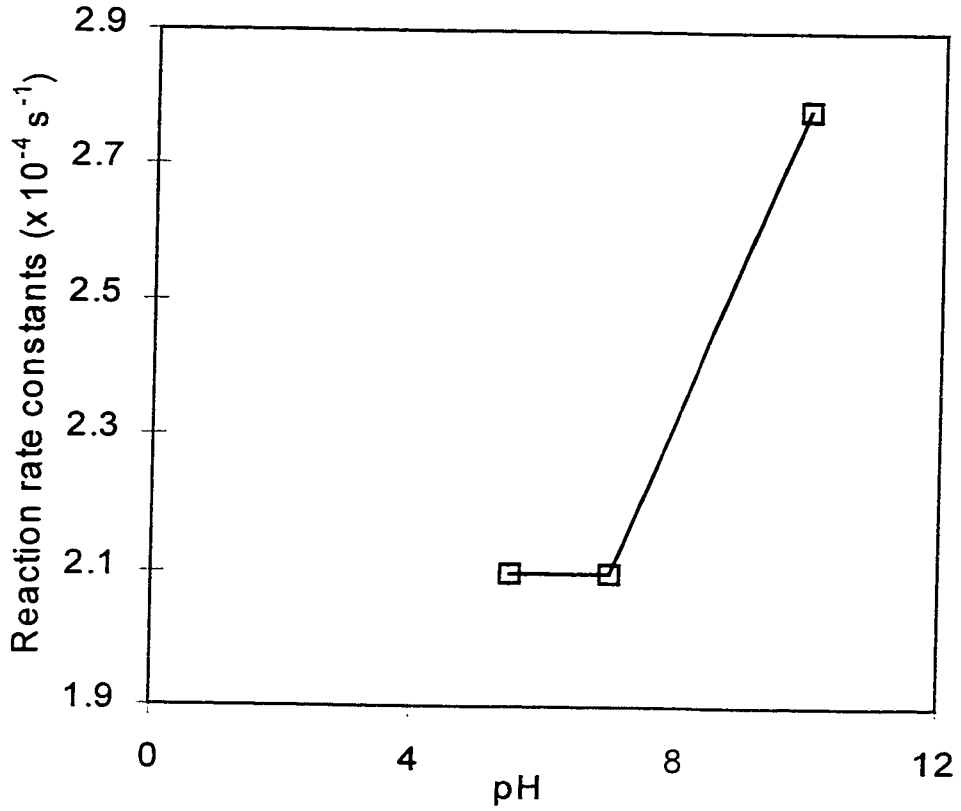

Figure 32: Reaction rates of DR photodecay at different initial pH level (5.5, 7 and 10).

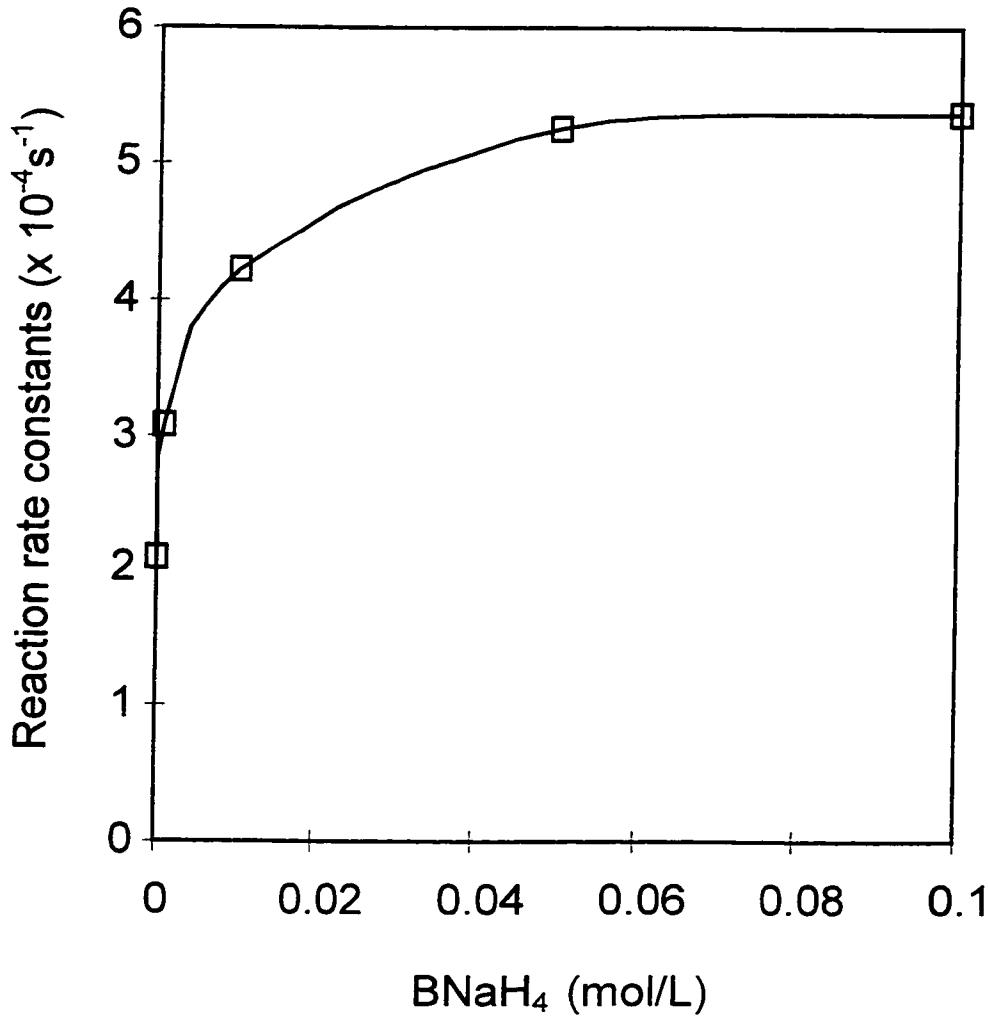

Figure 33: The rate enhancement of photodegradation of DR in the presence of hydrogen sources, $BNaH_4$. 10 mM of DR within Tween 80 solution was UV-irradiated under 253.7 nm indicates that $BNaH_4$ has a positive effect.

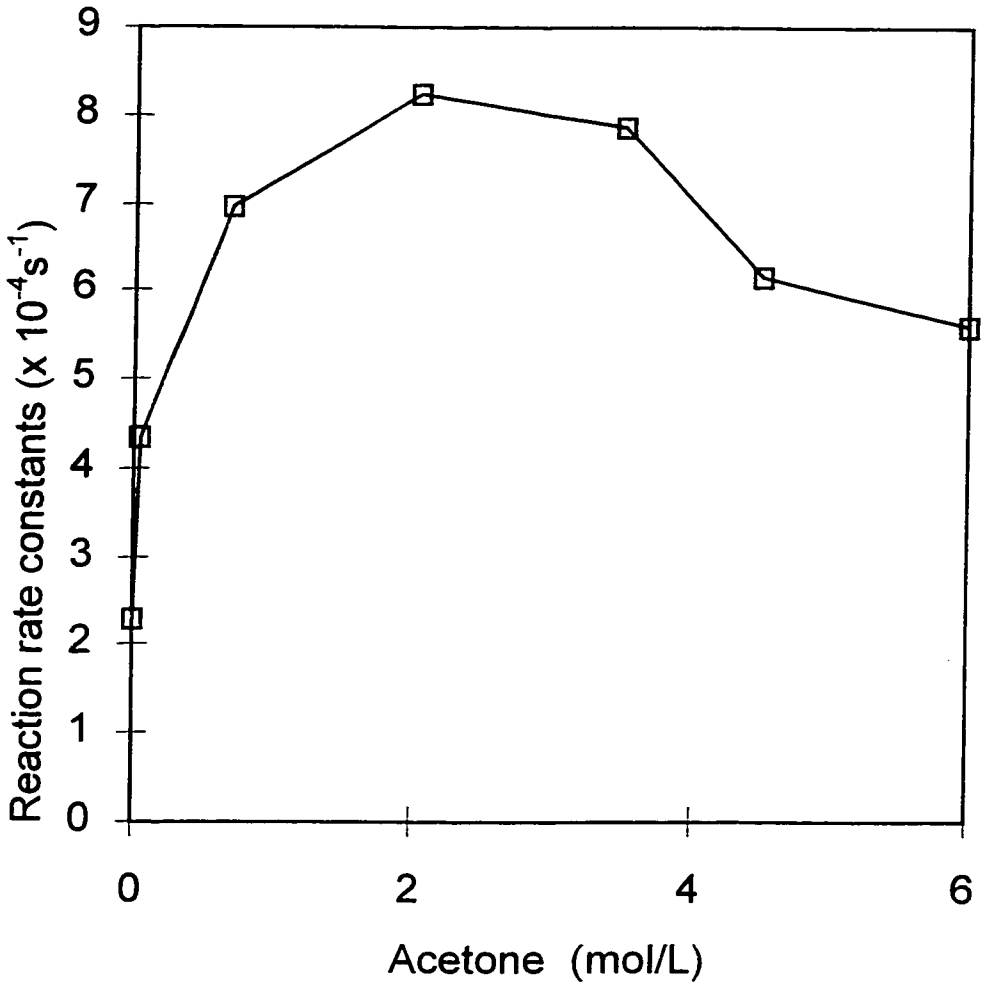

Figure 34: The rate enhancement of photodegradation of DR in the presence of acetone. DR within 10 mM Tween 20 solution was UV-irradiated under 253.7 nm indicates that lower acetone concentration (less than 2 mol/L) has a positive effect. High concentration of acetone, oppositely acts as a light barrier to slow down the photodegradation rate.

6.2. Photodegradation of Chlorinated Aromatic Dyes (CADs) in Micelle with the Presence of Humic Materials

6.2.1. Effect of humic materials

Surfactant can extract both Chlorinated Aromatic Dyes (CADs) and humic materials out of the contaminated soil during the soil-washing process. These extracts will therefore present in the follow up photodegradation process, in which the photodecay performance of target compound (CADs) is interfered by the humics. Two types of humic materials, i.e. soluble humic material from Aldrich Chemical Co. (Ha) and Soil Extracted Material (SEM), were used as additives in the surfactant-aided soil washing process to examine the impacts of humics to the photodegradation processes of CAD. The results of humic impact to the DR's photodegradation were showed in Figures 35 and 36.

From the experimental results, it was interesting to find that the low dose of humics (no matter the Aldrich humic (Ha) or Soil Extracted Material (SEM) would improve the photodecay rate of Disperse Red (DR) than that without the humics. On the other hand, excess humic substances would result in a retardation of the rate possibly due to the quenching of the reaction.

Obviously, low concentration of humics (Ha < 0.0333 μmol/L) can increase the photodegradation quantum yield (Φ) by about 16% from 1.068×10^{-4} (surfactant only without humic) to 1.238×10^{-4} (surfactant with 0.0333 μmol/L Ha). Likewise, in the presence of low concentration of Soil Extracted Materials (surfactant with 3.96 μmol/L SEM), the quantum yield of DR decay was significantly increased by 239% to 2.554×10^{-4}. The quantum yield improvement is likely due to the increment of available hydrogen sources in the solution, which was known critical to the photoreduction reactions.

However, as the humic concentration was further increased, the reduction of quantum yield in dye degradation was observed. Humics are known to absorb UV light, therefore, light attenuation by high dose of humic is expected. In addition, Zepp R.G.

et al., (1981) suggested that phenolic humic substances present on most inland waters could inhibit free radical chain reactions and therefore acted as a quencher of photochemical reaction. Thus, quantum yields for direct photolysis of chlorinated compounds in the aquatic environment are not likely to exceed unity.

6.2.2. Stern Volmer Plot

In order to verify the proposed explanations, a mathematical model based on possible reaction mechanisms in this system was proposed by assuming the rate improvement and quenching by humics are occurring simultaneously, in which the dominant sub-reactions will be different at high and low humic concentrations.

The reaction mechanisms of DR photodegradation in Tween 80 surfactant solution in the presence of humics, which acts as both quencher and hydrogen source, can be broken down in the following complex series of kinetic expressions:

Process	Rate		
Photon absorption	fI	$D_0 + hv \rightarrow D_1^*$	(68)
Deactivation of singlet	$k_{d1}[D_1^*]$	$D_1^* \rightarrow D_0 + \text{heat}$	(69)
Fluorescene	$k_f[D_1^*]$	$D_1^* \rightarrow D_0 + hv'$	(70)
Intersystem crossing	$k_{isc}[D_1^*]$	$D_1^* \rightarrow D_3^*$	(71)
Phosphorescence	$k_p[D_3^*]$	$D_3^* \rightarrow D_0 + hv''$	(72)
Deactivation of triplet	$k_{d3}[D_3^*]$	$D_3^* \rightarrow D_0 + \text{heat}$	(73)
Quenching of triplet	$k_q[D_3^*][H]$	$D_3^* + H \rightarrow D_0 + H_3^*$	(74)
Photochemical reaction	$k_r[D_3^*][H]$	$D_3^* + [H] \rightarrow \text{Products}$	(75)

The involvement of too many sub-reactions in a rate law makes the expression irresolvable. Several assumptions may be made based on earlier observations or hypotheses regarding the specific mechanisms of transformation, resulting in consideration simplification of the kinetic expression. Since the significant reactive intermediate is likely the long-lived triplet state for photochemical reaction, therefore if intersystem crossing is effective compared with all other singlet processes, a simpler mechanism may be proposed:

	Rate		
Absorption/Intersystem crossing	αfI	$D_0 + h\nu \rightarrow D_1^* \rightarrow D_3^*$	(76)
Photochemical reaction	$k_r[D_3^*][H]$	$D_3^* + [H] \rightarrow$ Products	(77)
Deactivation of triplet	$k_d[D_3^*]$	$D_3^* \rightarrow D_0$	(78)
Quenching of triplet	$k_q[D_3^*][H]$	$D_3^* + H \rightarrow D_0 + H_3^*$	(79)

Where I is the illuminating intensity; f is the efficiency of light absorption, α is the intersystem crossing efficiency. The proposed model can be divided into two cases:

a. Photodegradation enhancement of DR at low humic concentration

As the humic concentration in the reaction mixtures is low, the humic mainly acts as an additional hydrogen source to improve the reaction rate; therefore the quenching sub-reaction eq. 79 can be ignored in the process. By assuming a steady-state concentration of D_3^*, it will results in:

$$d[D_3^*]/dt = \alpha fI - K_r[D_3^*][H] - K_d[D_3^*] = 0 \quad (80)$$

$$\alpha fI = (K_r[H] + K_d)[D_3^*] \quad (81)$$

Because the quantum yield in this study is defined by the photodecay of DR, the rearrangement of eq. 81 in terms of quantum yield results in the first model which depends on the concentrations of hydrogen source, [H]:

$$\phi = \frac{k_r[D_3^*][H]}{fI} = \frac{k_r\alpha[H]}{k_r[H] + k_d} \quad (82)$$

Taking the reciprocal of the eq 82, a linear rate-enhancing model is established.

$$\frac{1}{\phi} = \frac{1}{\alpha} + \frac{k_d}{k_r\alpha} \times \frac{1}{[H]} \quad (83)$$

For low concentration ranges of Ha and SEM (lower than their corresponding optimum dosages), a plot of $1/\phi$ versus 1/[H] with an intercept of $1/\alpha$ and a slope of $k_d/k_r\alpha$ is shown in Figures 37 & 38. The model shows a good linear correlation with r^2 of 0.968 & 0.964 for SEM & Ha, respectively. These indicate that the proposed model and those assumptions are suitable for describing humics acting as a hydrogen source to enhance the photodegradation at low humic concentration levels.

b. Quenching effect at high humic concentration

When the humic concentration increases in the solution, humic was not only acted as a hydrogen source but also acted as a free radical scavenger. Judging from the rate retardation when humic is over dosed, it is rational to assume that the quenching effect of humic is dominant under this circumstance, and the concentration of humic in the eq. 77 is in excess and can be assumed to be a constant. Therefore, the eq. 77 can be rewritten to:

$$\text{Rate} = k_r' [D_3^*] \tag{84}$$

where $k_r' = k_r [H]$

By summing up the sub-reactions in eqs. 76, 78, 79 and 84, another steady state equation for high humic concentration is resulted:

$$\frac{d[D_3^*]}{dt} = \alpha f I - k_d[D_3^*] - k_r'[D_3^*] - k_q[D_3^*][H] = 0 \tag{85}$$

or $$\alpha f I = \left(k_d + k_r' + k_q[H]\right) \times [D_3^*] \tag{86}$$

The above equation can be rearranged into the format of quantum yield as follow:

$$\phi = \frac{k_r'[D_3^*]}{fI} = \frac{k_r'\alpha}{k_d + k_r' + k_q[H]} \tag{87}$$

By taking the reciprocal of eq. 87, a linear quenching model is established again:

$$\frac{1}{\phi} = \frac{k_r'+k_d}{k_r'\alpha} + \frac{k_q}{k_r'\alpha} \times [H] \tag{88}$$

where the $(k_r'+k_d)/k_r'\alpha$ and $k_q/k_r'\alpha$ are the intercept and the slope of the linear quenching model respectively. The plot of $1/\phi$ against [H] at high Ha and SEM dosage are shown in Figures 39 and 40, where good linear correlation with r^2 of 0.926 & 0.981 for SEM & Ha are observed, respectively. This indicates the proposed quenching model is valid at high humic concentrations. This evidence, together with the good correlation in Figures 39 and 40, suggest that triplet deactivation, triplet quenching by humic, and humic-enhanced photodecay are the major sub-reactions in this process and capable of describing the overall reaction successfully. Therefore, the initial hypothesis regarding the neglect of all singlet processes is valid.

The three rate constants, k_q, k_r, k_d, and one coefficient α, theoretically can be solved by the slopes and intercepts in eqs. 83 and 88. However, the intercept of Eq. 88 is a virtual intercept, which was physically meaningless since the y-intercept did not exist in the case of high humic concentration. (i.e. humic concentration cannot be zero in this model). Therefore, another equation is needed to solve the four constants. Practically, it is normally assumed that the rate for exothermic quenching is diffusion-controlled. The quenching rate, k_q, can therefore be evaluated from the modified Debye expression (William M., 1976).

$$k_q = \frac{8RT}{3000\eta} l M^{-1} s^{-1} \tag{89}$$

where η is the viscosity of the solution in poise. R is the constant at room temperature (i.e., T=298K). For pure water at room temperature, the kq is equal to 6.5 x 109 L $mol^{-1}s^{-1}$. Since the micellar micro-environments has a higher viscosity

(e.g. the viscosity within surfactant micelles normally ranged from 15 to 100 cp). By assuming an averaged η of 50 cp in our case, then

$$k_q = 1.303 \times 10^9 l M^{-1} s^{-1}$$

For soil extracted materials "SEM" (From Figures 37 and 39):

$$\frac{1}{\phi} = \frac{0.0018}{[H]} + 3691 \tag{90}$$

$$\frac{1}{\phi} = 8x10^8 [H] + 514 \tag{91}$$

By comparing their coefficients and constants,

$$\frac{1}{\alpha} = 3691 \tag{92}$$

$$\frac{k_d}{k_r \alpha} = 0.0018 \tag{93}$$

$$\frac{k_q}{k_r' \alpha} = 8x10^8 \tag{94}$$

From eq. (94), $k_r' = 6012 s^{-1}$

Since $k_r' = k_r [H]$, therefore

$$k_r = \frac{6012}{[H]} M^{-1} s^{-1} \tag{95}$$

From eq. (93),

$$k_d = \frac{2.93x10^{-3}}{[H]} s^{-1} \tag{96}$$

By using the same method, the corresponding kd, kr for addition of Ha in the reaction mixture could be found in following equation:

For Aldrich Humic materials "Ha" (From Figures 38 and 40):

$$\frac{1}{\phi} = \frac{1x10^{-5}}{[H]} + 7781 \tag{97}$$

$$\frac{1}{\phi} = 9x10^{9}[H] + 9840 \tag{98}$$

By comparing their coefficients and constants,

$$\frac{1}{\alpha} = 7781 \tag{99}$$

$$\frac{k_d}{k_r \alpha} = 1x10^{-5} \tag{100}$$

$$\frac{k_q}{k_r' \alpha} = 9x10^{9} \tag{101}$$

From eq. (101), $k_r' = 1127 s^{-1}$

Since $k_r' = k_r [H]$, therefore

$$k_r = \frac{1127}{[H]} M^{-1} s^{-1} \tag{102}$$

From eq. (100),

$$k_d = \frac{1.45x10^{-6}}{[H]} s^{-1} \quad (103)$$

As the quenching effect becomes more significant at high humic dosage, the quantity of humic involves as hydrogen source in the chemical reaction is overwhelmed, which leads to a lower k_r at higher humic concentration.

Table 15: summary of the reaction rate and deactivation rate of DR photodegradation in the presence of different humic substances.

Additives	Soil extracted material "SME"	Humic
k_r ($M^{-1}s^{-1}$)	6012/[H]	1127/[H]
k_d (s^{-1})	2.93×10^{-3}/[H]	1.45×10^{-6}/[H]

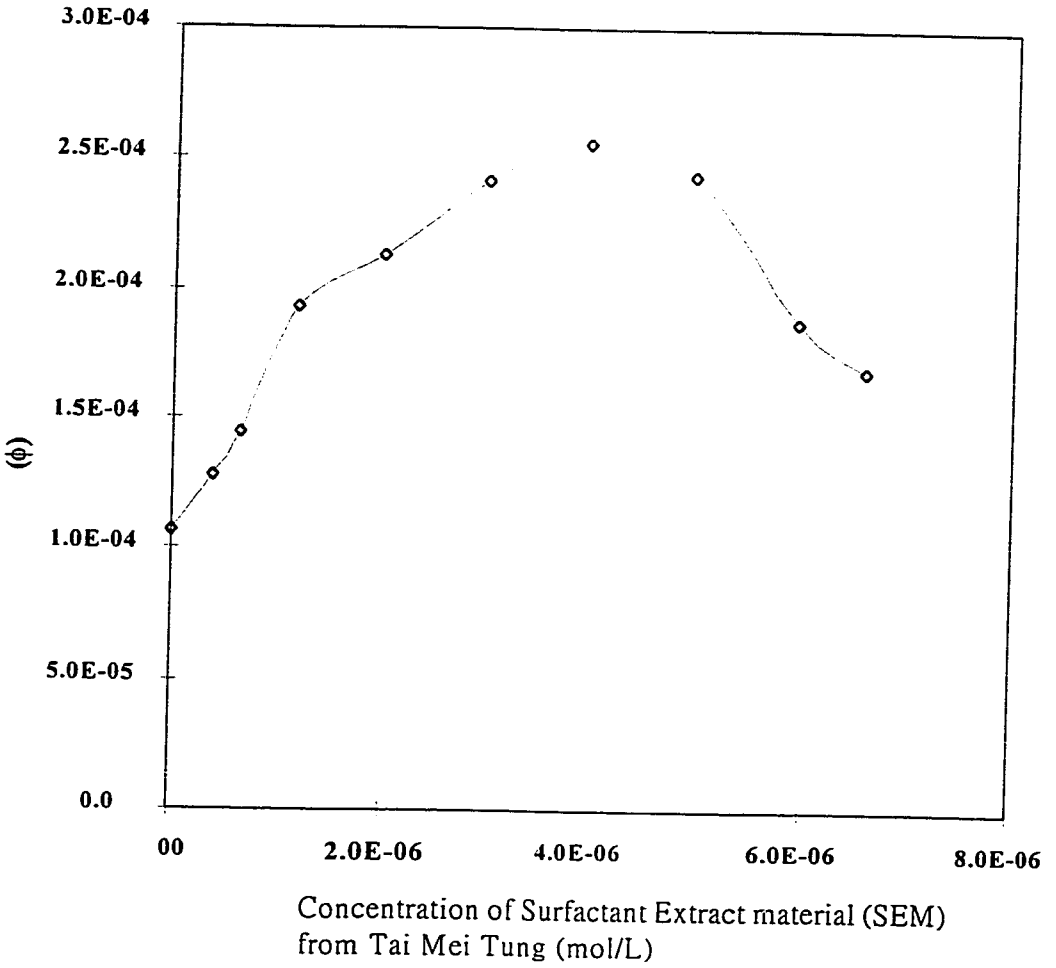

Figure 35: The photodegradation of Disperse Red (DR) within Tween 80 micelles: 0.01 mM of DR were UV-irradiated in 10 mM Tween 80 micelles with various initial concentration of Soil Extracted Materials (SEM).

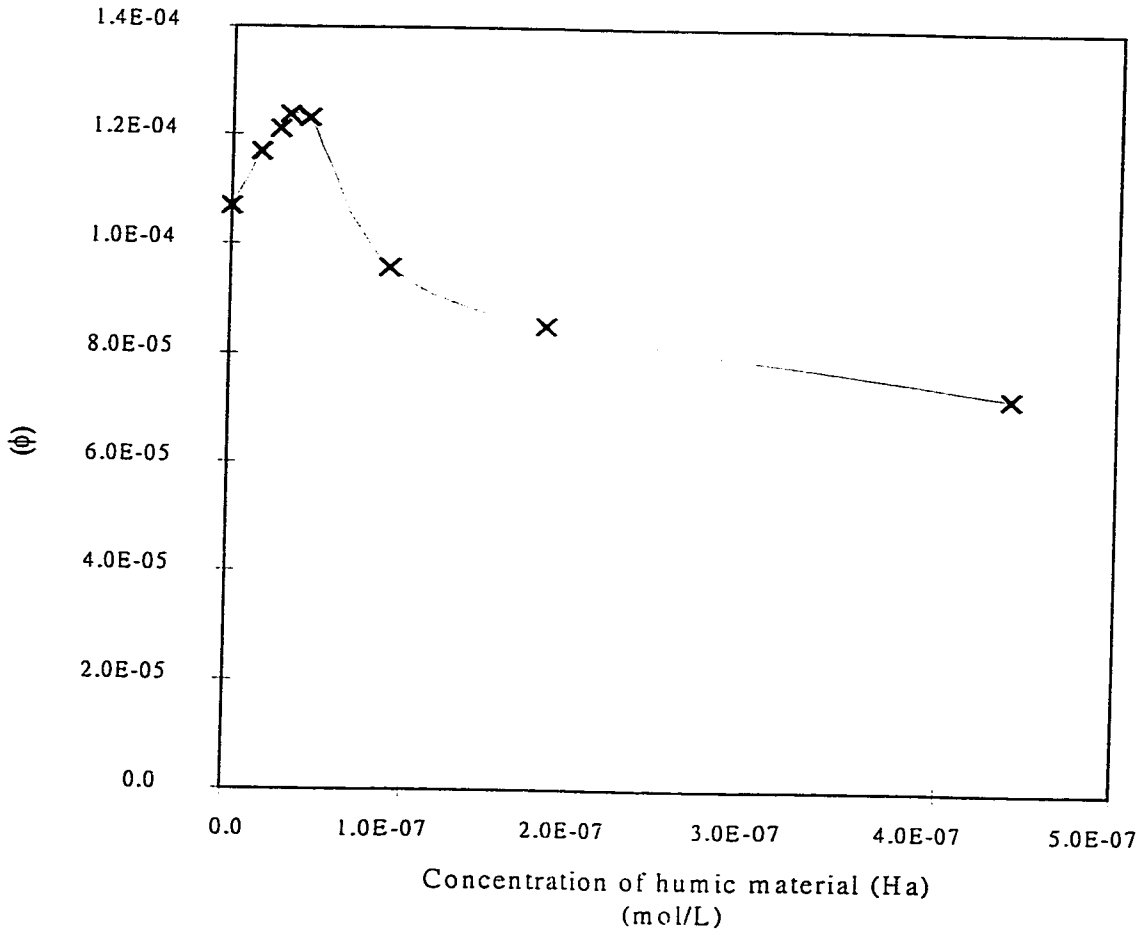

Figure 36:The photodegradation of Disperse Red (DR) within Tween 80 micelles: 0.01 mM of DR were UV-irradiated in 10 mM Tween 80 micelles with various initial Aldrich humic (Ha) concentration.

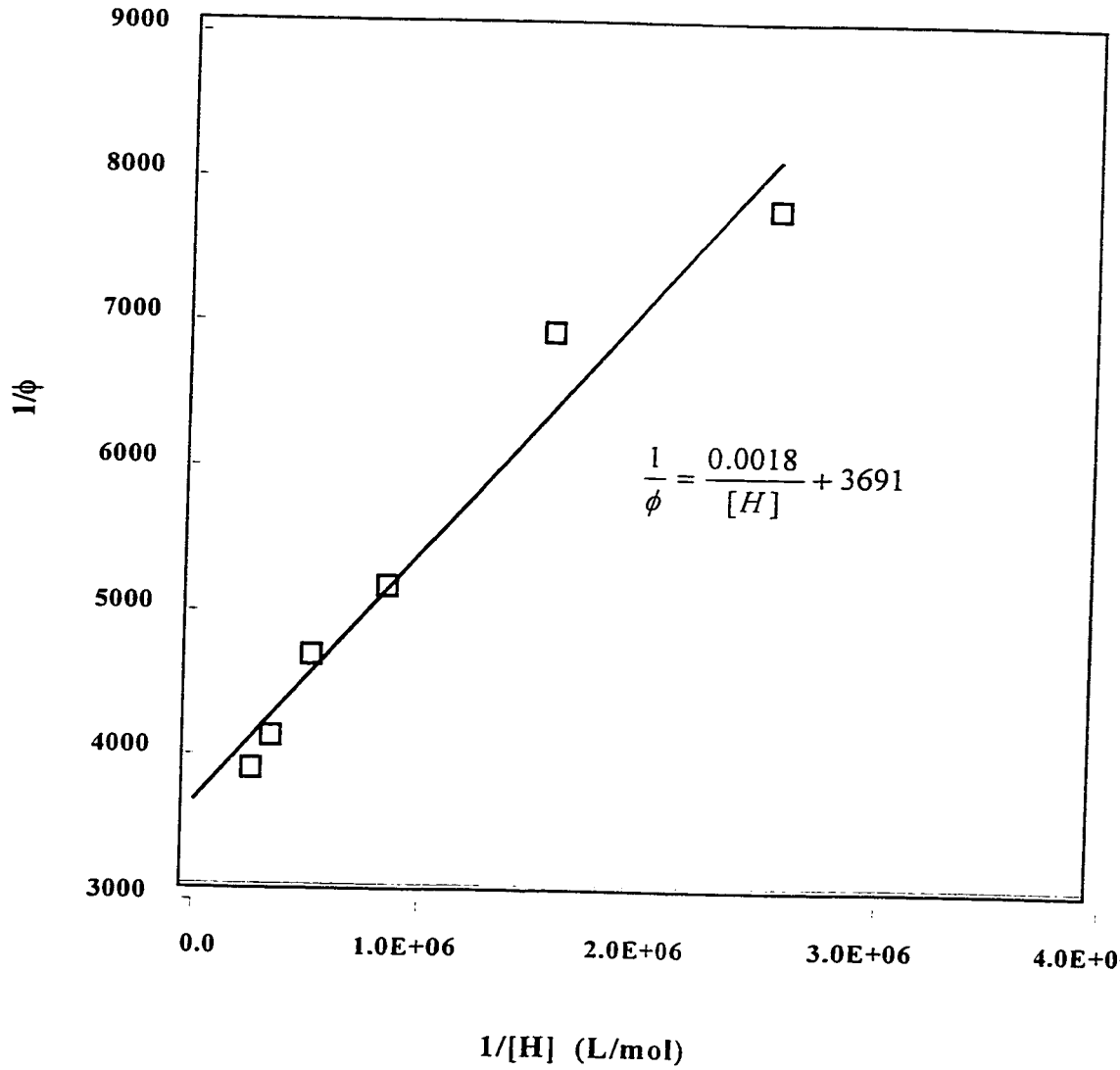

Figure 37: Photodegradation of DR at low concentration of Soil Extracted Materials (SEM): A plot of 1/ϕ against 1/[H] for the DR photodegradation within 10 mM Tween 80 micelle and various SEM concentrations.

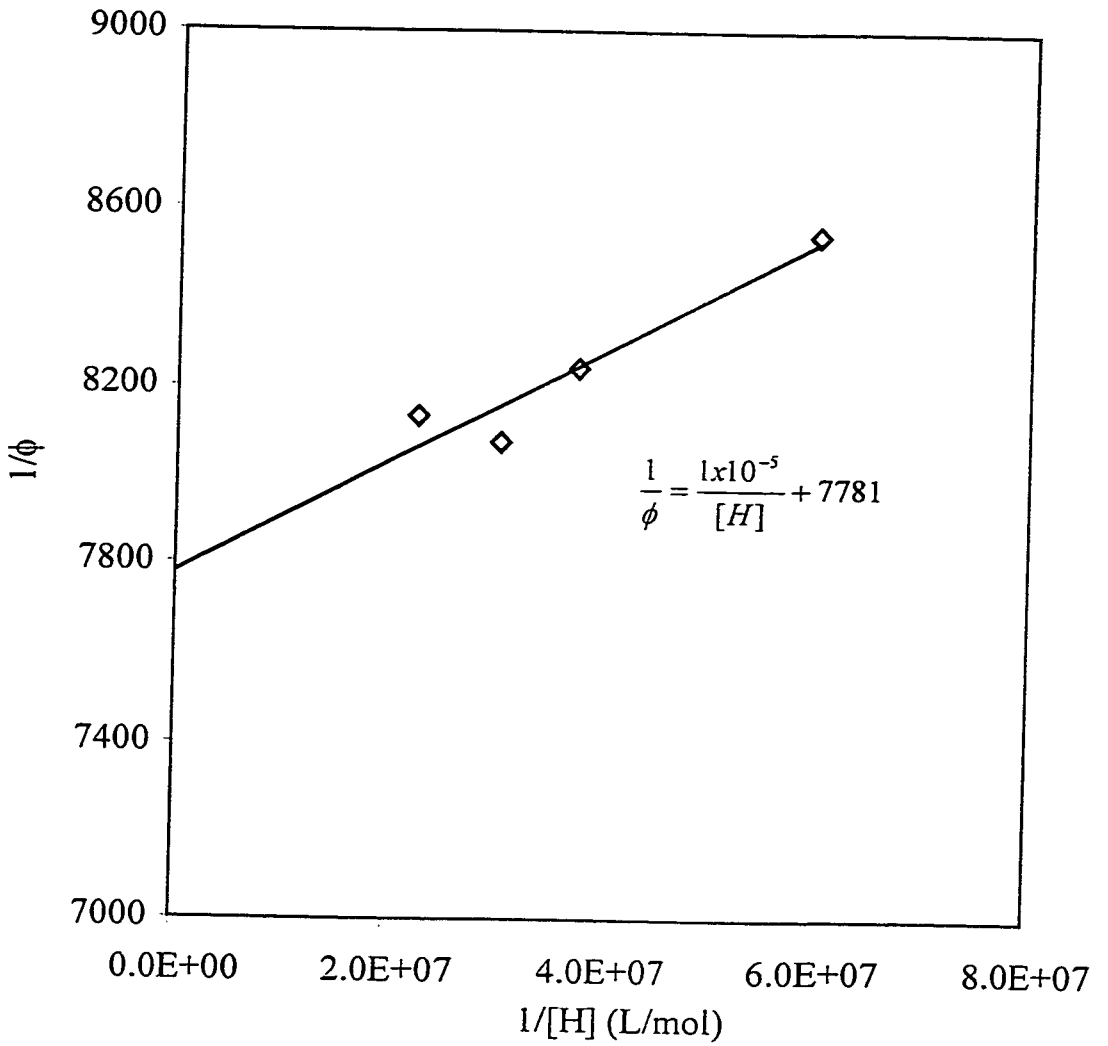

Figure 38: Photodegradation of DR at low concentration of Aldrach humic (Ha): A plot of 1/ϕ against 1/[H] for the DR photodegradation within 10 mM Tween 80 micelle and various humic concentrations.

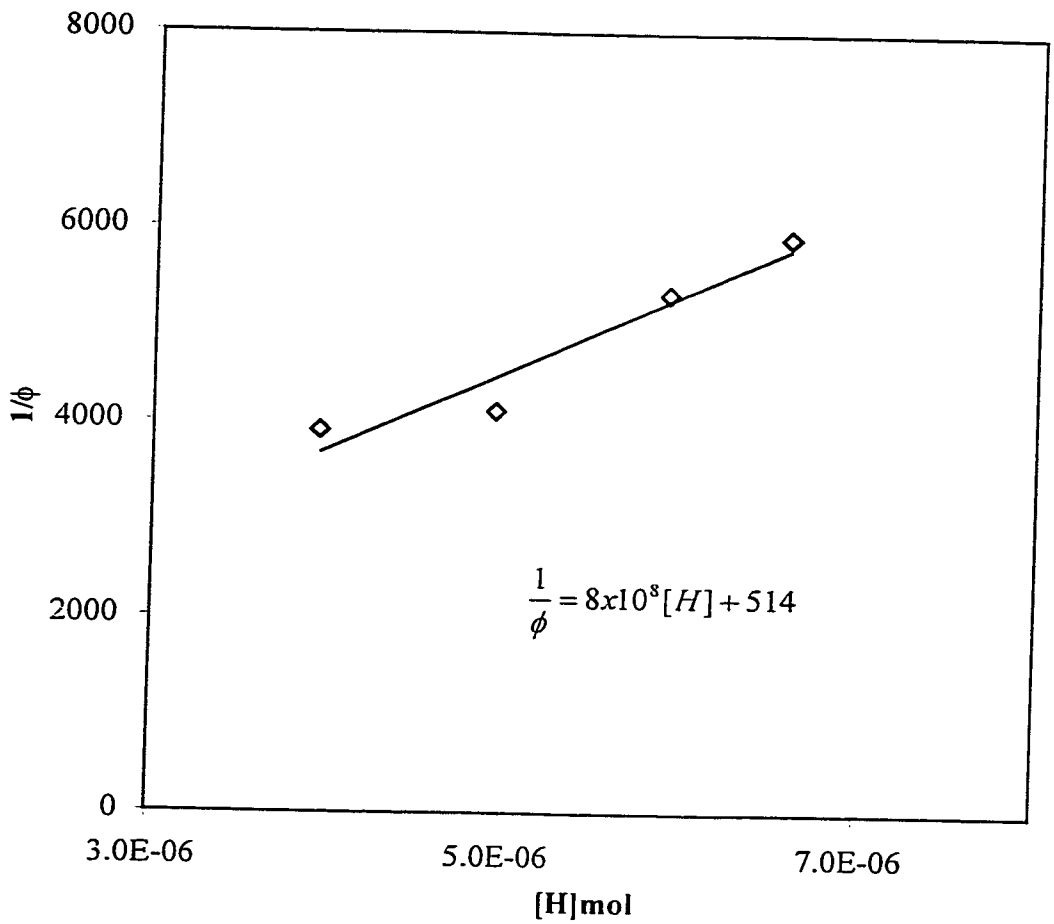

Figure 39: Photodegradation of DR at high concentration of Soil Extracted Material (SEM): A plot of 1/ϕ against [H] for the DR photodegradation within 10 mM Tween 80 micelle and various SEM concentrations.

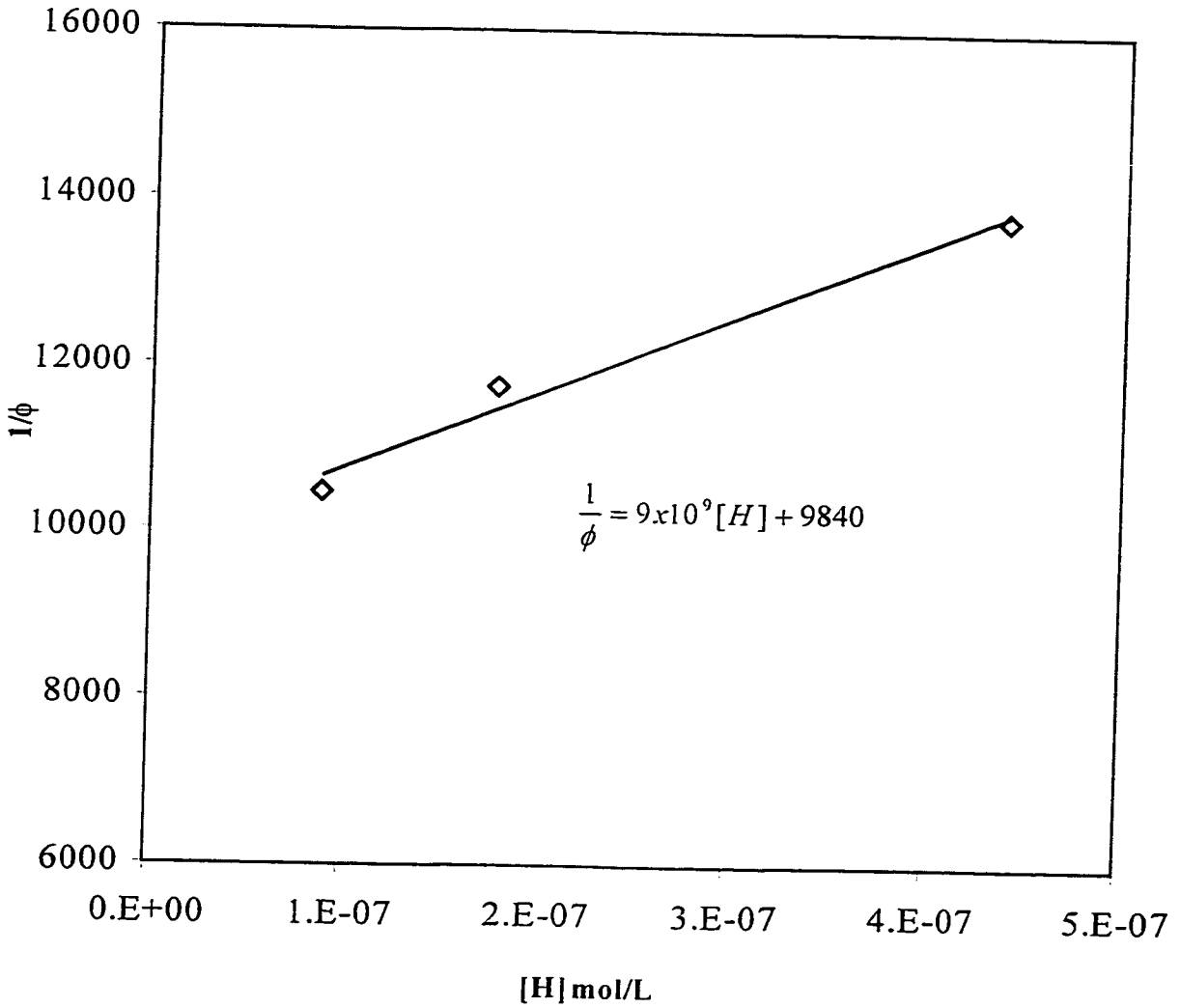

Figure 40: Photodegradation of DR at high concentration of Aldrich humic (Ha): A plot of 1/ϕ against [H] for the DR photodegradation within 10 mM Tween 80 micelle and various humic concentrations.

CHAPTER 7: CONCLUSION AND RECOMMENDATION

7.1. Conclusion

On the first part of this research, Advanced Chemical Oxidation, a quantitative estimation of direct ozonation and indirect free radical oxidation of dyes with assorted chromophores was studied through the examination of reaction kinetics in the ozonation process. The reaction kinetics of dye ozonation under different conditions was determined by adjusting the ozone doses, dye concentration, and reaction pH. The ozonation of dyes was found dominant by pseudo first-order reaction, and the rate constants decreased as the dye/ozone ratio increased. For all selected azo dyes, the dye decay rates increased as the initial pH of the solution increased, yet the decay rates of anthraquinone dyes would decrease in the same situation because of their insensible structure for ozone oxidation, formation of leuco-form, and higher solubility at a lower pH. The ozonation of dyes at a high pH contributed by hydroxyl free radicals was qualitatively verified by the use of a free radical scavenger. A proposed model, in another way, quantitatively determines the fraction of contribution for dye decomposition between free radical oxidation and direct ozonation.

For photodegradation reaction, the photodegradation rate of dye materials in water strongly depends on dye's physical, chemical characteristics and the initial pH of the solutions. The solubility of the dye molecules and the pH of the solution are the predominant factors to determine the efficiency of photodegradation at 253.7 nm. In general, the higher the dye solubility and the higher the initial pH, the higher the efficiencies of dye photodegradation. The free radical reaction can be proven as the dominant mechanism in photodegradation by the way of adding carbonate (the free radical quencher) to the solution. The photodegradation of dyes follows the pseudo first-order kinetics. The rate constants for selected dyes fall into the range of $3.3\times10^{-6}s^{-1}$ to $1.5\times10^{-4}s^{-1}$ depending on the solution pH, dye characteristics and the presence of sensitizers. The efficiency of dye degradation can be ranked in the following ascending order at high pH: insoluble anthraquinone < soluble anthraquinone < disazo ≈ triazo < polyazo < Cu monoazo. The ranking of polyazo dye will be depressed at lower pH due to

the insufficient free radicals in the solution and the change of electrophilic character of the azo groups. Moreover, Acetone, one of the well-known photo-sensitizer, can further speed up the UV-decolourization of dyes to 13 to 63 times faster for hydrophilic dyes and 139 times for hydrophobic dye.

On the second part of this research, remediation of CADs polluted soil by surfactant micellar/UV system, the photodegradation rate of hydrophobic chlorinated aromatic dye (CAD) within Brij 52, Tween 80, Tween 20 & Tween 60 micellar solution were 1.8, 1.9, 2.1 & 2.8 times higher than that of CAD dissolving within D.I. water only, respectively. This process may eventually prove to be a useful technology in the application of soil-washing of CAD polluted soil or sediments. In conclusion, the solubility of the dye molecules is found to be important in determining the efficiency of photodegradation. Various non-ionic surfactants can not only enhance the CAD's solubility, but also speed up the photodegradation. The degradation rate, in fact, depends on the micelle-water partition coefficient (K_m) and the potential of the selected surfactant to act as the hydrogen source. Three stages of photodegradation were identified, in which an initial lag stage is followed by a rapid decay stage (pseudo first-order) and a retardation stage.

Photoreduction of DR involves two major mechanisms: at first chlorine is removed from the dye molecules via photodechlorination in which HCl is generated as photoproducts. After the photodechlorination, photodecolorization of the dye is followed by breaking the azo bond in an extended exposure of UV light. The overall reaction rates can be further improved by using an additional hydrogen source or photosensitizer. Under these circumstances, the initial lag stage will vanish and the photodecay rate of DR will increase by 1.5, 2, 2.5 & 2.6 times than that without any $BNaH_4$ after 0.001, 0.01, 0.05 & 0.1 mol/L of $BNaH_4$ adding to the system, respectively. Likewise, decay rate of DR were also increased about 3.6 times from $2.28 \times 10^{-4} s^{-1}$ (surfactant only without acetone added) to $8.25 \times 10^{-4} s^{-1}$ (surfactant with 2.04 mol/L acetone).

From the study of the photodegradation rate of hydrophobic Chlorinated Aromatic Dye (CAD) in the presence of humic materials within micellar solution, it was interesting to

find that the low dose of humics (no matter the Aldrich humic (Ha) or Soil Extracted Materials (SME)) would improve the photodecay rate of Disperse Red (DR). Humics (Ha < 0.0333 μmol/L) can significantly increase the photodegradation quantum yield (Φ) by 16 % from 1.068×10^{-4} (surfactant only without humic) to 1.238×10^{-4} (surfactant with 0.0333 μmol/L Ha). Likewise, in the presence of low concentration of Soil Extracted Material (surfactant with 3.96 μmol/L SEM), the quantum yield of DR decay was increased by about 239% to 2.554×10^{-4}. The quantum yield improvement is likely due to the increment of available hydrogen sources in the solution, which was known critical to the photoreduction reactions. However, as the humic concentration was further increased, the reduction of quantum yield in dye degradation was observed. This is because light attenuation by high dose of humic and humic could inhibit free radical chain reactions i.e. acted as a quencher of photochemical reaction. In order to verify the proposed rate improving/quenching mechanisms, a mathematical model based on possible reaction mechanisms in this system was proposed.

7.3. Recommendation

According to the experimental results, Advanced Chemical Oxidation (ACO) can be employed for dye degradation. Nevertheless, the low degradation rate was considered to be the main drawback. In fact, other materials present like carbonates and low concentration of dyestuffs in the dye effluent may further lower the efficiency of the ACO performance. Therefore, further study should be concentrated to evaluate the ways to increase the degradation rate. For example, the indirect photodegradation: the selection of the solvent can not only enhance the dye solubility, but also act as a photosensitizer to speed up the degradation rate. Acetone and other ketone solvent may be a suitable class being selected. Moreover, there is still much room to explore the use of the sun light (i.e. low energy input by solar energy) in this photosensitization process. Moreover, the roles of intermediates during dye ozonation and photodegradation were still uncertain, further study for this aspect was encouraged.

For the use of surfactant for remediation of the hydrophobic aromatic dyes polluted soil or sediment, based on the results presented in this thesis, the solubility enhanced of CAD by surfactant follow by photolytic destruction is a promising method. A further study to examine the application of this technique in different type of soil or sediments to solve the real world problem. Finally, a continuous pilot scale reactor for the dyes removal by both ACO and surfactant soil remediation is needed as a next step to further develop.

APPENDIX A

DATA OF

OZONATION OF AROMATIC DYES

Ozonation of Aromatic Dyes:

Quantitative Analysis of Dissolving Ozone.

Exp. No OC-1

Aim: Calibration values for Ozone concentration measurement:

Solution:

Standard iodine solution 0.01 N: containing 6.4g potassium iodide and 1.2692 g of iodine in each 1000 mL of solution. One ml of 0.01 N iodine (triiodide) is equivalent to 240 μg ozone.

5 % Neutral potassium iodide reagent: containing 13.61 g potassium dihydrogen-phosphate, 14.2 g anhydrous disodium hydrogen phosphate and 20.0 g potassium iodide in each 1000 mL of solution.

Standard iodine solution was then diluted to a solution of iodine 4 x 10^{-5} N (1 ml = 0.96 μg ozone). Different portions of this standard iodine solution were diluted with 5% neutral potassium iodide reagent.

Table 16: The values of ozone calibration curve

[Ozone/I_2 measurement]	
Conc. [mg/L]	Abs*
0	0
0.096	0.049
0.24	0.103
0.48	0.232
0.96	0.513
1.44	0.751
1.92	1.022

*Absorbance of the ozone solution by UV/VIS spectrometer at λ= 352nm.

Ozone Concentration Measurement at Different pH Solutions under Different Air Input Flowrates and Different pH

Exp. No: OC-2

Solution:

Neutral potassium iodide reagent: containing 13.61g potassium dihydrogen-phosphate, 14.2 g anhydrous disodium hydrogen phosphate and 20.0 g potassium iodide in each 1000mL of solution.

Concentration of dissolving ozone (mmol/L) under input air flowrate: 1, 2, 3 and 4 L/min

	Solution pH: 4			Solution pH: 7				Solution pH: 10		
Time (min)	Flow rate (L/min)			Flow rate (L/min)				Flow rate (L/min)		
	1	2	3	1	2	3	4	1	2	3
0	0	0	0	0	0	0	0	0	0	0
1	0.11	0.12	0.14	0.04	0.10	0.08	0.17	0.09	0.10	0.11
2	0.13	0.18	0.15	0.06	0.14	0.11	0.20	0.09	0.16	0.12
3	0.14	0.20	0.18	0.10	0.18	0.14	0.23	0.10	0.15	0.15
4	0.16	0.21	0.22	0.12	0.18	0.18	0.27	0.11	0.23	0.22
5	0.15	0.21	0.27	0.14	0.19	0.20	0.33	0.15	0.25	0.25
10	0.18	0.21	0.28	0.18	0.21	0.24	0.34	0.19	0.25	0.27
15	0.17	0.23	0.28	0.18	0.23	0.26	0.35	0.20	0.25	0.28
20	0.17	0.22	0.29	0.19	0.23	0.24	0.35	0.20	0.26	0.29
25	0.18	0.22	0.30	0.20	0.23	0.25	0.36	0.20	0.25	0.30
30	0.18	0.21	0.30	0.20	0.22	0.26	0.36	0.21	0.25	0.29

Ozonation of Soluble Anthraquninone (A1)

Exp. No O-1:

Aim: effect of initial pH & different dye/ozone ratio in the reaction system:

Solution preparation:
Soluble Anthraquninone (A1): Molecular weight: 625 g/mol
Initial pH: 4,7,10
Initial A1 concentration: 0.036, 0.072 & 0.144 mmol/L

The concentration of A1 (mg/L) at different time interval

		Time (min)						
Dye (mmol/L)	pH	0	5	15	30	60	120	180
0.072	4	44.980	32.674	26.756	19.853	12.478	5.145	0.729
0.144	7	87.910	72.436	63.098	54.560	39.560	17.582	5.469
0.072	7	45.980	40.004	28.048	22.990	13.794	4.598	0.000
0.036	7	21.990	16.165	12.233	8.796	4.398		
0.072	10	44.680	32.681	25.142	17.683	10.933	4.500	1.697

C/Co of A1 at different time interval

		Time (min)						
Dye (mmol/L)	pH	0	5	15	30	60	120	180
0.072	4	1	0.726	0.595	0.441	0.277	0.114	0.016
0.144	7	1	0.824	0.718	0.621	0.450	0.200	0.062
0.072	7	1	0.870	0.610	0.500	0.300	0.100	0.000
0.036	7	1	0.735	0.556	0.400	0.200		
0.072	10	1	0.731	0.563	0.396	0.245	0.101	0.038

In (C/Co) of A1 at different time interval

		Time (min)						
Dye (mmol/L)	pH	0	5	15	30	60	120	180
0.072	4	0	-0.320	-0.519	-0.818	-1.282	-2.168	-4.122
0.144	7	0	-0.194	-0.332	-0.477	-0.799	-1.609	-2.777
0.072	7	0	-0.139	-0.494	-0.693	-1.204	-2.303	
0.036	7	0	-0.308	-0.586	-0.916	-1.609		
0.072	10	0	-0.313	-0.575	-0.927	-1.408	-2.296	-3.271

Reaction rates

Dye (mmol/L)	pH	Dye/ozone	Slope	Intercept	R square	Kinetic rate constant ($x\ 10^{-4}\ s^{-1}$)
0.072	4	0.42	-0.0208	- 0.1008	0.9747	3.47
0.144	7	0.80	-0.0145	- 0.0357	0.9878	2.42
0.072	7	0.40	-0.0186	- 0.0926	0.9922	3.10
0.036	7	0.20	-0.0254	- 0.1255	0.9819	4.23
0.072	10	0.38	-0.0171	- 0.2518	0.986	2.85

Changes of pH at different time interval

		Time (min)						
Dye (mmol/L)	pH	0	5	15	30	60	120	180
0.072	4	4.04	4	3.96	3.95	3.86	3.81	3.78
0.144	7	7.11	6.97	6.5	6.23	5.26	4.69	4.69
0.072	7	7.54	6.98	6.84	6.68	6.24	5.2	4.94
0.036	7	7.24	7.03	7.05	6.61	6.11	4.89	4.71
0.072	10	10.24	9.71	8.87	8.25	7.89	7.25	7.01

Ozonation of Insoluble Anthraquninone (A2)

Exp. No O-2:

Aim: effect of initial pH

Solution preparation:
Insoluble Anthraquninone (A2): Molecular weight: 307 g/mol

Initial pH: 4,7,10
Initial A2 concentration: 0.072 mmol/L

The concentration of A2 (mg/L) at different time interval

	Time (min)						
pH	0	5	15	30	60	120	180
4	22.300	21.790	18.112	12.846	8.294	4.928	3.591
7	23.210	21.192	16.913	14.528	12.304	10.699	9.516
10	22.690	21.105	19.764	17.248	11.416	8.545	7.473

C/Co of A2 at different time interval

	Time (min)						
pH	0	5	15	30	60	120	180
4	1	0.977	0.812	0.576	0.372	0.221	0.161
7	1	0.913	0.729	0.626	0.530	0.461	0.410
10	1	0.930	0.871	0.760	0.503	0.377	0.329

In (C/Co) of A2 at different time interval

	Time (min)						
pH	0	5	15	30	60	120	180
4	0	-0.023	-0.208	-0.552	-0.989	-1.510	-1.826
7	0	-0.091	-0.317	-0.468	-0.635	-0.774	-0.892
10	0	-0.072	-0.138	-0.274	-0.687	-0.977	-1.111

Reaction rates

Dye (mmol/L)	pH	Dye/ozone	slope	Intercept	R square	Kinetic rate constant ($\times 10^{-4}$ s^{-1})
0.072	4	0.42	-0.0105	- 0.1131	0.9494	1.75
0.072	7	0.40	-0.007	- 0.1886	0.8258	1.17
0.072	10	0.38	-0.0065	- 0.0867	0.928	1.08

Changes of pH at different time interval

	Time (min)						
pH	0	5	15	30	60	120	180
4	3.99	3.95	3.89	3.8	3.81	3.79	3.78
7	6.86	6.51	6.11	5.51	5.21	5.01	4.89
10	10.17	9.87	9.26	8.99	8.51	8.02	7.41

Ozonation of Disazo Vinylsulphonate (AZ2)

Exp. No O-3:
Aim: effect of initial pH & different dye/ozone ratio in the reaction system:

Solution preparation:
Disazo Vinylsulphonate (AZ2): Molecular weight: 976 g/mol

Initial pH: 4,7,10
Initial AZ2 concentration: 0.036, 0.072 & 0.144 mmol/L

The concentration of AZ2 (mg/L) at different time interval

		Time (min)						
Dye (mmol/L)	pH	0	5	15	30	60	120	180
0.072	4	70.32	63.3	46.83	35.37	16.04	4.44	2.01
0.144	7	140	128.54	109.43	90.72	63.84	41.44	24.64
0.072	7	69.98	60.89	42.55	22.39	11.2	3.359	1.12
0.036	7	35.23	27.22	12.97	6.482	2.255	0.282	
0.072	10	68.99	56.73	42.65	13.45	4.829	1.565	

C/Co of AZ2 at different time interval

		Time (min)						
Dye (mmol/L)	pH	0	5	15	30	60	120	180
0.072	4	1	0.900	0.666	0.503	0.228	0.063	0.029
0.144	7	1	0.918	0.782	0.648	0.456	0.296	0.176
0.072	7	1	0.870	0.608	0.320	0.160	0.048	0.016
0.036	7	1	0.773	0.368	0.184	0.064	0.008	
0.072	10	1	0.822	0.618	0.195	0.070	0.023	

In (C/Co) of AZ2 at different time interval

		Time (min)						
Dye (mmol/L)	pH	0	5	15	30	60	120	180
0.072	4	0	-0.105	-0.406	-0.687	-1.478	-2.762	-3.557
0.144	7	0	-0.085	-0.246	-0.434	-0.785	-1.217	-1.737
0.072	7	0	-0.139	-0.498	-1.139	-1.833	-3.037	-4.135
0.036	7	0	-0.258	-1.000	-1.693	-2.749	-4.828	
0.072	10	0	-0.196	-0.481	-1.635	-2.659	-3.786	

Reaction rate

Dye (mmol/L)	pH	Dye/ozone	Slope	Intercept	R square	Kinetic rate constant ($\times 10^{-4}$ s^{-1})
0.072	4	0.42	-0.0204	- 0.0923	0.9883	3.40
0.144	7	0.8	-0.0094	- 0.0924	0.9863	1.57
0.072	7	0.4	-0.0229	- 0.2009	0.9832	3.81
0.036	7	0.2	-0.0395	- 0.2416	0.9858	7.07
0.072	10	0.38	-0.0325	- 0.2151	0.9413	5.41

Changes of pH in different time interval

		Time (min)						
Dye (mmol/L)	pH	0	5	15	30	60	120	180
0.072	4	3.98	3.96	3.94	3.9	3.82	3.65	3.59
0.144	7	6.84	5.65	5.21	4.98	4.38	4.06	4.03
0.072	7	7.90	6.91	6.63	5.85	5.01	4.40	4.21
0.036	7	7.90	6.63	6.11	5.95	5.57	4.40	4.11
0.072	10	10.31	7.76	7.47	6.98	5.97	4.55	4.21

Ozonation of Triazo (AZ3)

Exp. No O-4:
Aim: effect of initial pH & different dye/ozone ratio in the reaction system:

Solution preparation:
Triazo (AZ3): Molecular weight: 1286 g/mol

Initial pH: 4,7,10
Initial AZ3 concentration: 0.036, 0.072 & 0.144 mmol/L

The concentration of AZ3 (mg/L) at different time interval

		Time (min)						
Dye (mmol/L)	pH	0	5	15	30	60	120	180
0.072	4	92.620	81.686	71.595	56.498	48.162	37.974	27.786
0.144	7	180.23	167.25	148.69	131.75	100.93	63.621	42.174
0.072	7	93.050	82.066	70.297	59.000	37.220	23.263	13.958
0.036	7	47.02	32.687	25.473	19.727	12.616	5.8722	
0.072	10	91.890	72.899	58.394	47.702	28.262	14.804	8.972

C/Co of AZ3 at different time interval

		Time (min)						
Dye (mmol/L)	pH	0	5	15	30	60	120	180
0.072	4	1	0.882	0.773	0.610	0.520	0.410	0.300
0.144	7	1	0.928	0.825	0.731	0.560	0.353	0.234
0.072	7	1	0.882	0.755	0.634	0.400	0.250	0.150
0.036	7	1	0.695	0.542	0.420	0.268	0.125	
0.072	10	1	0.793	0.635	0.519	0.308	0.161	0.098

In (C/Co) of AZ3 at different time interval

		Time (min)						
Dye (mmol/L)	pH	0	5	15	30	60	120	180
0.072	4	0	-0.126	-0.257	-0.494	-0.654	-0.892	-1.204
0.144	7	0	-0.075	-0.192	-0.313	-0.580	-1.041	-1.452
0.072	7	0	-0.126	-0.280	-0.456	-0.916	-1.386	-1.897
0.036	7	0	-0.364	-0.613	-0.869	-1.316	-2.080	
0.072	10	0	-0.232	-0.453	-0.656	-1.179	-1.826	-2.326

Reaction rates

Dye (mmol/L)	pH	Dye/ozone	slope	Intercept	R square	Kinetic rate constant ($\times 10^{-4}$ s^{-1})
0.072	4	0.42	-0.0062	- 0.1569	0 9358	1.03
0.144	7	0.8	-0.008	- 0.0544	0.9951	1.33
0.072	7	0.4	-0.0103	- 0.1171	0.9814	1.71
0.036	7	0.2	-0.0159	- 0.2624	0.9575	2.65
0.072	10	0.38	-0.0125	- 0.2183	0.9704	2.08

Changes of pH at different time interval

		Time (min)						
Dye (mmol/L)	pH	0	5	15	30	60	120	180
0.072	4	4.11	4.07	4.07	4.02	4	3.87	3.86
0.144	7	7.01	6.91	6.21	5.51	5.12	4.58	4.2
0.072	7	7.43	6.8	6.45	5.91	4.89	4.65	4.55
0.036	7	6.52	6.08	5.95	5.27	5.01	4.82	4.62
0.072	10	10.21	7.41	7.02	7.01	6.98	6.38	6.29

Ozonation of Polyazo (AZ5)

Exp. No O-5:
Aim: effect of initial pH & & quenching effect of additional carbonate:

Solution preparation:
Polyazo (AZ5): Molecular weight: 1373 g/mol

Initial pH: 4,7,10
Initial AZ5 concentration: 0.036, 0.072 & 0.144 mmol/L
Sodium Carbonate: 0.5 mol/L

The concentration of AZ5 (mg/L) at different time interval

	Time (min)						
pH	0	5	15	30	60	120	180
4	98.840	93.000	73.240	57.130	41.62	20.756	7.886
7	97.890	92.151	72.341	56.287	40.918	18.621	7.876
10	98.590	79.602	64.785	51.631	34.229	17.128	5.915
carbonate	97.900	92.831	83.326	74.138	53.100	28.451	21.227

C/Co of AZ5 at different time interval

	Time (min)						
pH	0	5	15	30	60	120	180
4	1	0.941	0.741	0.578	0.421	0.210	0.080
7	1	0.941	0.739	0.575	0.418	0.190	0.080
10	1	0.807	0.657	0.524	0.418	0.190	0.080
Carbonate	1	0.948	0.851	0.757	0.542	0.291	0.217

In (C/Co) of AZ5 at different time interval

	Time (min)						
pH	0	5	15	30	60	120	180
4	0	-0.060	-0.300	-0.548	-0.865	-1.561	-2.520
7	0	-0.060	-0.302	-0.553	-0.872	-1.660	-2.520
10	0	-0.214	-0.420	-0.647	-1.058	-1.750	-2.813
Carbonate	0	-0.053	-0.161	-0.278	-0.612	-1.236	-1.529

Reaction rates

Dye (mmol/L)	pH	Dye/ozone	Slope	Intercept	R square	Kinetic rate constant ($x\ 10^{-4}\ s^{-1}$)
0.072	4	0.42	-0.0137	-0.0553	0.996	2.28
0.072	7	0.4	-0.0137	- 0.0507	0.997	2.28
0.072	10	0.38	-0.0146	- 0.13	0.991	2.43
0.072	Carbonate	0.38	-0.0089	- 0.0324	0.985	1.48

Changes of pH in different time interval

	Time (min)						
pH	0	5	15	30	60	120	180
4	3.85	3.84	3.82	3.82	3.82	3.82	3.81
7	6.62	6.52	6.42	6.09	5.85	4.26	4.04
10	10.24	7.24	7.13	7.09	6.54	6.01	5.12
Carbonate	11.01	10.97	10.93	10.87	10.78	10.63	10.56

Ozonation of Monoazo (Cu Vinylsulphonate) (AM1)

Exp. No O-6:
Aim: effect of initial pH:

Solution preparation:
Monoazo (Cu Vinylsulphonate) (AM1): Molecular weight: 797 g/mol

Initial pH: 4,7,10
AM1 concentration: 0.072 mmol/L

The concentration of AM1 (mg/L) at different time interval

	Time (min)						
pH	0	5	15	30	60	120	180
4	57.830	47.848	29.451	18.725	10.225	0.000	0.000
7	57.450	47.353	35.456	18.002	9.314	0.000	0.000
10	56.980	44.861	32.442	16.936	5.419	0.000	0.000

C/Co of AM1 at different time interval

	Time (min)						
pH	0	5	15	30	60	120	180
4	1	0.827	0.509	0.323	0.177	0	0
7	1	0.824	0.617	0.313	0.162	0	0
10	1	0.787	0.569	0.297	0.095	0	0

In (C/Co) of AM1 at different time interval

	Time (min)						
pH	0	5	15	30	60	120	180
4	0	-0.189	-0.675	-1.128	-1.733		
7	0	-0.193	-0.483	-1.160	-1.819		
10	0	-0.239	-0.563	-1.213	-2.353		

Reaction rates

Dye (mmol/L)	pH	Dye/ozone	Slope	Intercept	R square	Kinetic rate constant ($\times 10^{-4}$ s^{-1})
0.072	4	0.4235	-0.030	-0.1261	0.9544	5.08
0.072	7	0.4	-0.031	- 0.0536	0.9803	5.13
0.072	10	0.3789	-0.039	- 0.0135	0.9991	6.52

Changes of pH at different time interval

	Time (min)						
pH	0	5	15	30	60	120	180
4	4.11	4.07	4.07	4.02	4	3.87	3.86
7	7.43	6.8	6.45	5.91	4.89	4.65	4.55
10	10.21	7.41	7.02	7.01	6.98	6.38	6.29

APPENDIX B

DATA OF

PHOTODEGRADATION OF AROMATIC DYES

Photodegradation of Soluble Anthraquninone (A1)

Exp. no: No UV1

Aim: effect of initial pH and photosensitization by acetone

Solution preparation:
Soluble Anthraquinone: Molecular weight: 625 g/mol
Initial pH: 4,7,10
Initial A1 concentration: 50 mg/L
Acetone: 0.05 mol/L
Light intensivity: 2.4 x 10^{-5} Einstein L^{-1} s^{-1}

The concentration of A1 (mg/L) in different time interval

	Time (min)							
pH	0	15	30	60	150	240	300	360
4	49.300	47.911	45.356	43.745	37.468	31.010	27.608	24.798
7	48.900	47.043	45.186	40.853	34.083	27.677	25.428	22.592
10	51.100	48.698	46.143	41.800	28.616	20.440	15.075	11.498
Acetone	57.000	2.481	2.608	2.290	0.891	0.827	0.954	0.954

C/Co of A1 at different time interval

	Time (min)							
pH	0	15	30	60	150	240	300	360
4	1	0.9718	0.92	0.8873	0.76	0.629	0.56	0.503
7	1	0.962	0.9241	0.8354	0.697	0.566	0.52	0.462
10	1	0.953	0.903	0.818	0.56	0.4	0.295	0.225
Acetone	1	0.0435	0.0458	0.0402	0.0156	0.0145	0.0167	0.0167

In (C/Co) of A1 at different time interval

	Time (min)							
pH	0	15	30	60	150	240	300	360
4	0	-0.029	-0.083	-0.12	-0.274	-0.464	-0.58	-0.687
7	0	-0.039	-0.079	-0.18	-0.361	-0.569	-0.654	-0.772
10	0	-0.048	-0.102	-0.201	-0.58	-0.916	-1.221	-1.492
Acetone	0	-3.134	-3.084	-3.214	-4.159	-4.233	-4.09	-4.09

Reaction rates

pH	Slope	Intercept	R square	Kinetic rate constant (x 10^{-5} s^{-1})
4	0.0019	-0.0059	0.9984	3.17
7	0.0021	-0.0211	0.996	3.50
10	0.0041	+0.0253	0.9979	6.83
Acetone	0.209	-5E-16	1	348

Changes of pH at different time interval

	Time (min)							
pH	0	15	30	60	150	240	300	360
4	4.08	4.07	4.07	4.05	4.02	4.01	4.01	3.99
7	7.05	6.95	6.89	6.5	6.02	5.68	5.5	5.39
10	9.95	9.25	9	8.65	7.8	7.21	6.75	6.56
Acetone	7.05	4.79	4.56	4.85	4.04	3.99	3.94	3.9

Photodegradation of Insoluble Anthraquninone (A2)

Exp. no: No UV2

Aim: effect of initial pH and photosensitization by acetone

Solution preparation:
Insoluble Anthraquninone (A2): Molecular weight: 307 g/mol
Initial pH: 4,7,10
Initial A2 concentration: 50 mg/L
Acetone: 0.05 M/L
Light intensivity: 2.4 x 10^{-5} Einstein L^{-1} s^{-1}

The concentration of A2 (mg/L) at different time interval

	Time (min)							
pH	0	15	30	60	150	240	300	360
4	48.23	47.401	47.125	46.296	45.468	45.468	44.661	43.258
7	49.12	48.979	48.557	48.135	47.995	47.010	46.588	45.181
10	49.50	48.906	47.717	47.420	46.826	46.232	45.935	45.340
Acetone	51.20	35.664	16.751	15.738	15.333	14.928	14.725	12.699

C/Co of A2 at different time interval

	Time (min)							
pH	0	15	30	60	150	240	300	360
4	1	0.983	0.977	0.960	0.943	0.943	0.926	0.897
7	1	0.997	0.989	0.980	0.977	0.957	0.948	0.920
10	1	0.988	0.964	0.958	0.946	0.934	0.928	0.916
Acetone	1	0.697	0.327	0.307	0.299	0.292	0.288	0.248

In (C/Co) of A2 at different time interval

	Time (min)							
pH	0	15	30	60	150	240	300	360
4	0	-0.017	-0.023	-0.041	-0.059	-0.059	-0.077	-0.109
7	0	-0.003	-0.012	-0.020	-0.023	-0.044	-0.053	-0.084
10	0	-0.012	-0.037	-0.043	-0.056	-0.068	-0.075	-0.088
Acetone	0	-0.362	-1.117	-1.180	-1.206	-1.233	-1.246	-1.394

Reaction rate

pH	Slope	Intercept	R square	Kinetic rate constant (x 10^{-5} s^{-1})
4	0.0002	-0.0135	0.9138	0.33
7	0.0002	-0.0013	0.9369	0.33
10	0.0002	-0.0179	0.8762	0.33
Acetone	0.0203	-0.1322	0.8071	33.83

Changes of pH at different time interval

	Time (min)							
pH	0	15	30	60	150	240	300	360
4	4.05	4.04	4.03	3.98	3.95	3.91	3.91	3.88
7	7.06	6.70	6.30	5.30	4.89	4.68	4.48	4.36
10	10.05	9.67	9.00	8.15	6.80	6.25	6.22	6.19
Acetone	7.06	5.10	4.18	4.27	4.09	3.97	3.96	3.91

Photodegradation of Disazo Vinylsulphonate (AZ2)

Exp. no: No UV3

Aim: effect of initial pH and photosensitization by acetone

Solution preparation:
Disazo Vinylsulphonate (AZ2): Molecular weight: 976 g/mol
Initial pH: 4,7,10
Initial AZ2 concentration: 50 mg/L
Acetone: 0.05 mol/L
Light intensivity: 2.4 x 10^{-5} Einstein L^{-1} s^{-1}

The concentration of AZ2 (mg/L) at different time interval

	Time (min)							
pH	0	15	30	60	150	240	300	360
4	50.220	46.562	44.948	40.107	33.437	26.659	21.280	19.128
7	51.110	44.035	42.320	38.435	29.778	21.096	18.706	16.662
10	49.950	44.409	40.437	33.223	23.815	16.497	11.239	7.992
Acetone	49.580	8.141	3.924	1.449	1.173	1.082	1.173	0.990

C/Co of AZ2 at different time interval

	Time (min)							
pH	0	15	30	60	150	240	300	360
4	1	0.927	0.895	0.799	0.666	0.531	0.424	0.381
7	1	0.862	0.828	0.752	0.583	0.413	0.366	0.326
10	1	0.889	0.810	0.665	0.477	0.330	0.225	0.160
Acetone	1	0.164	0.079	0.029	0.024	0.022	0.024	0.020

In (C/Co) of AZ2 at different time interval

	Time (min)							
pH	0	15	30	60	150	240	300	360
4	0	-0.076	-0.111	-0.225	-0.407	-0.633	-0.859	-0.965
7	0	-0.149	-0.189	-0.285	-0.540	-0.885	-1.005	-1.121
10	0	-0.118	-0.211	-0.408	-0.741	-1.108	-1.492	-1.833
Acetone	0	-1.807	-2.537	-3.533	-3.744	-3.825	-3.744	-3.914

Reaction rates

pH	Slope	Intercept	R square	Kinetic rate constant (x 10^{-5} s^{-1})
4	0.0026	-0.0286	0.9947	4.33
7	0.003	-0.0791	0.9867	5.00
10	0.0048	-0.0428	0.9937	8.00
Acetone	0.0846	-0.1795	0.9433	141

Changes of pH at different time interval

	Time (min)							
pH	0	15	30	60	150	240	300	360
4	4.14	4.14	4.14	4.13	4.12	4.11	4.07	4.1
7	7	6.43	6.34	6.27	6.2	5.82	5.73	5.61
10	10.06	9.68	9.65	9.2	8	7.5	7.2	6.96
Acetone	7	4.21	4	4.24	4.14	4.05	4.01	4

Photodegradation of Triazo (AZ3)

Exp. no: No UV4

Aim: effect of initial pH and photosensitization by acetone

Solution preparation:
Triazo (AZ3): Molecular weight: 1286 g/mol
Initial pH: 4,7,10
Initial AZ3 concentration: 50 mg/L
Acetone: 0.05 mol/L
Light intensivity: 2.4 x 10^{-5} Einstein L^{-1} s^{-1}

The concentration of AZ3 (mg/L) at different time interval

	Time (min)							
pH	0	15	30	60	150	240	300	360
4	49.910	48.090	43.843	40.809	33.390	26.802	21.411	17.968
7	50.650	47.245	43.273	38.190	31.251	24.869	22.845	19.095
10	49.330	46.870	43.918	37.639	22.199	14.889	11.444	7.646
Acetone	50.120	32.206	13.900	4.862	1.151	1.085	0.955	0.889

C/Co of AZ3 at different time interval

	Time (min)							
pH	0	15	30	60	150	240	300	360
4	1	0.964	0.878	0.818	0.669	0.537	0.429	0.360
7	1	0.933	0.854	0.754	0.617	0.491	0.451	0.377
10	1	0.950	0.890	0.763	0.450	0.302	0.232	0.155
Acetone	1	0.643	0.277	0.097	0.023	0.022	0.019	0.018

In (C/Co) of AZ3 at different time interval

	Time (min)							
pH	0	15	30	60	150	240	300	360
4	0	-0.037	-0.130	-0.201	-0.402	-0.622	-0.846	-1.022
7	0	-0.070	-0.157	-0.282	-0.483	-0.711	-0.796	-0.976
10	0	-0.051	-0.116	-0.270	-0.799	-1.198	-1.461	-1.864
Acetone	0	-0.442	-1.283	-2.333	-3.774	-3.833	-3.961	-4.032

Reaction rates

pH	Slope	Intercept	R square	Kinetic rate constant (x 10^{-5} s^{-1})
4	0.0027	-0.012	0.9945	4.50
7	0.0026	-0.0623	0.9867	3.33
10	0.0051	-0.0201	0.9977	8.50
Acetone	0.0428	+0.0663	0.9689	71.33

Changes of pH at different time interval

	Time (min)							
pH	0	15	30	60	150	240	300	360
4	3.98	3.95	3.94	3.96	3.92	3.89	3.88	3.86
7	7.21	6.98	6.70	6.60	6.40	6.20	6.10	6.07
10	10.15	9.90	9.68	9.24	8.60	7.23	7.15	7.12
Acetone	7.21	5.14	5.06	4.78	4.15	4.11	4.15	4.10

Photodegradation of Polyazo (AZ5)

Exp. no: No UV5
Aim: effect of initial pH, photosensitization by acetone & quenching effect of additional carbonate:

Solution preparation:
Polyazo (AZ5): Molecular weight: 1373 g/mol
Initial pH: 4,7,10
Initial AZ5 concentration: 50 mg/L
Acetone: 0.05 mol/L
Sodium carbonate solution: 0.1 mol/L
Light intensivity: 2.4 x 10^{-5} Einstein L^{-1} s^{-1}

The concentration of AZ5 (mg/L) in different time interval

	Time (min)							
pH	0	15	30	60	150	240	300	360
4	49.200	48.371	47.134	44.969	39.360	35.129	32.620	31.488
7	50.220	46.687	41.576	34.652	23.654	16.070	13.760	12.605
10	49.550	44.710	40.219	31.673	17.458	6.342	2.973	1.587
Carbonate	50	49.698	49.347	48.283	46.734	41.742	40.615	3.999
Acetone	49.860	29.567	4.613	0.015	0.272	0.000	0.000	0.000

C/Co of AZ5 at different time interval

	Time (min)							
pH	0	15	30	60	150	240	300	360
4	1	0.983	0.958	0.914	0.800	0.714	0.663	0.640
7	1	0.930	0.828	0.690	0.471	0.320	0.274	0.251
10	1	0.902	0.812	0.639	0.352	0.128	0.060	0.032
carbonate	1	0.994	0.987	0.966	0.935	0.835	0.812	0.800
Acetone	1	0.593	0.093	0.000	0.005	0.000	0.000	0.000

In (C/Co) of AZ5 at different time interval

	Time (min)							
pH	0	15	30	60	150	240	300	360
4	0	-0.017	-0.043	-0.090	-0.223	-0.337	-0.411	-0.446
7	0	-0.073	-0.189	-0.371	-0.753	-1.139	-1.295	-1.382
10	0	-0.103	-0.209	-0.448	-1.043	-2.056	-2.813	-3.441
carbonate	0	-0.006	-0.013	-0.0349	-0.0676	-0.181	-0.208	-0.223
Acetone	0	-0.523	-2.380	-8.128	-5.210			

Reaction rates

pH	Slope	Intercept	R square	Kinetic rate constant (x 10^{-5} s^{-1})
4	0.0013	-0.0082	0.9917	2.17
7	0.004	-0.0713	0.982	6.67
10	0.0095	-0.107	0.9898	15.83
carbonate	0.0007	+0.0057	0.9731	1.67
Acetone	0.0793	+0.2225	0.9051	132.17

Changes of pH in different time interval

	Time (min)							
pH	0	15	30	60	150	240	300	360
4	4.25	4.25	4.25	4.24	4.23	4.21	4.21	4.20
7	7.23	7.10	7.05	7.00	6.64	6.50	6.40	6.35
10	9.86	9.24	8.64	7.28	6.77	6.70	6.68	6.60
carbonate	11.08	11.02	10.88	10.56	10.32	10.09	10.01	9.89
Acetone	7.23	4.85	4.21	3.91	3.81	3.71	3.61	3.56

Spectrum analysis of AZ5 with Photosenitizer (acetone: 0.05 mol/L) and without Photosensitizer

Solution preparation:
Polyazo (AZ5): Molecular weight: 1373 g/mol
Initial pH: 7
Initial AZ5 concentration: 50 mg/L
Acetone: 0.05 mol/L
Light intensivity: 2.4 x 10^{-5} Einstein L^{-1} s^{-1}

Scanned spectrum λ: from 205 nm to 700 nm.

AZ5 at initial pH7						AZ5 with Acetone				
Wavelength (λ nm)	0hr	2 hr	3hr	4hr	6 hr	Wavelength (λ nm)	Acetone only	0hr	1 hr	5 hr
205	1.60	1.59	1.60	1.46	1.34	205	0.55	1.67	2.11	2.32
220	1.60	1.60	1.60	1.58	1.37	220	0.30	0.97	1.14	1.26
235	0.89	0.85	0.80	0.72	0.58	235	0.67	0.79	0.80	0.76
250	0.53	0.51	0.47	0.39	0.27	250	1.10	0.65	0.84	0.78
265	0.49	0.47	0.42	0.34	0.30	265	1.10	0.68	0.84	0.87
280	0.54	0.47	0.42	0.32	0.21	280	0.75	0.67	0.66	0.75
295	0.55	0.45	0.40	0.29	0.19	295	0.28	0.57	0.41	0.47
310	0.43	0.39	0.35	0.27	0.17	310	0.07	0.37	0.26	0.27
325	0.31	0.33	0.30	0.24	0.16	325	0.04	0.26	0.19	0.18
340	0.28	0.30	0.28	0.22	0.14	340	0.03	0.24	0.13	0.13
355	0.32	0.32	0.29	0.22	0.13	355	0.03	0.29	0.10	0.10
370	0.36	0.33	0.30	0.22	0.13	370	0.02	0.33	0.07	0.08
385	0.36	0.33	0.29	0.21	0.12	385	0.02	0.32	0.05	0.06
400	0.38	0.34	0.29	0.20	0.11	400	0.02	0.35	0.04	0.04
415	0.41	0.34	0.29	0.19	0.10	415	0.02	0.38	0.03	0.03
430	0.43	0.34	0.29	0.18	0.09	430	0.02	0.42	0.03	0.03
445	0.47	0.35	0.29	0.16	0.08	445	0.02	0.47	0.02	0.02
460	0.56	0.38	0.31	0.16	0.07	460	0.02	0.60	0.02	0.02
475	0.71	0.44	0.35	0.15	0.06	475	0.02	0.80	0.02	0.02
490	0.90	0.52	0.39	0.15	0.06	490	0.02	1.05	0.02	0.02
505	1.09	0.58	0.43	0.15	0.05	505	0.02	1.26	0.02	0.02
520	1.18	0.59	0.43	0.14	0.04	520	0.02	1.35	0.01	0.01
535	1.20	0.56	0.39	0.12	0.04	535	0.02	1.33	0.01	0.01
550	1.07	0.44	0.30	0.08	0.03	550	0.02	0.89	0.01	0.01
565	0.62	0.24	0.17	0.05	0.02	565	0.02	0.34	0.01	0.01
580	0.21	0.10	0.07	0.03	0.01	580	0.02	0.09	0.01	0.01
595	0.05	0.04	0.03	0.02	0.01	595	0.02	0.03	0.01	0.01
610	0.01	0.02	0.02	0.01	0.00	610	0.02	0.02	0.01	0.01
625	0.01	0.01	0.01	0.01	0.00	625	0.02	0.01	0.01	0.01
640	0.00	0.01	0.01	0.00	0.00	640	0.02	0.01	0.01	0.01
655	0.00	0.00	0.01	0.00	0.00	655	0.01	0.01	0.01	0.01
670	0.00	0.00	0.00	0.00	0.00	670	0.01	0.01	0.01	0.01
685	0.00	0.00	0.00	0.00	0.00	685	0.01	0.01	0.01	0.01
700	0.00	0.00	0.00	0.00	0.00	700	0.02	0.01	0.01	0.01

Photodegradation of Polyazo (AM1)

Exp. no: No UV6

Aim: effect of initial pH and photosensitization by acetone.

Solution preparation:
Monoazo (Cu Vinylsulphonate) (AM1): Molecular weight: 797 g/mol
Initial pH: 4,7,10
Initial AM1 concentration: 50 mg/L
Acetone: 0.05 mol/L
Light intensivity: 2.4 x 10^{-5} Einstein L^{-1} s^{-1}

The concentration of AM1 (mg/L) at different time interval

	Time (min)							
pH	0	15	30	60	150	240	300	360
4	49.870	47.835	45.061	38.200	26.780	19.649	16.507	13.964
7	50.210	46.149	40.168	30.410	17.774	11.245	9.405	7.438
10	49.660	45.958	42.923	35.033	19.616	10.027	6.992	4.817
Acetone	49.990	17.014	10.739	8.842	8.551	9.280	5.632	3.444

C/Co of AM1 at different time interval

	Time (min)							
pH	0	15	30	60	150	240	300	360
4	1	0.959	0.904	0.766	0.537	0.394	0.331	0.280
7	1	0.919	0.800	0.606	0.354	0.224	0.187	0.148
10	1	0.925	0.864	0.705	0.395	0.202	0.141	0.097
Acetone	1	0.340	0.215	0.177	0.171	0.186	0.113	0.069

In (C/Co) of AM1 at different time interval

	Time (min)							
pH	0	15	30	60	150	240	300	360
4	0	-0.042	-0.101	-0.267	-0.622	-0.931	-1.106	-1.273
7	0	-0.084	-0.223	-0.501	-1.038	-1.496	-1.675	-1.910
10	0	-0.077	-0.146	-0.349	-0.929	-1.600	-1.960	-2.333
Acetone	0	-1.078	-1.538	-1.732	-1.766	-1.684	-2.183	-2.675

Reaction rates

pH	Slope	Intercept	R square	Kinetic rate constant (x 10^{-5} s^{-1})
4	0.0036	-0.0187	0.9941	5.00
7	0.0054	-0.0852	0.9848	8.33
10	0.0066	-0.0302	0.9992	11.00
Acetone	0.05132	-0.103	0.949	85.5

Changes of pH at different time interval

	Time (min)							
pH	0	15	30	60	150	240	300	360
4	3.90	3.86	3.83	3.78	3.75	3.73	3.72	3.71
7	7.18	7.00	6.80	6.03	5.48	5.12	4.82	4.64
10	9.60	9.10	8.65	7.98	7.32	6.87	6.42	6.40
Acetone	7.18	6.60	4.00	4.40	3.95	3.86	3.82	3.82

Photodegradation of Disazo AZ2 within different pH buffer solution

Exp. no: No UV7
Aim: effect of pH buffer solution.

Solution: Disazo Vinylsulphonate (AZ2): Molecular weight: 976 g/mol
Initial concentration: 50 mg/L

For pH 7 buffer
Additives: 0.08M sodium di-hydrogen phosphate/0.12 M di-sodium hydrogen phosphate

For pH 10 buffer
Additives: sodium tetraborate/sodium hydroxide

Light intensivity: 2.4 x 10^{-5} Einstein L^{-1} s^{-1}

The concentration of AZ2 (mg/L) in different pH buffer solution at different time interval:

	Time (min)							
	0	15	30	60	150	240	300	360
pH 7 buffer	51.226	45.845	44.642	41.671	32.162	24.269	20.951	17.980
pH 10 buffer	51.116	47.584	45.230	34.503	26.836	18.197	13.035	9.200

C/Co of AZ2 in different time interval

	Time (min)							
	0	15	30	60	150	240	300	360
pH 7 buffer	1	0.895	0.871	0.813	0.628	0.474	0.409	0.351
pH 10 buffer	1	0.931	0.885	0.675	0.525	0.356	0.255	0.180

In (C/Co) of AZ2 in different time interval

	Time (min)							
	0	15	30	60	150	240	300	360
pH 7 buffer	0	-0.111	-0.138	-0.206	-0.465	-0.747	-0.894	-0.1047
pH 10 buffer	0	-0.072	-0.122	-0.393	-0.644	-1.033	-1.366	-1.715

Reaction rates

pH	Slope	Intercept	R square	Kinetic rate constant (x 10^{-5} s^{-1})
pH 7 buffer	0.0028	-0.0406	0.9969	4.67
pH 10 buffer	0.0046	-0.0092	0.9916	7.67

APPENDIX C

DATA OF

PHOTODEGRADATION OF CHLORINATED

AROMATIC DYES (CAD) IN MICELLE

Photodegradation of Disperse Red (DR) in different surfactant micelle solution.

Exp. No S-1:

Solution: Insoluble Chlorinated Aromatic Dyes (CAD): Disperse Red (DR)
Initial pH: 7
Initial DR concentration: various
Molecular weight: 404 g/mol
Non-ionic surfactant: Tween 20, Tween 60, Tween 80 and Brij 52.
Surfactant concentration: 10 mmol/L
Light intensivity: 2.4 x 10^{-5} Einstein L^{-1} s^{-1}

The concentration of A1 (10^{-3} mmol) in different time interval

		Time (min)								
Surfactant	pH	0	2.5	5	15	30	45	60	90	120
Tween 20	7	31.600	31.501	31.468	27.860	19.086	14.978	11.882	8.374	6.794
Tween 60	7	36.600	36.452	35.991	31.359	20.606	15.226	11.309	6.613	4.685
Tween 80	7	27.760	27.720	27.472	24.997	18.433	14.751	12.103	8.606	6.662
Brij 52	7	3.730	3.713	3.681	3.271	2.055	1.652	1.268	0.850	0.653
D.I. water	7	2.680	2.680	2.653	2.621	2.535	2.348	2.056	1.721	1.461

C/Co of DR in different time interval

		Time (min)								
Surfactant	pH	0	2.5	5	15	30	45	60	90	120
Tween 20	7	1	0.997	0.996	0.882	0.604	0.474	0.376	0.265	0.215
Tween 60	7	1	0.996	0.983	0.857	0.563	0.416	0.309	0.181	0.128
Tween 80	7	1	0.999	0.990	0.900	0.664	0.531	0.436	0.310	0.240
Brij 52	7	1	0.995	0.987	0.877	0.551	0.443	0.340	0.228	0.175
D.I. water	7	1	1.000	0.990	0.978	0.946	0.876	0.767	0.642	0.545

In (C/Co) of DR in different time interval

		Time (min)								
Surfactant	pH	0	2.5	5	15	30	45	60	90	120
Tween 20	7	1	-0.003	-0.004	-0.126	-0.504	-0.747	-0.978	-1.328	-1.537
Tween 60	7	1	-0.004	-0.017	-0.155	-0.574	-0.877	-1.174	-1.711	-2.056
Tween 80	7	1	-0.001	-0.010	-0.105	-0.409	-0.632	-0.830	-1.171	-1.427
Brij 52	7	1	-0.005	-0.013	-0.131	-0.596	-0.814	-1.079	-1.478	-1.743
D.I. water	7	1	0.000	-0.010	-0.022	-0.056	-0.132	-0.265	-0.443	-0.607

Reaction rate and the solubility K_m values

Dye (mmol/L)	Concentration (mM)	Km (L/ mol)	slope	Intercept	R square	Kinetic rate constant (x 10^{-4} s^{-1})
Tween 20	0.0316	1179.25	-0.014	-0.024	0.975	2.300
Tween 60	0.0366	1365.78	-0.018	-0.024	0.993	3.067
Tween 80	0.0278	1035.97	-0.013	-0.010	0.991	2.100
Brij 52	0.0037	139.34	-0.012	0.013	0.980	2.000
D.I. water	0.0027	—	-0.007	0.077	0.983	1.100

Photodegradation of Disperse Red (DR) in different concentration of Tween 80 micelle solution.

Exp. No S-2

Solution:
Insoluble DR concentration: various
Initial pH: 7
Molecular weight: 404 g/mole
Surfactant: Tween 80
Surfactant concentration: 5 mmol/L, 10 mmol/L & 20 mmol/L.
Light intensivity: 2.4 x 10^{-5} Einstein L^{-1} s^{-1}

The concentration of DR (10^{-3} mmol) at different time interval

		Time (min)								
(concentration) mmol/L	pH	0	2.5	5	15	30	45	60	90	120
5	7	15.000	14.708	14.595	13.095	9.960	7.980	6.270	5.040	3.960
10	7	27.600	27.560	26.568	24.853	18.326	14.666	12.034	8.556	6.624
20	7	47.300	46.922	45.408	39.732	30.272	23.650	18.920	13.764	9.460

C/Co of DR at different time interval

		Time (min)								
(concentration) mmol/L	pH	0	2.5	5	15	30	45	60	90	120
5	7	1	0.981	0.973	0.873	0.664	0.532	0.418	0.336	0.264
10	7	1	0.999	0.963	0.900	0.664	0.531	0.436	0.310	0.240
20	7	1	0.992	0.960	0.840	0.640	0.500	0.400	0.291	0.200

In (C/Co) of DR at different time interval

		Time (min)								
(concentration) mmol/L	pH	0	2.5	5	15	30	45	60	90	120
5	7	0	-0.020	-0.027	-0.136	-0.409	-0.631	-0.872	-1.091	-1.332
10	7	0	-0.001	-0.010	-0.105	-0.409	-0.632	-0.830	-1.171	-1.427
20	7	0	-0.008	-0.041	-0.174	-0.446	-0.693	-0.916	-1.234	-1.609

Reaction rate

Dye (mmol/L)	Concentration (mM)	Km (L/mol)	slope	Intercept	R square	Kinetic rate constant (x 10^{-4} s^{-1})
5	0.015	560.373	-0.0118	-0.0194	0.9769	1.9667
10	0.0278	1035.97	-0.013	-0.010	0.991	2.100
20	0.0473	1766.31	-0.0138	-0.0044	0.9933	2.3000

Photodegradation of Disperse Red (DR) in Tween 80 micelle solution & quantitative analysis of the change of chloride ion concentration & colour during photodegradation

Exp. No S-3

Initial DR concentration: 0.0277 mmol/L
Molecular weight: 404 g/mol
Non-ionic surfactant: Tween 80
Surfactant concentration: 10 mmol/L
Light intensivity: 2.4 x 10^{-5} Einstein L^{-1} s^{-1}

The results of pH, DR, and chloride ion analysis by HPLC, pH meter, IC and UV-visible spectrometer at time interval

	Time (min)									
	0	2.5	5	15	30	60	90	120	180	300
pH	5.60	5.60	5.59	5.58	5.57	5.40	5.17	4.94	4.78	4.61
Chloride ion	3155880	3155901	3155900	3191934	3235880	3396640	3801116	4212000	4696741	5601997
D.R	243734	243654	241475	219724	162021	106388	75642	58562	19354	8797
UV-spectra	*0.83*	*0.825*	*0.816*	*0.798*	*0.79*	*0.75*	*0.491*	*0.371*	*0.228*	*0.086*

Concentration analysis of H^+ ion, D.R. & chloride ion (mM) at different time interval

	Time (min)									
	0	2.5	5	15	30	60	90	120	180	300
H+ ion	0	-0.00001	0.00004	0.00015	0.000179	0.0015	0.0042	0.009027	0.014	0.0222
Chloride ion	0	2E-07	2E-07	0.000374	0.000831	0.0025	0.0067	0.010967	0.016	0.0254
D.R (mM)	0.0277	0.0277	0.0274	0.0250	0.0184	0.0121	00860	0.0666	0.0220	0.010
UV-spectra	0.0291	0.0289	0.0286	0.0279	0.0275	0.0260	0.0172	0.0130	0.080	0.030

Photodegradation of Disperse Red (DR) within Tween 80 micelle solution with different initial pH.

Exp. No S-4

Initial DR concentration: various
Molecular weight: 404 g/mol
Non-ionic surfactant: Tween 80
Surfactant concentration: 10 mmol/L
Light intensivity: 2.4 x 10^{-5} Einstein L^{-1} s^{-1}

The concentration of DR (10^{-3} mmol) at different time interval

	Time (min)								
pH	0	2.5	5	15	30	45	60	90	120
5.5	27.760	27.393	26.207	23.318	18.877	14.879	11.983	9.050	6.302
7	27.760	27.720	27.472	24.997	18.433	14.751	12.103	8.606	6.662
10	29.770	28.817	27.954	24.054	18.041	14.677	11.065	6.728	4.078

C/Co of DR at different time interval

	Time (min)								
pH	0	2.5	5	15	30	45	60	90	120
5.5	1	0.987	0.944	0.840	0.680	0.536	0.432	0.326	0.227
7	1	*0.999*	*0.990*	*0.900*	*0.664*	*0.531*	*0.436*	*0.310*	*0.240*
10	1	0.968	0.939	0.808	0.606	0.493	0.372	0.226	0.137

In (C/Co) of DR at different time interval

	Time (min)								
pH	0	2.5	5	15	30	45	60	90	120
5.5	*0*	-0.013	-0.058	-0.174	-0.386	-0.624	-0.840	-1.121	-1.483
7	0	-0.001	-0.010	*-0.105*	*-0.409*	*-0.632*	*-0.830*	-1.171	-1.427
10	*0*	-0.033	-0.063	-0.213	-0.501	-0.707	-0.990	-1.487	-1.988

Reaction rate

Dye (mmol/L)	Concentration (mM)	Km (L/mol)	slope	Intercept	R square	Kinetic rate constant (x 10^{-4} s^{-1})
5.5	0.0278	1036	-0.013	-0.0006	0.9970	*2.10*
7	0.0278	1036	-0.013	-0.010	0.991	*2.10*
10	0.0298	1111	-0.0167	0.0161	0.9995	*2.78*

Photodegradation of Disperse Red (DR) within Tween 80 micelle solution with addition of $NaBH_4$

Exp. No S-5

Aim: Photodegradation of Disperse Red (DR) within Tween 80 micelle solution with hydrogen sources ($NaBH_4$) addition:

Initial DR concentration: various
Molecular weight: 404 g/mol
Non-ionic surfactant: Tween 80
Surfactant concentration: 10 mmol/L
Light intensivity: 2.4 x 10^{-5} Einstein L^{-1} s^{-1}

Additive: various amount of $NaBH_4$: 0, 0.001, 0.01, 0.05 and 0.1 M

The concentration of DR (10^{-3} mmol/L) at different time interval

	Time (min)								
$NaBH_4$ (mol/L)	0	2.5	5	15	30	45	60	90	120
0	27.760	27.720	27.472	24.997	18.433	14.751	12.103	8.606	6.662
0.001	26.950	24.174	22.854	18.973	15.496	12.208	8.489	4.635	2.911
0.01	26.430	23.056	21.324	16.704	12.528	8.933	6.105	2.669	1.163
0.05	26.080	20.603	17.734	14.240	10.697	6.546	3.756	1.695	0.453
0.1	25.640	21.230	17.062	13.628	10.256	6.076	3.077	1.282	0.000

C/Co of DR at different time interval

	Time (min)								
$NaBH_4$ (mol/L)	0	2.5	5	15	30	45	60	90	120
0	1	0.999	0.963	0.900	0.664	0.531	0.436	0.310	0.240
0.001	1	0.897	0.848	0.704	0.575	0.453	0.315	0.172	0.108
0.01	1	0.872	0.807	0.632	0.474	0.338	0.231	0.101	0.044
0.05	1	0.790	0.680	0.546	0.410	0.251	0.144	0.065	0.017
0.1	1	0.828	0.665	0.532	0.400	0.237	0.120	0.050	0.000

In (C/Co) of DR in different time interval

	Time (min)								
$NaBH_4$ (mol/L)	0	2.5	5	15	30	45	60	90	120
0	0	-0.001	-0.010	-0.105	-0.409	-0.632	-0.830	-1.171	-1.427
0.001	0	-0.109	-0.165	-0.351	-0.553	-0.792	-1.155	-1.760	-2.226
0.01	0	-0.137	-0.215	-0.459	-0.747	-1.085	-1.465	-2.293	-3.124
0.05	0	-0.236	-0.386	-0.605	-0.891	-1.382	-1.938	-2.733	-4.054
0.1	0	-0.189	-0.407	-0.632	-0.916	-1.440	-2.120	-2.996	

Reaction rate

$NaBH_4$ (mol/L)	Concentration (mM)	Km (L/mol)	slope	Intercept	R square	Kinetic rate constant (x 10^{-4} s^{-1})
0	0.0278	1036	-0.013	-0.010	0.991	2.10
0.001	0.0270	1006	-0.0184	-0.0377	0.997	3.07
0.01	0.0264	986	-0.0252	-0.0291	0.997	4.20
0.05	0.0261	973	-0.0315	-0.0709	0.990	5.25
0.1	0.0256	957	-0.0321	-0.0943	0.990	5.35

Photodegradation of Disperse Red (DR) within Tween 20 micelle solution with addition of acetone.

Exp. No S-6

Initial DR concentration: various
Molecular weight: 404 g/mol
Non-ionic surfactant: Tween 20
Surfactant concentration: 10 mmol/L
Light intensivity: 2.4 x 10^{-5} Einstein L^{-1} s^{-1}

Additive: various acetone addition: 0, 0.034, 0.68, 2.04, 3.5, 4.5 and 6 mol/L

The concentration of DR (10^{-3} mmol/L) at different time interval

	Time (min)								
Acetone (mol/L)	0	2.5	5	15	30	45	60	90	120
0	32.000	31.267	30.596	25.681	19.328	15.168	12.032	8.480	6.880
0.034	33.000	28.148	25.567	19.062	13.368	9.937	7.398	2.669	0.000
0.68	34.000	27.825	24.752	17.952	11.968	7.344	4.080	0.544	0.000
2.04	33.311	25.388	20.200	12.791	7.195	3.703	1.332	0.000	0.000
3.5	34.300	26.178	20.998	13.686	7.580	4.596	1.509	0.000	0.000
4.5	35.900	27.370	25.756	17.771	11.093	6.965	3.267	0.000	0.000
6	34.500	25.930	24.797	19.391	12.916	8.494	5.175	1.295	0.000

C/Co of DR at different time interval

	Time (min)								
Acetone (mol/L)	0	2.5	5	15	30	45	60	90	120
0	1	*0.977*	*0.956*	*0.803*	*0.604*	*0.474*	*0.376*	*0.265*	*0.215*
0.034	1	*0.853*	*0.775*	*0.578*	*0.405*	*0.301*	*0.224*	*0.081*	*0.000*
0.68	1	*0.818*	*0.728*	*0.528*	*0.352*	*0.216*	*0.120*	*0.016*	*0.000*
2.04	1	*0.762*	*0.606*	*0.384*	*0.216*	*0.111*	*0.040*	*0.000*	*0.000*
3.5	1	*0.763*	*0.612*	*0.399*	*0.221*	*0.134*	*0.044*	*0.000*	*0.000*
4.5	1	*0.762*	*0.717*	*0.495*	*0.309*	*0.194*	*0.091*	*0.000*	*0.000*
6	1	*0.752*	*0.719*	*0.562*	*0.374*	*0.246*	*0.150*	*0.038*	*0.000*

In (C/Co) of DR at different time interval

	Time (min)								
Acetone (mol/L)	0	2.5	5	15	30	45	60	90	120
0	0	-0.023	-0.045	-0.220	-0.504	-0.747	-0.978	-1.328	
0.034	0	-0.159	-0.255	-0.549	-0.904	-1.200	-1.495	-2.515	
0.68	0	-0.200	-0.317	-0.639	-1.044	-1.532	-2.120	-4.135	
2.04	0	-0.272	-0.500	-0.957	-1.532	-2.197	-3.219		
3.5	0	-0.270	-0.491	-0.919	-1.510	-2.010	-3.124		
4.5	0	-0.271	-0.332	-0.703	-1.174	-1.640	-2.397		
6	0	-0.286	-0.330	-0.576	-0.982	-1.402	-1.897	-3.283	

Reaction rates

Acetone(mol/L)	Concentration (mM)	Km (L/mol)	Slope	Intercept	R square	Kinetic rate constant (x 10^{-4} s^{-1})
0	0.032	1179.25	*-0.014*	0.040	*0.979*	*2.283*
0.034	0.033	1237.73	-0.026	-0.079	0.990	*4.333*
0.68	0.034	1268.88	-0.042	0.046	0.965	*6.967*
2.04	0.033	1242.95	-0.050	-0.126	0.989	*8.250*
3.5	0.034	1279.81	-0.047	-0.127	0.983	*7.867*
4.5	0.036	1340.44	-0.037	-0.104	0.990	*6.133*
6	0.035	1287.78	-0.034	-0.058	0.983	*5.583*

APPENDIX D

DATA OF

PHOTODEGRADATION OF CHLORINATED AROMATIC DYES (CAD) IN MICELLE WITH THE PRESENCE OF HUMIC MATERIALS

Photodegradation of Disperse Red (DR) within Tween 80 micelle solution with addition of Soil Extracted Material (SEM)

Exp. No: H-1

Initial DR concentration: various
Molecular weight: 404 g/mol
Concentration of Soil Extracted Materials "SEM": various
Non-ionic surfactant: Tween 80
Surfactant concentration: 10 mmol/L
Initial pH: 7

SEM concentration: various
Light intensivity: 2.4 x 10^{-5} Einstein L^{-1} s^{-1}
Molar absorptivity of DR: 35305 ($M^{-1}cm^{-1}$)
Molecular Weight of humic: 150000

The concentration of DR (10^{-3} mmol/L) in different time interval

	Time (min)								
SEM (μ mol/L)	0	2.5	5	15	30	45	60	90	120
0	27.760	27.720	26.722	24.997	18.433	14.751	12.103	8.606	6.662
0.40	24.111	23.718	20.821	17.616	14.289	11.744	8.123	5.554	4.159
0.65	23.720	23.375	22.539	17.932	13.840	11.232	7.346	4.738	3.487
1.19	23.190	22.463	20.732	15.928	12.847	9.924	6.168	3.000	1.543
1.98	22.196	21.551	19.346	13.759	10.010	7.512	4.452	2.313	1.133
2.97	21.220	20.544	18.053	13.323	9.125	6.684	4.154	1.910	0.637
3.96	20.200	19.334	17.392	12.045	8.444	6.121	3.676	1.616	0.485
4.94	19.920	19.446	17.217	12.093	8.395	6.178	3.795	1.671	0.607
5.93	19.450	17.927	15.867	12.194	8.558	7.130	4.104	2.334	1.420
6.59	19.028	18.901	18.881	18.780	12.235	9.133	5.449	3.044	2.188

C/Co of DR at different time interval

	Time (min)								
SEM (μ mol/L)	0	2.5	5	15	30	45	60	90	120
0	1	0.999	0.954	0.855	0.664	0.532	0.436	0.310	0.240
0.40	1	0.984	0.864	0.731	0.593	0.487	0.337	0.230	0.173
0.65	1	0.985	0.950	0.756	0.583	0.474	0.310	0.200	0.147
1.19	1	0.969	0.894	0.687	0.554	0.428	0.266	0.129	0.067
1.98	1	0.971	0.872	0.620	0.451	0.338	0.201	0.104	0.051
2.97	1	0.968	0.851	0.628	0.430	0.315	0.196	0.090	0.030
3.96	1	0.957	0.861	0.596	0.418	0.303	0.182	0.080	0.024
4.94	1	0.976	0.864	0.607	0.421	0.310	0.191	0.084	0.030
5.93	1	0.922	0.816	0.627	0.440	0.367	0.211	0.120	0.073
6.59	1	0.993	0.992	0.987	0.643	0.480	0.286	0.160	0.115

In (C/Co) of DR at different time interval

	Time (min)								
SEM (μmol/L)	0	2.5	5	15	30	45	60	90	120
0	0	-0.011	-0.048	-0.156	-0.409	*-0.632*	*-0.830*	-1.171	-1.427
0.40	0	-0.016	-0.147	-0.314	-0.523	-0.719	-1.088	-1.468	-1.757
0.65	0	-0.015	-0.051	-0.280	-0.539	-0.748	-1.172	-1.611	-1.917
1.19	0	-0.032	-0.112	-0.376	-0.591	-0.849	-1.324	-2.045	-2.710
1.98	0	-0.029	-0.137	-0.478	-0.796	-1.083	-1.607	-2.261	-2.975
2.97	0	-0.032	-0.162	-0.455	-0.844	-1.155	-1.631	-2.408	-3.507
3.96	0	-0.044	-0.150	-0.517	-0.872	-1.194	-1.704	-2.526	-3.730
4.94	0	-0.024	-0.146	-0.499	-0.864	-1.171	-1.658	-2.478	-3.491
5.93	0	-0.082	-0.204	-0.467	-0.821	-1.004	-1.556	-2.120	-2.617
6.59	0	-0.007	-0.008	-0.013	-0.442	-0.734	-1.250	-1.833	-2.163

Quantum yield

SEM (μmol/L)	Concentration (mM)	slope	Intercept	R square	Kinetic rate constant ($\times 10^{-4} s^{-1}$)	1/[humic] (L/mol)	Yield ($\times 10^{-3}$)	1/yield
0	0.0278	-0.013	-0.010	0.991	*2.10*	*0*	1.068	3691
0.40	0.0241	-0.015	0.054	0.988	*2.500*	2528090	1.281	7806
0.65	0.0237	-0.017	0.014	0.989	*2.817*	1532176	1.443	6928
1.19	0.0232	-0.023	0.030	0.996	*3.767*	842697	1.930	5181
1.98	0.0222	-0.025	0.025	0.997	*4.150*	505618	2.127	4702
2.97	0.0212	-0.028	0.215	0.996	*4.717*	337079	2.417	4137
3.96	0.0202	-0.030	0.029	0.994	*4.983*	252809	2.554	3916
4.94	0.0199	-0.029	0.015	0.997	*4.750*	202247	2.434	4108
5.93	0.0195	-0.022	0.087	0.991	*3.667*	168539	1.879	5322
6.59	0.0190	-0.020	0.092	0.980	*3.300*	151837	1.691	5913

Photodegradation of Disperse Red (DR) within Tween 80 micelle solution with addition of Soluble Humic (Ha)

Exp. No: H-2

Initial DR concentration: various
Molecular weight: 404 g/mol
Non-ionic surfactant: Tween 80
Surfactant concentration: 10 mmol/L
pH: 7

Concentration of Humic "Ha" additive: various

Light intensivity: 2.4 x 10^{-5} Einstein L^{-1} s^{-1}
Molar absorptivity of DR: 35305 ($M^{-1}cm^{-1}$)
Molecular weight of humic: 150000

The concentration of DR (10^{-3} mmol/L) in different time interval

	Time (min)								
Ha (μ mol/L)	0	2.5	5	15	30	45	60	90	120
0	27.800	27.509	26.510	23.782	18.459	14.790	12.121	8.618	6.672
0.017	31.200	31.197	30.298	26.957	21.559	16.692	11.482	8.702	6.864
0.027	27.500	27.492	27.225	24.063	18.783	14.823	10.065	7.260	5.775
0.033	26.300	26.287	26.068	22.934	18.778	14.176	8.758	6.812	5.423
0.044	31.200	30.356	29.850	27.335	21.122	16.318	10.760	8.081	6.427
0.089	27.400	26.214	25.562	27.374	23.180	22.012	16.550	10.960	7.097
0.177	30.200	30.054	29.966	27.939	26.183	24.060	19.928	14.194	8.788
0.440	31.600	30.996	31.934	30.543	28.219	24.986	21.700	16.021	11.186

C/Co of DR in different time interval

	Time (min)								
Ha (μ mol/L)	0	2.5	5	15	30	45	60	90	120
0	1	*0.999*	0.954	0.855	0.664	0.532	*0.436*	*0.310*	*0.240*
0.017	1	1.000	0.971	0.864	0.691	0.535	0.368	0.279	0.220
0.027	1	1.000	0.990	0.875	0.683	0.539	0.366	0.264	0.210
0.033	1	1.000	0.991	0.872	0.714	0.539	0.333	0.259	0.206
0.044	1	*0.973*	*1.005*	*0.876*	*0.677*	*0.523*	*0.345*	*0.259*	*0.206*
0.089	1	*0.957*	*1.024*	*0.999*	*0.846*	*0.803*	*0.604*	*0.400*	*0.259*
0.177	1	*0.975*	*1.034*	*1.008*	*0.867*	*0.797*	*0.660*	*0.470*	*0.291*
0.440	1	*0.981*	*1.011*	*0.967*	*0.893*	*0.791*	*0.687*	*0.507*	*0.354*

In (C/Co) of DR in different time interval

	Time (min)								
Ha (μ mol/L)	0	2.5	5	15	30	45	60	90	120
0	0	-0.001	-0.038	*-0.105*	*-0.409*	*-0.632*	*-0.830*	-1.171	-1.427
0.017	0	0.000	-0.029	-0.146	-0.370	-0.625	-1.000	-1.277	-1.514
0.027	0	0.000	-0.010	-0.134	-0.381	-0.618	-1.005	-1.332	-1.561
0.033	0	0.000	-0.009	-0.137	-0.337	-0.618	-1.100	-1.351	-1.579
0.044	0	-0.027	0.005	-0.132	-0.390	-0.648	-1.065	-1.351	-1.580
0.089	0	-0.044	0.024	-0.001	-0.167	-0.219	-0.504	-0.916	-1.351
0.177	0	-0.025	0.033	0.008	-0.143	-0.227	-0.416	-0.755	-1.234
0.440	0	-0.019	0.011	-0.034	-0.113	-0.235	-0.376	-0.679	-1.038

Quantum yield

Ha (μ mol/L)	Concentration (mM)	slope	Intercept	R square	Kinetic rate constant (x $10^{-4}s^{-1}$)	1/[humic] (L/mol)	Yield (x 10^{-5})	1/yield
0	0.0278	0.013	-0.010	0.991	*2.10*	0	1.068	7781
0.017	0.0312	0.015	0.024	0.968	*2.28*	60000000	1.170	8546
0.027	0.0275	0.014	0.013	0.974	*2.37*	37500000	1.213	8245
0.033	0.0263	0.011	0.104	0.956	*2.42*	30000000	1.238	8075
0.044	0.0312	0.010	0.102	0.954	*2.40*	22727273	1.230	8131
0.089	0.0274	0.009	0.071	0.968	*1.87*	11278195	0.957	10454
0.177	0.0302	0.002	0.048	0.854	*1.67*	5639098	0.854	11708
0.440	0.0318	0.001	0.003	0.984	*1.42*	2272727	0.726	13774

REFERENCE

REFERENCE

Almgren M.A., Grieser F. and Thomas J.K., "Dynamic and static aspects of solubilization of neutral arenes in ionic micellar solutions". *J. American Chemistry Society.*, 121, 279-291. (1979)

Alton G. C., "Recycling dye wastewater through ozone treatment". *Textile Industries.* no 7:26-30. (1983)

American Chemical Society., "Ozone Chemistry and Technology". *International ozone conference,* Chicago. (1956)

Attwood D. and Florence A.T., "*In Surfactant Systems: Their Chemistry, Pharmacy and Biology*". Chapman & Hall, New York. (1983)

Benitez F. J., "Degradation by ozone & UV radiation of the herbicide cyanazine". *Ozone Science & Engineering,* vol 16, 212-234. (1994)

Blaisdell B.E., "The photochemistry of aromatic azo compounds in organic solvent". *J. Soc. Dyers and Colourists*, 65, 618. (1949)

Bruno L., David A. R. and Deborah R. B., "Fundamental Aspects, *Ozone in water treatment application and engineering: cooperative research report".* Lewis Publishers, p. 13-15. (1991)

Buffle J.A.E., "Les Substances Humiques et leurs Interactions avec les Ions Mineraux" *in Conferenced Preceedings de la Commission d'Hydrologie Applique de l';AGHTM,* I'U-niversite d'Orday, p.3-10. (1977)

Bunce N.J., Kumar Y., Ravanal L., and Safe S., "Photochemistry of chlorinated biphenyls in iso-octane solution". *J.C.S. Perkin II*, 880-884. (1978)

Carriere J., Jones J. P. and Broadbent A.D., "Decolorization of textile wastewaters by ozonation". *AATCC Book of paper*, 232 (1991).

Charpentier., "*Gas-Liquid Absorptions and Reactions, Advances in Chemical Engineering*". T.B. Drew et. Al., Academic Press, New York. (1981)

Choudhry G.G. and Webster G.R.B., " Quantum wields of polychlorodibenzo-p-dioxins, Photochemistry of environmental aquatic system". *American Chemistry Society,* p. 61-73. (1987)

Choudhry G.G., "Photophysical and photochemical properties of soil and aquatic humic substances". *Environ. Toxicol. Chem,*. 92, 59-112 (1984)

Chu W. and Javert C. T., "Photodechlorination of Polychlorobenzene Congeners in Surfactant Micelle Solutions". *Environ. Sci. Technol.*, vol. 28, No13, 2415 –2422. (1994)

Chu W. and Ma C. W., "Quantitative Prediction of Direct and Indirect Dye Ozonation Kinetics". *Water Research*, vol.34, No.12, p.3453-3160. (2000)

Chu W. and Ma C. W., "Reaction Kinetics of UV-decolorization for Dye Materials". *Chemosphere*, 37, 961-974. (1998)

Chu W. and Ma C.W., "Effect of UV-decolouring of aromatic dyes with different chemical structures". *Toxicological and Environmental Chemistry.*, 63, 247-255. (1997)

Chu W. and So W.S., "Modelling the two stages of Surfactant Aided Soil-Washing Process". Submit to Water Research. (2000)

Chu W. and Tsui S.M., "Photo-sensitization of diazo disperse dye in aqueous acetone". *Chemosphere,* 39, 1667-1677. (1999)

Chu W., "Photodechlorination Mechanism of DDT in UV/Surfactant System". *Environ. Sci. Technol.*, 33, 421-425. (1999)

Colour Index., (third edition) The society of Dyers and Colourists. (1971, 1987)

Cooper W.J, Zika R.G., Petsane R.G. and Fisher A.M., "Sunlight-induced photochemistry of humic substances in natural water, in Aquatic humic substances: Influence on fate and treatment of pollutants". I.H. Suffet and P. MacCarthy, eds., pp. 333-362. *American Chemical Society*, Washington DC. (1989)

Cooper W.J. and Herr F.L., "Introduction and overview, Photochemistry of environmental aquatic system". *American Chemistry Society*, pp. 1-8. (1987)

Daryner A., Nicholls C.H. and Palithorpe M.T., "Some Aspects of the light fastness of reactive azo dyes on cellulose under wet conditions". *J. Soc. Dyers and Colourists,* 93, 213 - 216. (1977)

David M. H. and Warren S. P., "Practical methods for purification of anion dyes as their sodium, potassium and lithium salts". *AATCC*, 1871. (1971)

Davidson R.S., Goodin J. W. and Kemp G., "The Photochemistry of aryl halides and related compounds". *Advanced in physical organic chemistry, Vol. 20,* Academic Press, London, pp. 192-233. (1984)

Davies G. and Ghabbour E.A., "*Humic substance Structures Properties and Uses*"., The Royal Society of Chemistry, U.K. (1998)

Eckenfelder W.W., "Industrial Wastewater Seminar on Water Pollution Control in the Textile Industry". *Soc. Dyers and Colourists*, Hong Kong, September. (1994)

Edwards D.A., Liu Z. and Luthy R.G., "Surfactant solubilization of organic compounds in soil/aqueous systems". *Journal of Environmental Engineering*, vol.120, No.1, p.5 – 18, (1994)

Edwards D.A., Luthy R.G. and Liu Z., "Solubilization of Polycyclic Aromatic Hydrocarbons in Micellar Nonionic Surfactant Solutions". *Environ. Sci. Technol.* 25, 127-133. (1991)

Egger K.W. and Cocks A.T., "Homopolar and heterpolor bond dissociation energy and heat of formation of radicals and ions in the gas phase. I. Data on organic molecules". *Helvetica Chimica Acta*, 56, 5, Nr. 148-149, 1516-1536. (1973)

Fendler J.H., "*Catalysis in micellar and macromolecular systems*". Academic Press, 86-103 (1975)

Frimmel F.H., "Photochemical aspects related to humic substances". *Environ. Int.*, 20, 373-385. (1994)

Frimmel F.H., Bauer H., Putzien J., Muraseecco P. and Braun A.M., "Laser flash photolysis of dissolved aquatic humic material and the sensitized production of singlet oxygen". *Environ. Sci. Technol.*, 21 4541-4545. (1987)

Green J.M. and Sokol C., "Using color to decolorize dyeing plant wastewater". *American Dyestuff Reporter*, 74, No.4: 50-51, 67. (1985)

Hana S., "Spectrophotometric method for determination of ozone in aqueous solutions". *Water Research*, vol. 7, pp. 729-739. (1973)

Hartley, *Proc. Roy. Soc. London A168*, 420. (1938)

Hawari J., Demeter A., and Samson R., "Sensitized photolysis of polychlorobiphenyls in alkaline 2-propanol: Dechlorination of Aroclor 1254 in soil samples by solar radiation". *Environ. Sci. Technol.*, 26: 10, 2022-2027. (1992)

Hirashima T. and Manabe O., *Kagaku Kogyo*, 24, 1164. (1973)

Hoigne J. and Bader H., "The role of hydroxyl radical reaction in ozonation processes in aqueous solution". *Water research*, 10, 377. (1976)

Huang C.R., Lin Y.K. and Shu H.Y., "Wastewater decoloration & TOC [Total Organic Carbon] – Reduction by sequential treatment". *American Dyestuff Reporter*, 83, No. 10: 15-16. (1994)

Hung Y.S., "Degradation of commercial azo dyes in water using ozonation and UV enhanced ozonation process". *Chemosphere*, vol., no.8, pp. 3813-3825. (1995)

Hung Y.S., Huang C.R. and Chang M.C., "Decolourization of mono-azo dyes in wastewater by advanced oxidation process. A case study of acid red 1 and acid yellow 23". *Chemosphere,* vol 29, no12, p.2597-2607. (1994)

Jacques K., "*Organic photochemistry Principal and Application*". London; San Diego; Academic Press,c, p.15 -16. (1993)

Jafvert C.T., "Sediment- and saturated-soil-associated reactions involving an anionic surfactant (dodecsulfate). 2. Partition of PAH compounds among phases". *Enviro. Sci. Technol.* 25, 6, 1039-1045. (1991)

Jafvert C.T., Van Hoof P.L. and Heath J.K., "Solubilization of non-polar compounds by non-ionic surfactant micelles". *Water Research.* 28, 1009-1017. (1994)

John H. C., "Rmoval of dyewaste colour from sewage effluent – The use of a full scale ozone plant". *Water Science Technology*, vol. 30, 275-283. (1994)

Jurgen B., " Mixed results: Latest study adds skepticism, hope to ozone debate", *Textile Rental,* February, 78-84. (1995)

Kile D.E. and Chiou C.T., "Water Solubility enhancement of DDT and trichlorobenzene by some surfactants below & above the critical micelle concentration". *Environ. Sci. Technol.* 23, 832-838. (1988)

Leaver I.H., "Photochemistry of dyed and pigmented polymers" Normans. Allen, *Photooxidation and Photoreduction of dyes in ploymers*, Applied Science Publishers Ltd, England, p.161 – p.239. (1980)

Lin S.H., "Looking to treat wastewater? Try ozone". *Chemical Engineering*, 100, no.5: 112-116 May (1993)

Liu Z. and Shonali L., "Surfactant solubilization of polycyclic aromatic hydrocarbon compounds in soil-water suspension". *Water Science Technology*, v23, 475-485. (1991)

Mamoru K., "Photochemical effects of humic substances on the degradation of orgenophorous pesticides". *Chemosphere*, vol. 36 part: n10, p. 2337(8) (1998)

Michelsen D.L., Powell W.W., Woodby R.M., Fulk L.L. and Boardman G.D. "Pretreatment of textile dye concentrates using fenton's reagent and ozonation prior to biodegradation". *AATCC Book of paper*, p.135-p.149 (1992)

Mirat D. G. and Vatistas R., "Oxidation of phenolic compounds by ozone and ozone + UV radiation: A comparative study". *Water Research*, vol 21, no.8, 895-900". (1987)

Mishra G. and Tripathy M., "A critical review of the treatments for decolourization of textile effluent". *Colourage*, 10, 35-38 (1993)

Mittal K.L., *Micellization, solubilization, and microemulsions*, Volume 1 & 2, Plenum Press, N.Y. (1977)

Miyamoto J. T., "Sorption of a Disperse Dyes by sands and Soil". *J. Environmental Qual.*, Vol.8, no.3, 412 - 417. (1979)

Namboodri C.G., "Decolorizing dyes with chlorine and ozone Part 1". *American Drycleaner*, 83, no.3 : 17-22. (1994)

Nebel C., "Ozone decolorization of secondary dye-laden effluents, 2 nd Symp on ozone technology". *Montreal*, May 11-14, 336-358. (1975)

Neter J., Wasserman W. and Whitmore G.A., "*Applied statistics, 3rd ed*". Allyn and Bacon, Inc., 958-959. (1988)

Poon C. and Vittimberga B. M., "UV photodecomposition of color in dyeing wastewater". *Industrial waste, Processing of 13 th Mid-Atlantic Conference*. 427-433. (1981)

Rabek J.K., "*Experimental methods in photochemistry and photophysics Part 2*". John Wiley & Sons, 937-959. (1982)

Ramnath N., Ramesh V. and Ramamurthy V., "Micellar structure and micellar control of photochemical reactions". *Journal of Photochemistry*, 31, 75-95, (1985).

Risk Reduction Engineering Laboratory., "The superfund innovation technology evaluation program: Technology profiles fourth edition". *EPA/540/5-91/008*, November. (1991)

Roth J.A., "Design of completely mixed ozonation reactors". *Chemical Oxidation – Technologies for the Nineties*, pp. 114-129. (1991)

Ruppert G. and Rupert .B., "UV-O_3, UV-H_2O_2, UV-TiO_2 and the photo-fenton reaction comparison of advanced oxidation processes for wastewater treatment". *Chemosphere*, vol. 28, No.8. p.1447-1454. (1994)

Rygalov L.N. and Chibisov A.K., *Khim. Vys. Energ.*, 5, 545. (1971)

Rys P. and Zollinger H., "*Fundamentals of the Chemistry and Application of Dyes*". Wiley-Interscience. (1972)

Schultz G., "Oxidative decomposition of dyestuffs by means of ozone – effluent decolorozation, reactions, decomposition products". *Textile-praxis International* 47, no.11: 1055-1060, 1062., XXVI-XXI. (1992)

Spadaro J.T., Isabelle L. and Renganathan V., "Hydroxyl radical mediated degradation of azo dyes – evidence for benzene generation". *Environ. Sci. and Technol.*, 28, no7: 1383-1393. (1994)

Staehelin J. and Hoigne J., "Decomposation of ozone in water: rate of initiation by hydroxide ions and hydrogen peroxide". *Environ. Sci. Technol*". 16, 676-681. (1982)

Stevenson F.J., "*Humus Chemistry: Genesis, Composition, Reactions*". Wiley-Interscience, New York. (1982)

Thomas J.K., "Radiation induced reactions in organized assemblies". *Chemical Reviews*, 80, 4, 283-299, Aug. (1980)

Turro N.J., "*Modern molecular photochemistry*". The Benjamin/Cummings publishing Co, Inc., 246-248. (1978)

Turro N.J., Cox G.S., Paczkowski., "*Photochemistry in micelles, Current Chemistry – Photochemistry and organic synthesis*". 129, 57-97. (1985)

Vigon B.W. and Rubin A.J., "Practical considerations in the surfactant-aided mobilization of contaminants in aquifers". *Journal WPCF*, 61,7, 1233-1240. (1989)

Wayt H. J. and Wilson D. J., "Soil clean up by in-situ surfactant flushing, II. Theory of micellar solubilization," *Separation Science and Technology*, 24, 905-937. (1989)

West C.C. and Harwell J.H., "Surfactants and subsurface remediation". *Environ. Sci. Technol.*, 26, 12, 2324-2330. (1992)

Whiten D.G., Russell J.C., and Schmehl, R.H., "Photochemical reactions in organized assemblies: environmental effects on reactions occurring in micelles, vesicles, films and multilayer assembles and at interfaces". *Tetrahedron*, 38, 16, 2455-2487. (1982)

William M. H., "*Aspects of Organic Photochemistry*". Academic Press Inc. (London) Ltd. (1976)

Woldman M. L. and Weston R. F., "Techniques for decoloring mill wastewater". *Textile Chemist and Colorist*, 9, 175-179 (1974).

Yang Y., Wyatt D. and Bahorsky M., "Decolorization of Dyes using UV/H_2O_2 photochemical oxidation". *Text. Chem. Color.*, 30, 27-35. (1998)

Zepp R.G., Baugham G.L. and Schlotzhauer P.F., "Comparison of photochemical behaviour of various humic substance in water". *Chemosphere*. 10, 109-117. (1981)

Zepp R.G., Wolfe N.L., Gordon J.A. and Baughman G.L., "Dynamics of 2,4-D ester in surface water – Hydrolysis, Photlysis, and Vaporizatio". *Environ. Sci. & Technol.*, 9:13, 1144-1149. (1975)

Zollinger H., "*Azo and Diazo Chemistry. Aliphatic and Aromatic Compounds*". Interscience, New York. (1961)